The Dissertation Committee for Xiaoyue Wang Certifies that this is the approved version of the following dissertation:

Improvement of Random Vibration Theory Site Response Analysis

Committee:

Ellen M. Rathje, Supervisor

Lance Manuel

Robert B. Gilbert

Clark R. Wilson

Brady R. Cox

Improvement of Random Vibration Theory Site Response Analysis

by

Xiaoyue Wang, B.E.; M.S.E.

Dissertation

Presented to the Faculty of the Graduate School of

The University of Texas at Austin

in Partial Fulfillment

of the Requirements

for the Degree of

Doctor of Philosophy

The University of Texas at Austin

May 2017

Dedication

To my husband and parents

Acknowledgements

I would like to say that I am beyond words of gratitude, because there are a lot of memorable moments during my past five years at UT. However, I am going to convey my appreciation as much as I can in this acknowledgement.

My deep gratitude goes to Dr. Ellen M. Rathje, my supervisor, who expertly and kindly guided me throughout the graduate education. My experience working with her is joyful and rewarding. Her energy and enthusiasm for research is infectious. Without her support, guidance, and persistent help this dissertation would not have been possible.

I am grateful to my committee members, Drs. Lance Manuel, Robert B. Gilbert, Clark R. Wilson, and Brady R. Cox for the reviewing of this dissertation. Dr. Lance Manuel has kindly provided me with inspiring ideas and valuable feedback for my research. Drs. Robert B. Gilbert, Clark R. Wilson, and Brady R. Cox have offered me a wealth of knowledge through their inspiring teaching in class. It is a great pleasure and honor to have them in my committee.

Financial support for this research and my education was provided by the Pacific Gas & Electric, Co. through Dr. Norman Abrahamson and the Nuclear Regulatory Commission (grant NRC-HQ-60-15-C-0005). This support is greatly acknowledged.

I would also like to give my appreciation to my friends at Austin – it is their support and company that made my life outside school at Austin – and to my family who forgives me for pursuing education at places further and further away from home and have supported me as always. And finally, I want to acknowledge my husband, Chenyang Bi, who offered unconditional love and support and have always been there for me.

Improvement of Random Vibration Theory Site Response Analysis

Xiaoyue Wang, Ph.D.

The University of Texas at Austin, 2017

Supervisor: Ellen M. Rathje

Random Vibration Theory (RVT) site response analysis is a standard in seismic hazard analysis for nuclear facilities to compute the dynamic response of soil deposits. However, studies have shown that the RVT analysis predicts site amplification at natural site frequencies that are considerably larger than the time series (TS) analysis. The objectives of this research are to identify improvements to the current approaches used in RVT site response analysis and to incorporate these improvements so that the discrepancy between RVT and TS site amplification are reduced.

This research first investigates a critical part of the RVT approach – the peak factor, defined as the peak to root-mean-square (*rms*) ratio of a signal. It is shown that by accounting for the statistical dependence between peaks, the peak factor model developed by Vanmarcke (1975) is superior to the model developed by Cartwright and Longuet-Higgins (1956) when applied to seismic site response analysis. The use of the Vanmarcke peak factor model reduces the RVT site amplification at the natural site frequencies and makes the RVT amplification more similar to the TS analysis.

This research also investigates the duration used in the computation of the *rms* value from the Fourier Amplitude Spectrum. It is shown that by accounting for the influence of the dynamic site response on the duration of the oscillator response, the RVT analysis generally predicts site amplification within +/- 10% of TS analysis. To apply

the modification of duration to RVT without the use of time series, a duration model is developed that empirically predicts the change of duration at the ground surface due to site response.

In the last part of the research, the improved RVT approach, which utilizes the Vanmarcke (1975) peak factor and incorporates the change in duration due to site response, is applied to more complex and realistic shear wave velocity profiles and for strain-compatible properties associated with equivalent-linear analysis. The site amplification results indicate that the improved RVT site response analysis generally works well to reduce the discrepancy between RVT and TS amplification for a wide range of situations.

Table of Contents

List of Tables xi

List of Figures xii

Chapter 1: Introduction 1

1.1 Research Significance 1

1.2 Organization of Dissertation 2

Chapter 2: Influence of Peak Factors on Site Amplification from Random Vibration Theory Based Site Response Analysis 4

2.1 Introduction 5

2.2 RVT Approach and Peak Factor Models 7

2.2.1 Parseval's Theorem 7

2.2.2 Extreme Value Statistics: Cartwright and Longuet-Higgins (1956) 8

2.2.3 Extreme Value Statistics: Vanmarcke (1975) 10

2.2.4 Comparisons of Peak Factor Models 13

2.3 Analyses Performed 17

2.4 Site Amplification Results 19

2.4.1 Influence of CL and Vanmarcke Peak Factor Models on RVT-TS Comparison 20

2.4.2 Site and Input Motion Characteristics that Influence RVT-TS Comparison 24

2.4.3 Influence of Duration on RVT-TS Comparisons 27

2.4.4 Influence of Input Motion Frequency Content on RVT-TS Comparisons 31

2.4.5 Influence of $V_{s,rock}$ and Seismological Parameters on the RVT- TS Comparisons 33

2.5 Discussion and Conclusions 36

2.6 Data and Resources 39

2.7 Acknowledgements 39

2.8 References 39

Chapter 3: Development of Ground Motion Duration Models for Use in Random Vibration Theory Site Response Analysis 43
3.1 Introduction 44
3.2 RVT Site Response Analysis 45
3.3 Durations Used in RVT Analysis 48
3.3.1 *RMS* Duration 48
3.3.2 Effect of Site Response on Ground Motion Durations 49
3.4 Analyses Performed 54
3.4.1 Input Ground Motions 54
3.4.2 Site Profiles 55
3.5 Oscillator Durations for Rock Motions 57
3.6 Oscillator Durations for Surface Motions 61
3.7 Incorporating a Duration Modification in RVT Site Response Analysis 70
3.8 Discussion and Conclusions 74
3.9 Data and Resources 76
3.10 Acknowledgements 76
3.11 References 76

Chapter 4: Accounting for Changes in Duration in Random Vibration Theory Based Site Response Analysis 79
4.1 Introduction 80
4.2 Modified RVT Approach for Site Response Analysis 81
4.2.1 RVT Framework 81
4.2.2 Outline of RVT Approach Using Modified Duration 82
4.3 Analyses Performed 85
4.3.1 Input Ground Motions 85
4.3.2 Site Profiles 86
4.4 RVT-TS Site Response Comparisons: Linear-Elastic Conditions 89
4.4.1 Results for Hypothetical Sites 89
4.4.2 Results for Realistic Sites 95
4.5 RVT-TS Site Response Comparisons: Equivalent-Linear Conditions 98
4.6 Conclusions 105

4.7 Data and Resources.....107
4.8 Acknowledgements.....107
4.9 References.....107

Chapter 5: Conclusions And Recommendations For Future Work.....110
5.1 Conclusions.....110
5.2 Recommendations for Future Work.....113

References.....115

List of Tables

Table 2.1: Stochastic input parameters used in development of time series input motions using SMSIM 15

Table 3.1: Stochastic input parameters used in development of time series input motions using SMSIM 55

Table 4.1: Stochastic input parameters used in development of time series input motions using SMSIM 86

List of Figures

Figure 2.1: (a) Time series (TS) and (b) random vibration theory (RVT) approaches to site response analysis. 6

Figure 2.2: Illustration of first-passage problem for a two-sided, D-type barrier (after Crandall et al. 1966) 10

Figure 2.3: (a) Cartwright and Longuet-Higgins (CL) peak factor as a function of the number of zero-crossings (Nz) for different values of bandwidth ξ, (b) Vanmarcke peak factor as a function of Nz for different values of bandwidth δ, and (c) influence of δ on the Vanmarcke peak factor. Bandwidth factors ξ and δ cannot be uniquely related and thus the results in the different panels of this figure cannot be directly compared. 14

Figure 2.4: (a) Fourier amplitude spectrum (FAS) for a broad-band rock motion and its narrow-band oscillator response. (b) CL and Vanmarcke peak factors as a function of Nz for the broad-band rock motion and narrow-band oscillator response. 16

Figure 2.5: FAS, ground motion duration (Dgm), and corner frequencies (fc) for the earthquake scenarios considered in this study for central and eastern North America (CENA). 19

Figure 2.6: RVT and TS site response results for H = 32 m and H = 316 m sites excited by *M* 6.5 earthquake. Amplification factors, ratios of RVT to TS amplification, bandwidth factor δ, and peak factors are plotted as a function of oscillator frequency. 21

Figure 2.7: RVT and TS site response results for H = 316 m site excited by *M* 5 and *M* 8 earthquake motions. Amplification factors, ratios of RVT to TS amplification, and bandwidth factor δ are plotted as a function of oscillator frequency. 23

Figure 2.8: Rock FAS, surface FAS, and FAS of the oscillator response of the surface motion for $f = fsite$ for three scenarios: (a) *M* 8.0 and H = 316 m, (b) *M* 5.0 and H = 316 m, and (c) *M* 5.0 and H = 32 m. 25

Figure 2.9: Ratio of RVT/TS site amplification at first-mode site frequency as a function of $fsite/fc$ for sites with $Vs,rock$ = 3000 m/s and CENA input motions. 26

Figure 2.10: (a) The ratio of the duration of the oscillator response for the surface motion ($D5\text{-}95, oscsurface$) to the duration of the oscillator response for the input rock motion ($D5\text{-}95, oscrock$) as a function of $fsite$ for three different earthquake magnitudes. The duration increases most for low frequency sites and small magnitude earthquakes. (b) Ratio of $D5\text{-}95, oscsurface/D5\text{-}95, oscrock$ as a function of $fsite/fc$ for all scenarios considered. 29

Figure 2.11: Ratio of RVT/TS site amplification at first-mode site frequency as a function of $fsite/fc$ when using duration correction due to site response. Results for sites with $Vs,rock$ = 3000 m/s and CENA input motions. 30

Figure 2.12: Effect of frequency content of input motion, as indicated by earthquake magnitude, on (a) TS and (b) RVT site amplification for H = 316 m site. 32

Figure 2.13: Ratio of RVT/TS site amplification at first-mode site frequency as a function of f_{site}/f_c for sites with $V_{s,rock}$ = 1000 m/s and CENA input motions.....34
Figure 2.14: Ratio of RVT/TS site amplification at first-mode site frequency as a function of f_{site}/f_c for sites with $V_{s,rock}$ = 1000 m/s and western North America (WNA) input motions. 35
Figure 3.1: Ratio of RVT/TS site amplification at first mode site frequency as a function of $f_{site}f_c$ for a range of earthquake magnitudes (data from Wang and Rathje 2016). 47
Figure 3.2: Acceleration-time histories of rock and surface motions, as well as the oscillator responses for these motions for different oscillator frequencies. 51
Figure 3.3: Average significant duration (D5-95) of oscillator responses for time-domain, stochastically-simulated rock motions and *rms* durations (D_{rms}) from different empirical models. 53
Figure 3.4: Ground motion durations (D_{gm}) for all earthquake scenarios used in this study. 56
Figure 3.5: Theoretical site transfer functions for selected hypothetical site profiles used in this study. 56
Figure 3.6: Variation of $D_{5\text{-}95,rock}$ and $D_{5\text{-}95,rockDgm}$ with oscillator frequency for a range of D_{gm}. 58
Figure 3.7: Functional form of model to predict $D_{5\text{-}95,rockDgm}$ as a function of frequency.....59
Figure 3.8: Parameters in $D_{5\text{-}95,rockDgm}$ model and predicted values of $D_{5\text{-}95,rockDgm}$ for a range of D_{gm}. 61

Figure 3.9: Variation of $D5\text{-}95, surf$ and $D5\text{-}95, rock$ with oscillator frequency for a site with H = 316 m and $Vs, rock$ = 3,000 m/s for two earthquake scenarios.....63

Figure 3.10: The change in the duration of the oscillator response ($\Delta D = D5\text{-}95, surf - D5\text{-}95, rock$) as a function of frequency due to site response for (a) different Dgm, (b) different site thicknesses, and (c) different $Vs, rock$. 64

Figure 3.11: Functional form of model to predict $\Delta D = D5\text{-}95, surf - D5\text{-}95, rock$.65

Figure 3.12: Variation of amplitude Ai with Dgm for (a) different $Vs, rock$, (b) different site thicknesses, and (c) different modes.....67

Figure 3.13: Parameters in predictive model for $\Delta D = D5\text{-}95, surf - D5\text{-}95, rock$.69

Figure 3.14: Ratio of RVT/TS site amplification at first-mode site frequency as a function of Dgm for RVT analyses using the $Drms$ model and using the modified $Drms, surf$ model. (a) Site with H = 316 m and $Vs, rock$ = 3,000 m/s and (b) site with H = 100 m and $Vs, rock$ = 3,000 m/s.72

Figure 4.1: Framework of the RVT approach using a modified duration at the ground surface.....83

Figure 4.2: Shear wave velocity profiles of hypothetical and realistic sites used in this study. 87

Figure 4.3: Linear-elastic transfer functions for hypothetical and realistic site profiles. 88

Figure 4.4: *AF* results from linear-elastic RVT and TS analyses for H = 316 m and 100 m hypothetical sites with $V_{s,rock}$ = 3,000 m/s and selected earthquake scenarios.....90

Figure 4.5: Ratio of RVT/TS at the first mode frequency from linear-elastic analysis for the H = 316 m and 100 m hypothetical sites ($V_{s,rock}$ = 3,000 m/s) and all earthquake scenarios. RVT analyses use the original, unmodified duration. 92

Figure 4.6: Ratio of RVT/TS at modal frequencies as a function of $Dgm \cdot fsite$ from linear-elastic analysis for all hypothetical sites and all earthquake scenarios.....93

Figure 4.7: *AF* results from linear-elastic RVT and TS analyses for selected realistic sites and earthquake scenarios. 96

Figure 4.8: Ratio of RVT/TS at modal frequencies as a function of $Dgm \cdot fsite$ from linear-elastic analysis for all realistic sites and all earthquake scenarios. 97

Figure 4.9: Response spectra of input motions generated using SMSIM (Boore 2005) and accounting for finite-source effects. 99

Figure 4.10: *AF* results and shear strain profiles from equivalent linear RVT and TS analyses for the CC site subjected to ground motions with different intensities. 101

Figure 4.11: Ratio of RVT/TS at modal frequencies as a function of $Dgm \cdot fsite$ from equivalent-linear analysis for all realistic sites and all earthquake scenarios.....103

Figure 4.12: Maximum shear strain from RVT analysis vs. maximum shear strain from TS analysis. 104

Chapter 1: Introduction

1.1 RESEARCH SIGNIFICANCE

One dimensional site response analysis is frequently used to quantify the influence of local soil conditions on the earthquake ground motions. This analysis uses as input an acceleration-time history for rock conditions, propagates this motion through a one-dimensional soil column, and computes acceleration-time history and associated acceleration response spectrum at the ground surface. Traditional site response analysis selects and scales a suite of time histories for use as input into the analysis, and averages the results from these motions to obtain a stable estimate of the site response. However, this approach requires a sufficient amount of appropriate input time histories and the computation process can be very time consuming when performing a large number of analyses. As an alternative to the traditional time series (TS) approach, site response analysis based on random vibration theory (RVT) eliminates the use of input time series by using as input only a Fourier Amplitude Spectrum and the duration of ground motion. The RVT approach reduces the computation time because a single RVT analysis represents the average of a large number of TS analyses, and RVT analysis is applicable in regions where ground motion recordings of large magnitude earthquakes may not be available. As a result, RVT site response analysis is commonly used to estimate site amplification in probabilistic seismic hazard analysis for nuclear facilities.

The RVT approach uses Parseval's theorem to compute the root-mean-square (*rms*) acceleration from the FAS and converts this *rms* value to a peak value using a peak factor (*pf*). The peak factor, defined as the peak-to-*rms* ratio, is derived from extreme value statistics and can be represented through a probability distribution, with its

expected value used in RVT analysis. While the application of RVT in site response analysis has been investigated by many researchers (Silva et al. 1997, Rathje and Ozbey 2006), recent comparisons between TS and RVT site response analyses have shown that RVT analysis may predict amplification at the natural frequencies of a site that are significantly larger than TS analysis (e.g., Kottke and Rathje 2013, Graizer 2014). This discrepancy between RVT and TS site amplification may be caused by the simplified assumptions used in the peak factor models incorporated in the RVT approach or by the durations used in the calculation of the *rms* acceleration.

Modifications to and improvements of the procedures used for RVT site response analysis are the main goals of this research. This research consists of three parts: (1) investigating the influence of different peak factor models and the influence of the surface ground motion duration on the results from RVT site response analysis; (2) developing a model of duration that predicts the change in duration due to dynamic ground response and can be used in RVT site response when computing the ground surface motion; and (3) evaluating the improvement in the results from RVT site response analysis relative to TS analysis when incorporating the most adequate peak factor model and a duration model that account for the effects of site response on ground motion duration.

1.2 ORGANIZATION OF DISSERTATION

After this introduction, this dissertation is organized into three main chapters, each chapter being a self-contained journal article consisting of an introduction, previous research, research methods, research findings, and conclusions.

Chapter 2 investigates the influence of different peak factor models on the site amplification predicted by RVT site response analysis. Site amplification results obtained from RVT and TS analyses using different peak factor models are compared. Linear-elastic site response analyses are performed for hypothetical sites with different natural frequencies subjected to input motions from a large range of earthquake magnitudes in an effort to understand how the natural site frequency, frequency content of the input motion, and duration of shaking influence the results.

Chapter 3 investigates the influence of site response on the duration of oscillator responses for use in RVT analysis. Using the surface acceleration-time histories computed by linear-elastic TS site response analyses, an empirical model is developed that predicts the modification of duration for use in the RVT *rms* calculation due to site response as a function of various properties of the site.

Chapter 4 evaluates the performance of the improved RVT approach that utilizes the peak factor model recommended by Chapter 2 and the model of duration developed in Chapter 3. The improved RVT site response analysis is applied to various shear velocity profiles, including simple hypothetical sites and more complex realistic sites, and for strain-compatible soil properties associated with equivalent-linear analysis.

Chapter 5 represents conclusions and recommendations for future work.

Chapter 2: Influence of Peak Factors on Site Amplification from Random Vibration Theory Based Site Response Analysis[1]

Xiaoyue Wang[2], Ellen M. Rathje[2]*

Abstract

Studies have shown that random vibration theory (RVT) site response analysis predicts site amplification at the natural site frequencies that are systematically larger than the results obtained from time series (TS) analysis using a suite of input TS. A critical part of the RVT approach is the peak factor, defined as the ratio of the peak to root mean square (RMS) value of a signal. This study investigates the influence of different peak factor models on the site amplification estimated by RVT site response analysis. It is shown that the use of the Vanmarcke (1975) peak factor model rather than the Cartwright and Longuet-Higgins (1956) peak factor model predicts site amplification in better agreement with those predicted by TS analysis, although some differences remain for some cases. Larger differences between the RVT and TS results occur for sites with smaller natural frequencies, for earthquakes of smaller magnitude, and for sites with larger bedrock shear-wave velocities. Accounting for the increase in duration due to site response in the RVT analysis minimizes the differences between RVT and TS analysis. Recommendations are provided regarding the cases where RVT provides site amplification reasonably similar to TS analysis.

---

[1]This chapter previously appeared as an article in the Bulletin of Seismological Society of America. The original citation is as follows: Wang, X., and Rathje, E. M. (2016). Influence of Peak Factors on Site Amplification from Random Vibration Theory Based Site-Response Analysis. *Bull. Seism. Soc. Am.* **106(4)** 1733-1746. The analyses in this article were all performed by Wang under the supervision of Dr. Rathje.

[2]Department of Civil, Architectural and Environmental Engineering, The University of Texas, 301 E Dean Keeton Stop C1792, Austin, TX, USA 78712

*Corresponding author. Phone: +1-512-232-3683. E-mail: e.rathje@mail.utexas.edu.

2.1 INTRODUCTION

Local soil conditions play an important role in determining the characteristics of earthquake ground motions. These effects are often quantified numerically via site response analysis. Site response analysis uses seismic wave propagation to compute a surface motion given an input rock motion and a profile of the soil properties. One-dimensional site response analysis is used because in many cases earthquake waves near the ground surface can be considered predominantly vertically propagating, horizontally polarized shear waves. Site response analysis typically specifies the input rock motion as an acceleration-time history and a suite of input time histories are used to account for motion-to-motion variability and to provide a stable estimate of the surface response (Figure 2.1a). The effort to select suites of input time series (TS) for site response analyses can be significant, particularly when considering multiple hazard levels with distinct earthquake scenarios, as well as different oscillator frequencies of importance. As a result, thousands of input motions may be required, which quickly becomes difficult to manage. Also, it may be unrealistic to identify a sufficient number of appropriate input motions for analysis in regions with few earthquake recordings, such as central and eastern North America (CENA).

The random vibration theory (RVT) approach to site response analysis (e.g., Silva et al., 1997; Rathje and Ozbey, 2006; Kottke and Rathje, 2013) is an alternative to the TS approach. Rather than using an acceleration-time history as input, RVT site response analysis uses only the Fourier amplitude spectrum (FAS) and duration of a rock motion as input (Figure 2.1b). Because the FAS includes only amplitudes, but not phase angles, RVT site response analysis cannot be used to obtain the surface acceleration-time history and it cannot be used for nonlinear site response analysis in the time domain. However, the RVT approach can be used with equivalent-linear site response analysis in the

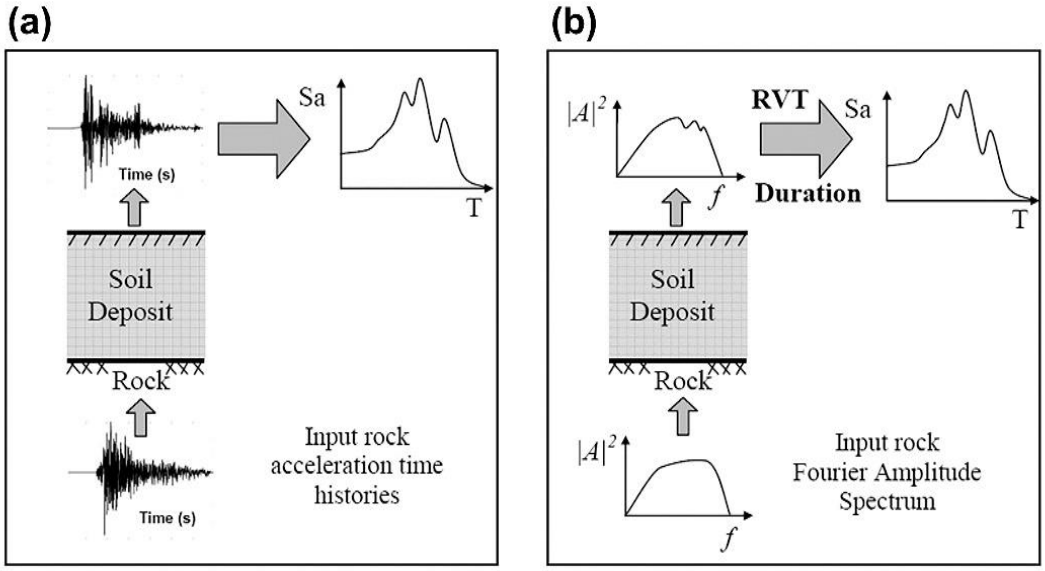

Figure 2.1: (a) Time series (TS) and (b) random vibration theory (RVT) approaches to site response analysis.

frequency domain to calculate peak time-domain parameters of the surface motion, such as peak ground acceleration (PGA), surface acceleration response spectra, and response spectral amplification.

The RVT approach uses Parseval's theorem to compute the root-mean-square (*rms*) acceleration from the FAS and converts this *rms* value to a peak value using a peak-to-*rms* ratio, known as the peak factor. The peak factor is derived from extreme value statistics and can be represented through a probability distribution, with its expected value used in RVT analysis. Researchers have validated the application of RVT in site response analysis (Silva et al., 1997, Rathje and Ozbey, 2006), but more recent comparisons between TS and RVT equivalent-linear site response analysis have shown that RVT analysis may predict amplification at the natural frequencies of a site that are 20 to 50% larger than TS analysis (Kottke and Rathje, 2013). Graizer (2011,

2014) has also questioned the accuracy of the RVT approach to site response analysis and Seifried and Toro (2015) considered some possible improvements to RVT analysis.

This article investigates the influence of different statistical models of the peak factor on the site amplification predicted by RVT based site response analysis. Site amplification results obtained from TS and RVT analyses using different peak factor models are compared. Linear-elastic site response analyses are performed for sites with different natural frequencies subjected to input motions from a large range of earthquake magnitudes in an effort to understand how the natural site frequency, frequency content of the input motion, and duration of shaking influence the results.

2.2 RVT Approach and Peak Factor Models

2.2.1 Parseval's Theorem

The basis of the RVT approach is that the peak of a signal is the product of its *rms* value and an estimated peak factor (*pf*). The *rms* value is computed using Parseval's theorem which states that the integral of the square of a motion in the time domain is equal to the integral of its square in the frequency domain. Applying Parsevel's theorem to an acceleration-time history with a duration D_{rms} to compute the *rms* acceleration (a_{rms}) results in (Boore and Joyner 1984):

$$a_{rms} = \sqrt{\frac{1}{D_{rms}} \int_0^{D_{rms}} |a(t)|^2 dt} = \sqrt{\frac{2}{D_{rms}} \int_0^{\infty} |A(f)|^2 df} = \sqrt{\frac{m_0}{D_{rms}}} \quad (2.1)$$

in which $A(f)$ is the Fourier amplitude at frequency f and m_0 is the zero-th order spectral moment of the FAS. The i-th order spectral moment of the FAS is defined by:

$$m_i = 2\int_0^\infty (2\pi f)^i |A(f)|^2 df \quad (2.2)$$

The first few order spectral moments (e.g., m_0, m_1, m_2, m_4) typically are used as descriptions of the frequency content of a signal (Vanmacke, 1972).

The *rms* duration (D_{rms}) represents the duration of the signal. For an analysis where the goal of the RVT analysis is to predict PGA, D_{rms} is taken as the duration of the ground motion (D_{gm}). When considering the oscillator response where the goal of the RVT analysis is to compute the spectral acceleration (S_a), D_{rms} is larger than D_{gm} because the duration of the signal is increased due to the response of the oscillator (Boore and Joyner, 1984). Boore and Joyner (1984) originally considered simply adding the oscillator decay time to D_{gm}, but found that this approach resulted in excessively long values of D_{rms} for long period oscillators excited by short duration motions. Instead, they developed an empirical D_{rms} model that uses D_{gm} and the oscillator decay time within an empirically derived functional form developed to make RVT predictions of response spectra best match response spectra from stochastic simulations in the time domain. Other empirical D_{rms} models have been proposed over the years (e.g., Liu and Pezeshk, 1999; Boore and Thompson, 2012, 2015).

2.2.2 Extreme Value Statistics: Cartwright and Longuet-Higgins (1956)

Extreme value statistics is used to evaluate the probability distribution associated with the peak factor. The expected value of the peak factor ($\overline{pf}$) is commonly used in RVT analysis and is computed from an assumed probability distribution. Various models for the probability distribution of the peak factor have been proposed (e.g.,

Cartwright and Longuet-Higgins, 1956; Davenport, 1964; Vanmarcke, 1975; Der Kiureghian, 1980).

The Cartwright and Longuet-Higgins (1956) peak factor model has been used most commonly in engineering seismology and site response applications. Following the assumption that the peaks of a signal are independent and follow a Poisson process, Cartwright and Longuet-Higgins (1956) proposed that the expected value of peak factor can be estimated using:

$$\overline{pf} = \sqrt{2}\int_0^\infty \left\{1 - \left[1 - \xi e^{-\eta^2}\right]^{N_e}\right\} d\eta \tag{2.3}$$

in which ξ is the bandwidth factor (Cartwright and Longuet-Higgins, 1956; Boore, 2003) defined as:

$$\xi = \frac{m_2}{\sqrt{m_0 m_4}} = \frac{N_z}{N_e} \tag{2.4}$$

The bandwidth is a function of the zeroth, second, and fourth order spectral moments of the FAS, but also has the physical meaning of representing the ratio of the number of zero-crossings (N_z) to the number of extrema (N_e). N_e and N_z can be computed using (Boore 1983):

$$\mathrm{N}_e = \frac{1}{\pi}\sqrt{\frac{m_4}{m_2}} D_{gm} = 2 \cdot f_e \cdot D_{gm} \tag{2.5}$$

and

$$\mathrm{N}_z = \frac{1}{\pi}\sqrt{\frac{m_2}{m_0}}D_{gm} = 2 \cdot f_z \cdot D_{gm} \tag{2.6}$$

in which f_e and f_z are the rates of extrema and zero-crossings, respectively. Davenport (1964) derived an asymptotic expression that approximates the Cartwright and Longuet-Higgins (CL) *pf* model for large values of N_z. This asymptotic form provides a more convenient calculation of the peak factor for large value of N_z while sacrificing some accuracy. The full integral form of CL peak factor model (equation 2.3) has been incorporated into most RVT procedures in engineering seismology (e.g., Boore 2003) and site response (e.g., Kottke and Rathje 2008), but it fails to take into account the fact that for narrow-band processes peaks tend to occur in clumps and are not independent (Vanmarcke 1975).

2.2.3 Extreme Value Statistics: Vanmarcke (1975)

The estimation of the peak factor can also be considered a first-passage problem. A first-passage problem in the theory of probability (Crandall and Mark 1963) solves for

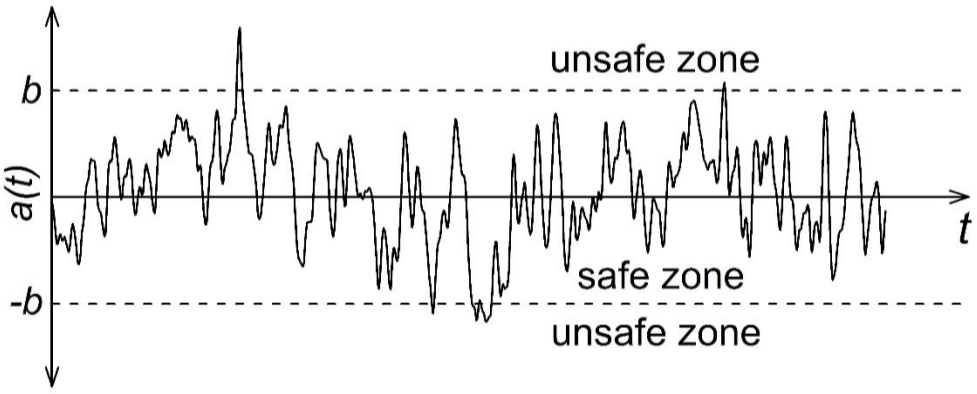

Figure 2.2: Illustration of first-passage problem for a two-sided, D-type barrier (after Crandall et al. 1966)

the probability distribution of the time at which a random signal first passes a specified barrier (i.e., amplitude). A two-sided barrier problem that considers the barrier $a(t) = \pm b$ is relevant for earthquake motions because both positive and negative maxima need to be considered. Figure 2.2 shows an example of a two-sided barrier, often called a D-type barrier (Crandall et al., 1966), with the safe (i.e. $|a(t)| < b$) and unsafe (i.e., $|a(t)| \geq b$) zones indicated. This barrier is commonly normalized by the *rms* value (i.e., $r = b/a_{rms}$, referred to as barrier level) and therefore the parameter *r* represents the peak factor. Assuming that the starting condition is random and stationary (Crandall et al. 1966) and statistical independence of the peaks (i.e., incorporating the Poisson assumption), the probability that there is no crossing of barrier level *r* during the time interval $(0, t)$ is given by:

$$P_{no\ crossing}(t) = Ae^{-\alpha t} \tag{2.7}$$

in which A is the probability of starting below the barrier level (i.e., in the safe zone) and α is the decay rate. Both A and α are functions of the barrier level r, under consideration. The value of A can be expressed as $[1 - \exp(-r^2/2)]$; for large values of r the parameter A is equal to 1.0. For D-type barriers, the parameter α represents twice the average rate of crossings of the barrier level r, and can be taken as $\alpha = 2 \cdot f_z \cdot \exp(-r^2/2)$ (Vanmarcke 1975). Equation 2.7 predicts that the probability of staying below the barrier level decreases with time.

If the time t is specified in equation 2.7 (e.g., $t = D_{gm}$) and *r* is considered the independent variable, equation 2.7 represents the cumulative distribution function (CDF) of the peak factor (i.e., the probability that the value of the peak factor is less than a specific barrier level over a specified time interval). Rearranging equation 2.7

accordingly, the resulting probability that the *pf* is less than the barrier level *r* over a given time *t* is taken as (Crandall et al. 1966):

$$P(pf < r) = [1 - \exp(-r^2/2)] \cdot \exp[-2 \cdot f_z \cdot \exp(-r^2/2) \cdot t] \quad (2.8)$$

where f_z is the rate of zero crossings (Equation 2.6). Equation 2.8 is asymptotically exact when r increases to infinity (Cramer 1966) and it matches with the result derived independently by Davenport (1964).

Vanmarcke (1975) improved the model for the first-passage problem in equation 2.8 to account for the time spent above the barrier level as well as the statistical dependence of peaks. The time spent above the barrier level is important for broad-band processes and low barrier levels (Ditlevsen 1971) and the statistical dependence, or clumping, of peaks is important for narrow-band processes and high barrier levels (Crandall et al. 1966). The resulting CDF of the *pf* provided by Vanmarcke (1975) is:

$$P(pf < r) = [1 - \exp(-r^2/2)] \cdot \exp\left[-2 \cdot f_z \cdot \exp(-r^2/2) \cdot t \cdot \frac{\left(1-e^{-\delta^{1.2} r\sqrt{\pi/2}}\right)}{\left(1-e^{r^2/2}\right)}\right] \quad (2.9)$$

in which δ is a bandwidth factor. Note that δ is different than the bandwidth factor used by CL and δ is defined as (Vanmarcke 1970):

$$\delta = \sqrt{1 - \frac{{m_1}^2}{m_0 m_2}} \quad (2.10)$$

Compared with the Crandall et al. (1966) peak factor model in equation 2.8, the Vanmarcke (1975) model in equation 2.9 includes a multiplier that modifies the decay

rate α. The expected value of the peak factor (i.e. $\overline{pf}$) from the Vanmarcke (1975) model can be obtained from equation 2.9 by integrating $\int_0^\infty [1 - P(pf < r)] \cdot dr$. Der Kiureghian (1980) and Igusa and Der Kiureghian (1985) empirically modified the Davenport (1964) asymptotic $\overline{pf}$ equation to predict values consistent with the expected value of the *pf* from the Vanmarcke (1975) model. The Der Kiureghian models are in general agreement with the Vanmarcke model, but they start to deviate at smaller N_z and should not be used for $N_z < 10$.

2.2.4 Comparisons of Peak Factor Models

The variation of the expected value of the *pf* with the number of zero-crossings (i.e., $N_z = 2 \cdot f_z \cdot t$) is shown in Figure 2.3 for the CL and Vanmarcke peak factor models and for different values of bandwidth. It is important to note that although both the CL and Vanmarcke bandwidth factors (ξ and δ) take on values between zero and one, ξ approaches 1 for a narrow-band process while δ approaches 0 for a narrow-band process. Because of the different definitions of ξ and δ, the results in Figures 2.3a and b cannot be compared directly.

For both the CL and Vanmarcke models, the $\overline{pf}$ increases with increasing N_z because a large peak is more likely to occur when more extrema are sampled. The CL $\overline{pf}$ is only influenced by the bandwidth for N_z less than 20 and the effect is minor (Figure 2.3a). For values of N_z greater than 20, the CL $\overline{pf}$ becomes independent of the bandwidth and is equal to the value provided by the asymptotic model of Davenport (1964). The Vanmarcke $\overline{pf}$ is more sensitive to changes in bandwidth (Figure 2.3b),

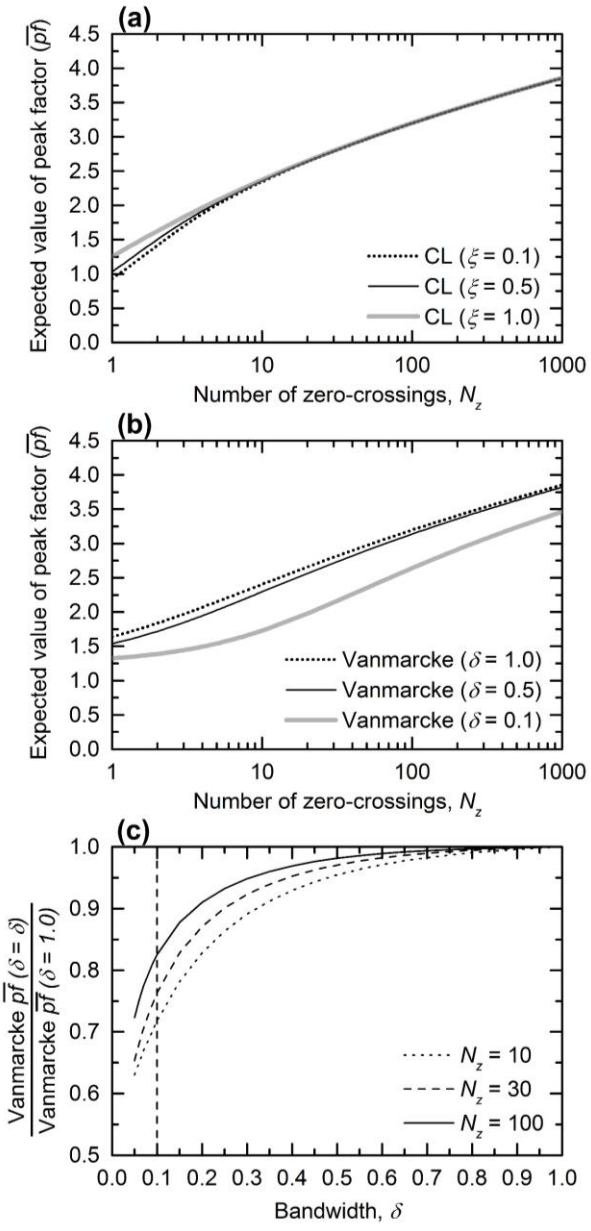

Figure 2.3: (a) Cartwright and Longuet-Higgins (CL) peak factor as a function of the number of zero-crossings (N_z) for different values of bandwidth ξ, (b) Vanmarcke peak factor as a function of N_z for different values of bandwidth δ, and (c) influence of δ on the Vanmarcke peak factor. Bandwidth factors ξ and δ cannot be uniquely related and thus the results in the different panels of this figure cannot be directly compared.

particularly for $\delta < 0.5$ (i.e., narrow-band motions). Figure 2.3c shows the variation of the Vanmarcke $\overline{pf}$ with δ for three different values of N_z. The Vanmarcke $\overline{pf}$ for $\delta = 0.1$ is 20 to 30% smaller than the $\overline{pf}$ for $\delta = 1.0$, depending on the value of N_z. This reduction is due to the effect of clumping of extrema in narrow-band motions. For $\delta \geq 0.5$ (i.e., relatively broad-band motions), the effect of δ on the Vanmarcke $\overline{pf}$ is typically less than 5%. Comparing the Vanmarcke $\overline{pf}$ with the CL $\overline{pf}$, the values are similar for broad-band motions and large N_z. However, the Vanmarcke $\overline{pf}$ is influenced more by bandwidth such that its values are much smaller than the CL $\overline{pf}$ for narrow-band motions.

Because the bandwidth factors ξ and δ are defined differently and cannot be uniquely related, it is not possible to systematically compare the CL and Vanmarcke peak factors without prescribing the frequency content of the signal. Thus, the FAS for an earthquake event is used to define the bandwidth factors and compare directly the CL and Vanmarcke peak factors. The FAS of an earthquake motion for *M* 6.5 and *R* 20 km is defined using a theoretical seismological model (Brune 1970, 1971) for conditions in Central and Eastern North America (CENA) using the parameters from Atkinson and

Table 2.1: Stochastic input parameters used in development of time series input motions using SMSIM

Parameter	**Value**
Source spectrum	Brune ω-squared point source
Stress drop $\Delta\sigma$ (bar)	400
Site diminution κ (s)	0.006
Density of crust ρ (g/cm^3)	2.8
Shear wave velocity of crust β (km/sec)	3.7
Geometrical spreading	Atkinson and Boore (2014)
Path attenuation	Atkinson and Boore (2014)
Crustal amplification	Boore (2014)

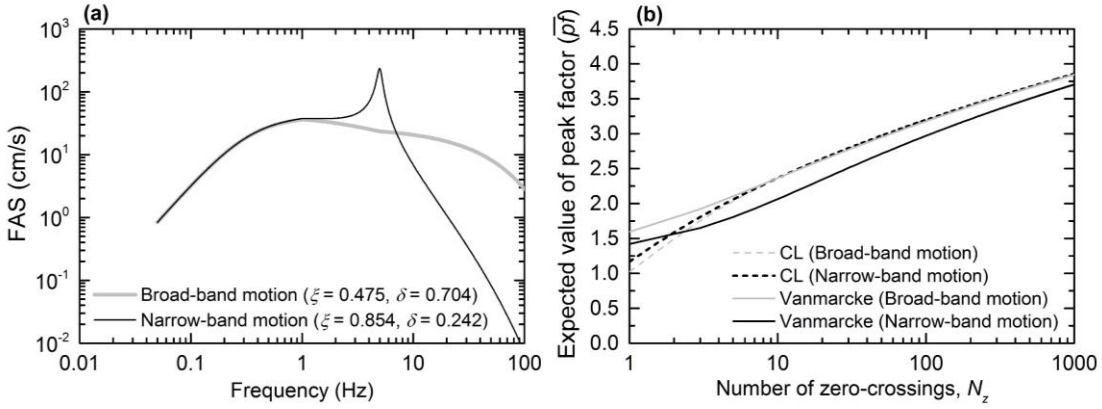

Figure 2.4: (a) Fourier amplitude spectrum (FAS) for a broad-band rock motion and its narrow-band oscillator response. (b) CL and Vanmarcke peak factors as a function of N_z for the broad-band rock motion and narrow-band oscillator response.

Boore (2014) and Boore (2015), as listed in Table 2.1. The rock FAS and its oscillator response for an oscillator frequency of 5 Hz and 5% damping are shown in Figure 2.4a. The ξ and δ for the rock FAS equal 0.475 and 0.704, respectively, indicating a relatively broad-band motion. The FAS of the oscillator response to the rock motion represents a more narrow-band process with larger ξ (i.e., 0.854) and smaller δ (i.e., 0.242). Figure 2.4b shows the CL $\overline{pf}$ and Vanmarcke $\overline{pf}$ for the rock motion and oscillator response as a function of N_z. For the broad-band rock motion the CL and Vanmarcke $\overline{pf}$ are similar, yet for the narrow-band oscillator response the Vanmarcke $\overline{pf}$ is generally about 10% smaller than the CL $\overline{pf}$. This comparison shows that for narrow-band processes, such as the oscillator response of earthquake motions, the Vanmarcke (1975) model predicts a smaller peak factor than CL model because it considers the dependence/clumping between peaks. This effect will be magnified for surface ground motions which have peaks in the FAS associated with the dynamic modes

of the site as well as the oscillator response, and thus using the Vanmarcke $\overline{pf}$ will influence predicted site amplification from RVT.

It is important to note that the D_{rms} models that are used to modify D_{gm} to account for the oscillator duration are linked to a peak factor model because they were developed from empirical comparisons between RVT response spectra and the average response spectra for stochastically generated acceleration-time histories. As noted earlier, Boore and Joyner (1984) provided the first empirical model for D_{rms} (BJ84) and later Boore and Thompson (2012, BT12) proposed an improved D_{rms} model for a wide range of magnitudes, distances, and seismological parameters. Both the BJ84 and BT12 D_{rms} models were developed using the CL peak factor model. However, Boore and Thompson (2015, BT15) recently developed a D_{rms} model using the Vanmarcke peak factor model. The BT15 D_{rms} model is used for the analyses presented here. The influence of site response on the ground motion duration is investigated later in this article.

2.3 ANALYSES PERFORMED

Linear-elastic site response analyses using both the TS and RVT approach are conducted for a range of site conditions and earthquake magnitudes. Hypothetical sites similar to those used by Kottke and Rathje (2013) are used. Each site consists of a single layer soil deposit underlain by a rock half-space. The shear wave velocity and the unit weight of the soil layer are 400 m/s and 18 kN/m^3, respectively, and for the rock layer they are 3,000 m/s and 22 kN/m^3, respectively. The damping ratio for both layers is 1%. Sites 32 m, 100 m and 316 m thick are used to investigate the influence of the

natural site frequency. The corresponding first mode site frequencies are 3.1 Hz, 1.0 Hz, and 0.32 Hz.

Earthquake scenarios for CENA with a fixed distance of 20 km and seven magnitudes between M 5.0 to M 8.0 are considered. CENA motions were considered because of recent work updating seismological parameters and durations for this region through the Next Generation Attenuation (NGA) – East project (Boore 2015). The input motions for the RVT analyses are FAS generated by the program Stochastic-Method SIMulation (SMSIM) (Boore 2005) using a single-corner-frequency source spectrum (Boore 2003) and ground motion durations (D_{gm}) derived from Boore and Thompson (2015). The important seismological parameters describing the shape of the FAS include the stress drop ($\Delta\sigma$) and site diminution (κ). These values, along with the other important seismological parameters used to define the FAS, are summarized in Table 2.1. For each magnitude, the input for the TS analyses is a suite of 100 time series generated by the program SMSIM (Boore 2005) using stochastic simulation (Boore 1983) and the input for the RVT analyses is the same FAS used to develop the stochastic time series. As a result, the average FAS of the time series matches the FAS used in the RVT analysis. Figure 2.5 shows the FAS and the D_{gm} used for the seven magnitude events considered. The corner frequency (f_c), which is the frequency below which the FAS begins to decrease, is also shown in Figure 2.5 for each magnitude. RVT site response analyses are performed using the CL peak factor model coupled with the BT12 D_{rms} model and the Vanmarcke peak factor model coupled with the BT15 D_{rms} model. The different duration models were used because the BT12 D_{rms} model was developed to minimize the difference between TS and RVT rock simulations when using the CL peak factor model, whereas the BT15 D_{rms} model was developed to minimize the differences when using the Vanmarcke peak factor model.

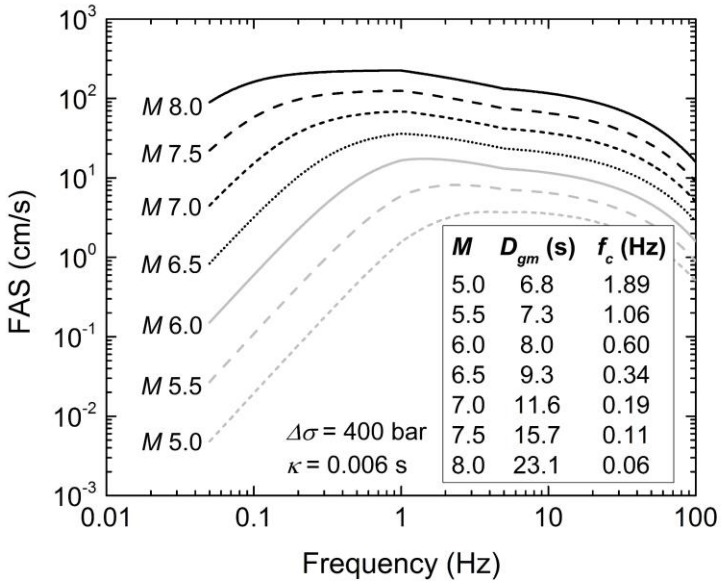

Figure 2.5: FAS, ground motion duration (D_{gm}), and corner frequencies (f_c) for the earthquake scenarios considered in this study for central and eastern North America (CENA).

2.4 SITE AMPLIFICATION RESULTS

The site response results are shown in terms of amplification factor (*AF*), defined as the ratio of the surface spectral acceleration to the rock spectral acceleration at each frequency. For the TS analysis, the median of the results from the 100 input time series is shown. To illustrate the results more clearly, the ratio of the RVT *AF* to the median TS *AF*, labeled RVT/TS, is also shown.

2.4.1 Influence of CL and Vanmarcke Peak Factor Models on RVT-TS Comparison

The RVT and TS site response results for the 32 m and 316 m sites subjected to the M 6.5 earthquake event are shown in Figure 2.6. The RVT results are shown for both the CL and Vanmarcke peak factor models. For the 32 m site, the amplification predicted at the modal frequencies by RVT with the CL peak factor is about 10 to 20% larger than predicted by TS analysis. When using the Vanmarcke peak factor, this difference is essentially removed at the first mode and is less than 10% at all other frequencies. The improvement when using the Vanmarcke peak factor is due to the influence of the bandwidth on the peak factor. At the modal frequencies, the oscillator response becomes narrow-band with δ less than about 0.1 to 0.15 (Figure 2.6c) and for these bandwidth levels the peak factor is significantly reduced (Figure 2.6d) leading to a prediction of less amplification. The reduction in peak factor is most significant for the first mode, and less significant for each higher mode.

For the 316 m site, the RVT analysis using the CL peak factor predicts amplification about 25% – 45% larger than the TS analysis at the modal frequencies (Figures 2.6e, f). When using the Vanmarcke $\overline{pf}$ this difference is reduced to about 15 to 20%. Again, the reason for the improvement is the small bandwidth at these frequencies and the associated reduced peak factor when using the Vanmarcke model. As shown in Figures 2.6g and h, δ is as small as 0.1 to 0.15 at the modal frequencies where significant improvements are observed.

The results in Figure 2.6 show that RVT analysis using the CL peak factor predicts larger site amplification than TS analysis at the modal frequencies, but using the Vanmarcke peak factor in RVT analysis reduces this difference and improves the RVT amplification results. This improvement is due to the influence of the bandwidth on the peak factor. However, the results in Figure 2.6 demonstrate that this improvement is

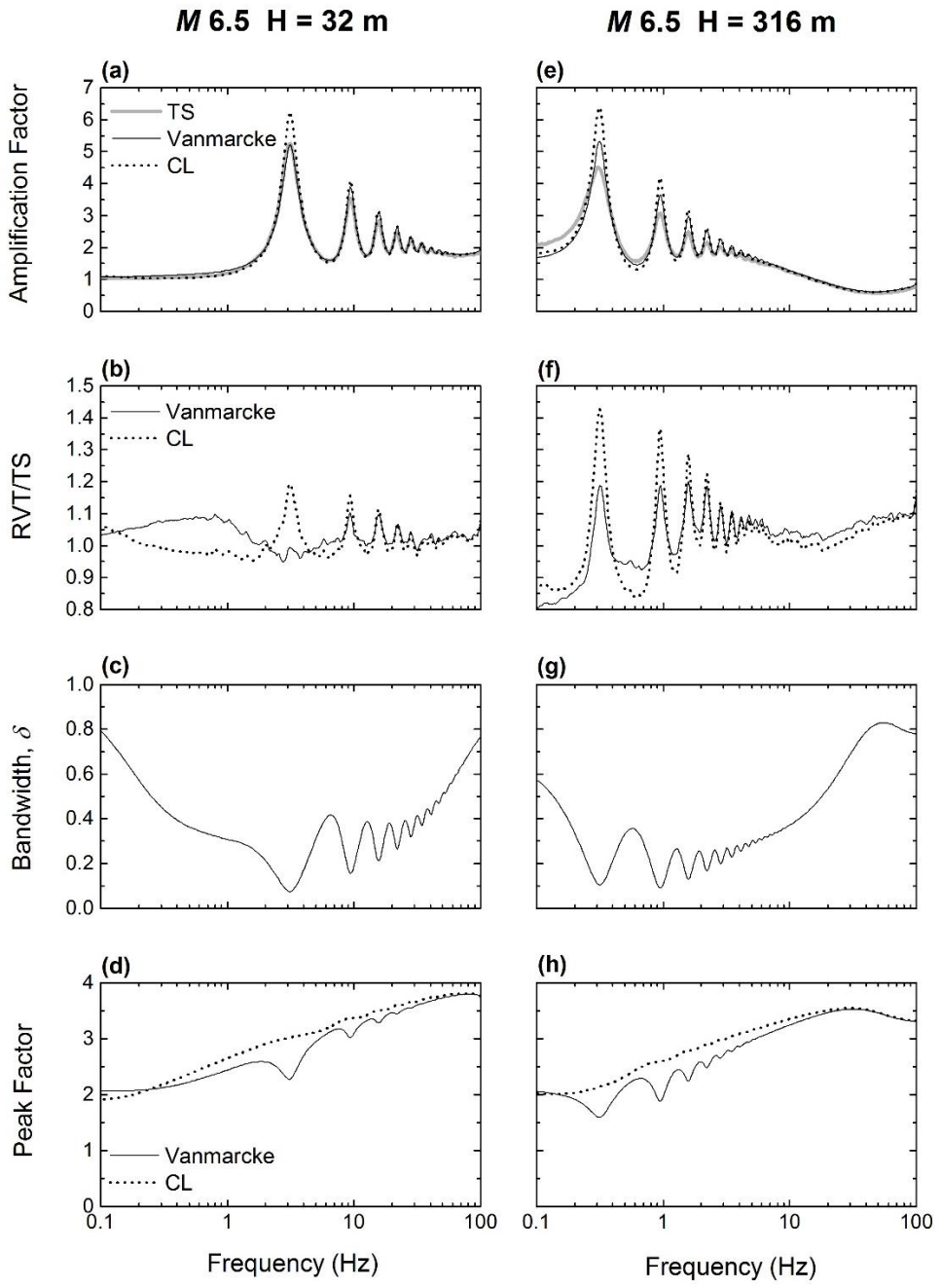

Figure 2.6: RVT and TS site response results for H = 32 m and H = 316 m sites excited by *M* 6.5 earthquake. Amplification factors, ratios of RVT to TS amplification, bandwidth factor δ, and peak factors are plotted as a function of oscillator frequency.

mode-dependent and differs for the two sites shown, with the most favorable comparison observed for the shallow site.

To investigate the influence of earthquake magnitude on the differences between RVT and TS analyses, the site amplification for the 316 m thick site is calculated for *M* 5.0 and *M* 8.0 earthquakes (Figure 2.7). For the *M* 5.0 event, there is a significant difference between the amplification predicted by RVT and TS analysis at the modal frequencies (Figures 2.7a, b). At the first mode, the RVT analysis predicts amplification as much as 60% larger than the TS analysis, and there is no improvement when using the Vanmarcke peak factor. Here, the oscillator response is rather broad-band with δ about 0.5, such that the amplification is not reduced by using the Vanmarcke peak factor. Some improvement is observed at the higher modes because at these modes δ is less than about 0.1 – 0.15, which decreases the RVT amplification at these frequencies when using the Vanmarcke peak factor. For the *M* 8.0 event, there is very good agreement between the site amplification obtained from RVT and TS analyses when using the Vanmarcke peak factor, with the maximum difference being about 15% (Figures 2.7d, e). Improvement when using the Vanmarcke peak factor is greatest at the first mode but less at the higher modes because the bandwidth is not as small for the higher modes (Figure 2.7f). These comparisons indicate that the improvement obtained when using the Vanmarcke peak factor is dependent on the earthquake magnitude, with better improvement in RVT results observed for larger magnitude events. This trend is observed not only for the 316 m site, but also for the 32 m and 100 m sites (results not shown).

Figures 2.6 and 2.7 indicate that RVT site response analyses using the Vanmarcke peak factor generate smaller site amplification than analyses using the CL peak factor, which results in a more favorable agreement between RVT and TS amplification results

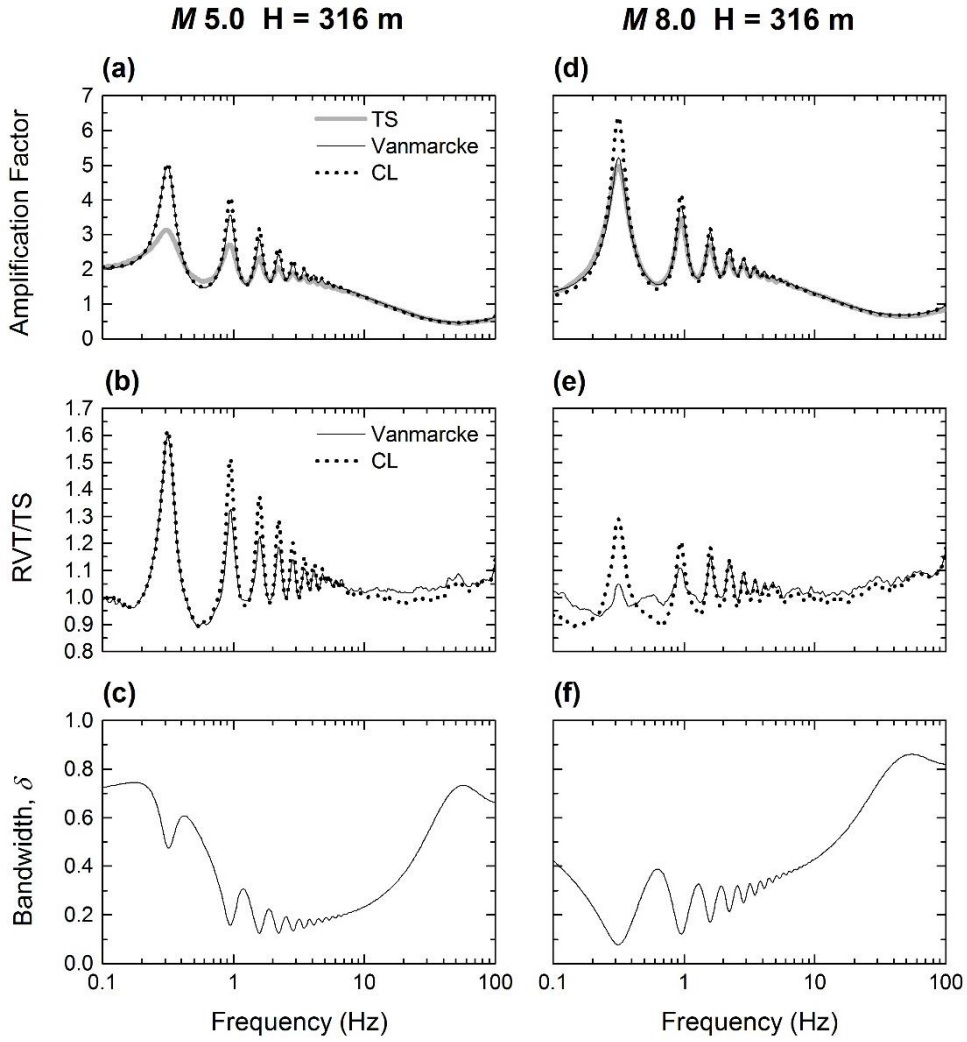

Figure 2.7: RVT and TS site response results for H = 316 m site excited by *M* 5 and *M* 8 earthquake motions. Amplification factors, ratios of RVT to TS amplification, and bandwidth factor δ are plotted as a function of oscillator frequency.

when using the Vanmarcke peak factor. The improvement is the most significant at the first mode, which is of importance because the first mode is the frequency that experiences the largest site amplification. Furthermore, the improvement when using the Vanmarcke peak factor tends to be better for larger earthquakes and shallower sites.

2.4.2 Site and Input Motion Characteristics that Influence RVT-TS Comparison

To better understand the influence of the site conditions and input motion characteristics on the results from RVT and TS analyses, the FAS are considered for three different scenarios of earthquake magnitude and site thickness (Figure 2.8). For each scenario, the rock and surface FAS are shown along with the FAS of the oscillator response corresponding to an oscillator with a natural frequency equal to the first mode site frequency. For the response of the 316 m site subjected to the *M* 8.0 earthquake (Figure 2.8a), where the RVT analysis agree well with TS analysis at the first mode (Figure 2.7b), the bandwidth (δ) is 0.078 indicating a very narrow-band response. This smaller bandwidth leads to a smaller Vanmarcke peak factor and the more favorable comparison with TS analysis, as compared with the CL peak factor. For the response of the same site subjected to the *M* 5.0 earthquake (Figure 2.8b), where the RVT result is not improved at the first mode (Figure 2.7a), δ is 0.484 indicating a broad-band response. The large δ occurs because the first mode frequency (f_{site}) is located on the decaying portion of the rock FAS below the corner frequency (f_c). When $f_{site} < f_c$, the amplitudes of the higher modes are close enough to the amplitude of the first mode such that they contribute more to the bandwidth and the bandwidth becomes larger. For the response of the 32 m site subjected to the *M* 5.0 earthquake (Figure 2.8c), f_{site} is larger than f_c such that the amplitude associated with the first mode dominates the bandwidth and a smaller δ is obtained (δ = 0.073).

The results presented in Figure 2.8 demonstrate that the improvement in site amplification predicted by RVT with the Vanmarcke peak factor is a function of both f_{site} and f_c. The RVT results become more similar to the TS results as f_{site} increases

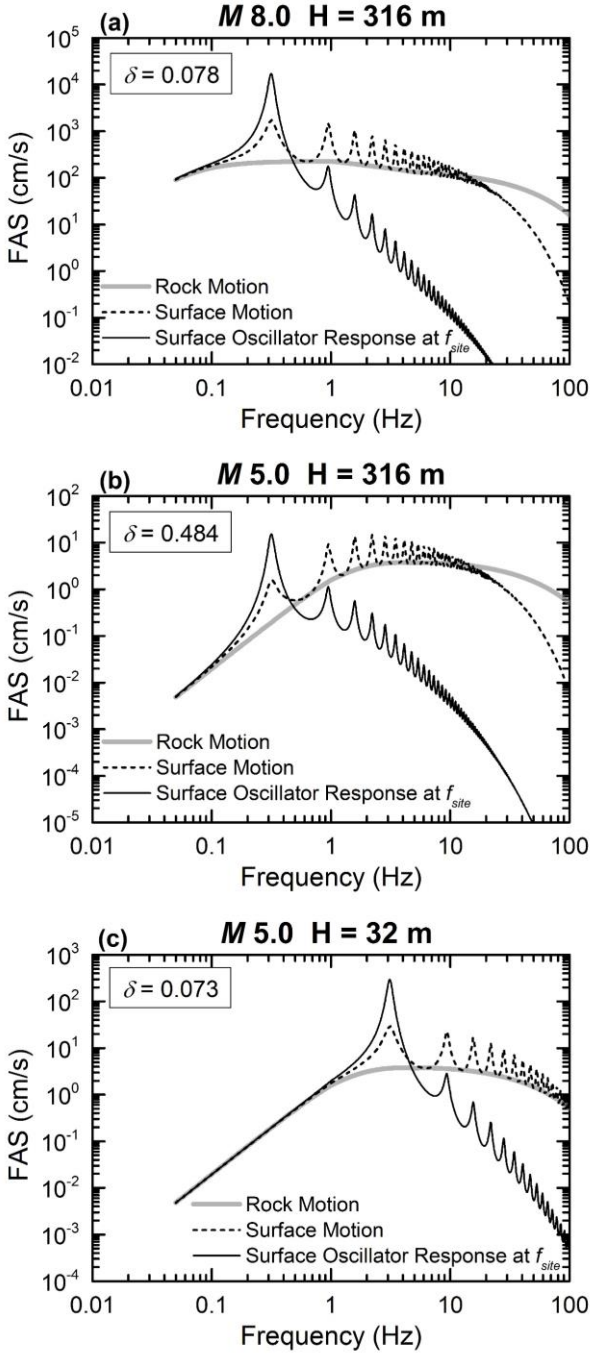

Figure 2.8: Rock FAS, surface FAS, and FAS of the oscillator response of the surface motion for $f = f_{site}$ for three scenarios: (a) M 8.0 and H = 316 m, (b) M 5.0 and H = 316 m, and (c) M 5.0 and H = 32 m.

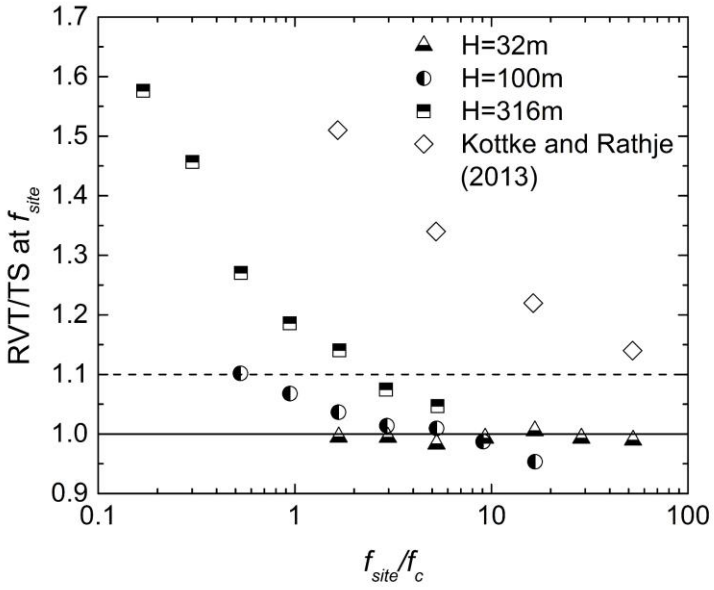

Figure 2.9: Ratio of RVT/TS site amplification at first-mode site frequency as a function of f_{site}/f_c for sites with $V_{s,rock}$ = 3000 m/s and CENA input motions.

and f_c decreases (i.e., magnitude increases). To investigate this relationship quantitatively, the ratio of RVT/TS at the first mode is plotted against the ratio of the first mode site frequency to the corner frequency (f_{site}/f_c) for all three sites (32 m, 100 m, and 316 m) and all seven earthquake magnitudes (Figure 2.9). For each site the ratio of RVT/TS approaches 1.0 as f_{site}/f_c increases, but the values of RVT/TS are different for each site at a common value of f_{site}/f_c. Nonetheless, when f_{site}/f_c is greater than about 2, the RVT *AF* is within +/- 10 % of the TS *AF* for all the scenarios considered. Among all the cases in Figure 2.9, the worst case occurs for the thickest site (i.e. 316 m thick, $f_{site} = 0.32$ Hz) subjected to the smallest earthquake event with the largest corner frequency (i.e. M 5.0, $f_c = 1.89$ Hz). For this case, the RVT prediction of site amplification is almost 60% larger than for TS analysis. Also shown in Figure 2.9 are

results from Kottke and Rathje (2013), which were computed for hypothetical sites similar to those used in this study (i.e., $V_{s,soil} = 400$ m/s, $V_{s,rock} = 3000$ m/s, variable soil thickness), subjected to SMSIM input motions from a *M* 6.5 earthquake, and using the CL peak factor model. The RVT/TS ratios from Kottke and Rathje (2013) are much larger than those from this study for similar values of f_{site}/f_c, which further demonstrates the improvement realized by using the Vanmarcke peak factor.

2.4.3 Influence of Duration on RVT-TS Comparisons

As noted above, scenarios with the same f_{site}/f_c exhibit different values of RVT/TS. For example, the two cases with $f_{site}/f_c \sim 0.5$ (i.e., the 100 m site for the *M* 5.0 event and the 316 m site for the *M* 6.0 event) display values of RVT/TS of 1.1 and 1.3, respectively. Therefore, the effect of bandwidth as indicated by the ratio of f_{site}/f_c cannot fully explain the differences between RVT and TS analyses.

The change in ground motion duration due to site response is an issue that potentially can explain the differences between RVT and TS shown in Figure 2.9. Site response will typically increase the ground motion duration and this effect needs to be taken into account in the a_{rms} calculation (Equation 2.1). A larger D_{rms} in equation 2.1 with the same FAS will result in a smaller a_{rms} and thus smaller spectral acceleration and *AF*. Kottke and Rathje (2013) related the overprediction of site amplification by RVT analysis to changes in duration caused by the site response, although the duration effect did not fully explain the differences they observed. Based on the results presented here, it appears that duration did not fully explain these differences because Kottke and Rathje (2013) used the CL peak factor model which does not accurately model a narrow-band process such as the oscillator response.

To investigate this ground motion duration issue, the duration of the oscillator response for an oscillator with a natural frequency equal to f_{site} was computed for the time series analyses. The duration was calculated as the time between the buildup of 5% and 95% of the Arias Intensity of the oscillator acceleration response ($D_{5-95,osc}$). This definition of duration was used because the $D_{5\text{-}95}$ of the stochastically simulated rock motions was consistent with the specified D_{gm} values for these motions. Figure 2.10a shows the ratio of the duration of the oscillator response for the surface motions ($D_{5-95,osc}^{surface}$) to the duration of the oscillator response for the input rock motion ($D_{5-95,osc}^{input}$) for the three different sites, as a function of the natural site frequency (f_{site}). This ratio is shown for three earthquake magnitudes of 5.0, 6.5, and 8.0. For the shallow 32 m site (f_{site} = 3.13 Hz) the ratio of the durations is close to 1.0 for all three earthquake magnitudes, which indicates that the dynamic response of the site is not changing the duration characteristics of the motions. This similarity in durations is consistent with the RVT/TS values of about 1.0 for the shallow site (Figure 2.9). For the 100 m site (f_{site} = 1.0 Hz) the ratio of the durations is close to 1.0 for the *M* 8.0 event, but is between 1.1 and 1.2 for the *M* 6.5 and *M* 5.0 events, respectively. For these smaller magnitude events, which have shorter durations (Figure 2.5), the response of this deeper site elongates the duration slightly. This modest increase in duration for the smaller magnitude events for the 100 m site is consistent with the RVT/TS values of about 1.0 to 1.1 for the site for f_{site}/f_c less than about 3 in Figure 2.9. Finally, for the 316 m site (f_{site} = 0.32 Hz) there is a considerable increase in duration for the oscillator response of the surface motions. This increase is modest for the *M* 8.0 event (~ 1.15), but it is as large as 1.4 – 1.6 for the smaller magnitude events because the duration of the smaller magnitude events is smaller. Again, this increase in duration is consistent with the RVT/TS values shown in Figure 2.9 for the 316 m site.

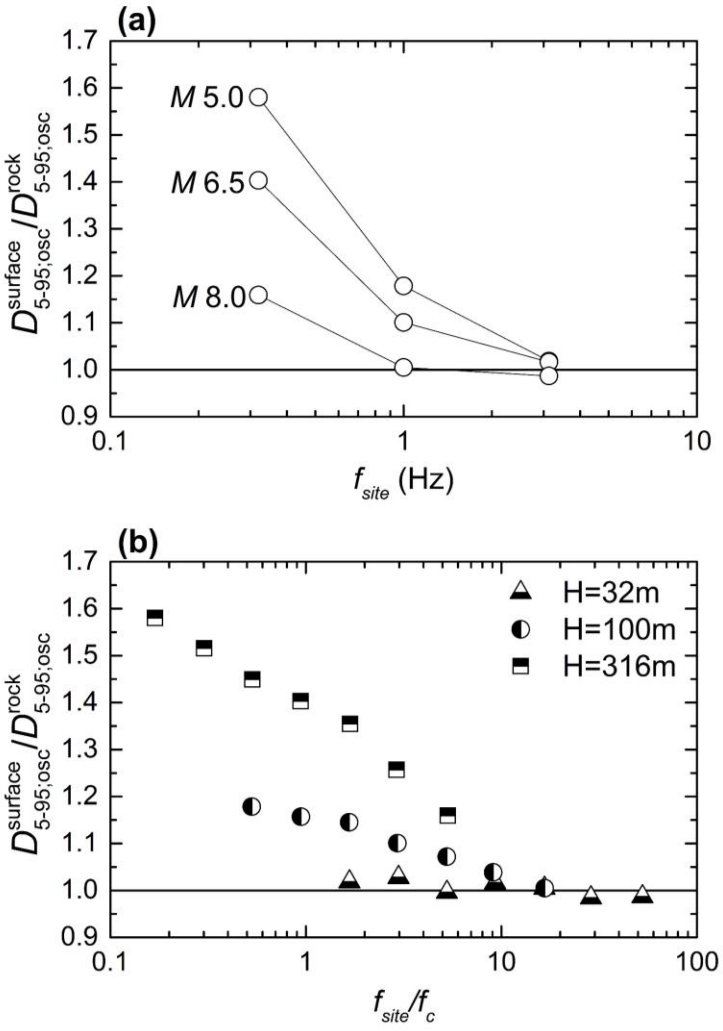

Figure 2.10: (a) The ratio of the duration of the oscillator response for the surface motion ($D^{surface}_{5-95,osc}$) to the duration of the oscillator response for the input rock motion ($D^{rock}_{5-95,osc}$) as a function of f_{site} for three different earthquake magnitudes. The duration increases most for low frequency sites and small magnitude earthquakes. (b) Ratio of $D^{surface}_{5-95,osc}/D^{rock}_{5-95,osc}$ as a function of f_{site}/f_c for all scenarios considered.

Figure 2.10b compiles $D^{surface}_{5-95,osc}/D^{input}_{5-95,osc}$ for all three sites for all of the magnitudes considered in this study and plots them as a function of f_{site}/f_c. The data in Figure 2.10b demonstrate the increasing effect of duration elongation as f_{site}/f_c

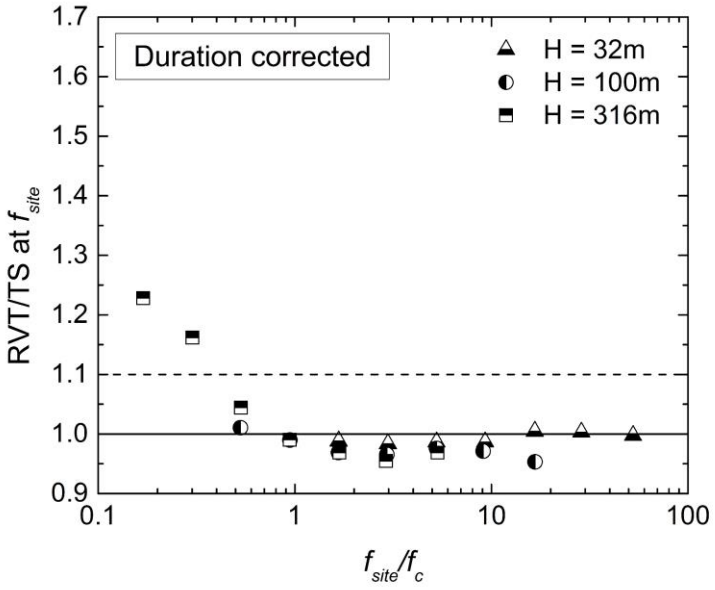

Figure 2.11: Ratio of RVT/TS site amplification at first-mode site frequency as a function of f_{site}/f_c when using duration correction due to site response. Results for sites with $V_{s,rock}$ = 3000 m/s and CENA input motions.

decreases, which is caused by a low frequency site (small f_{site}) being excited by a small magnitude, short duration motion (large f_c). The similarity in the data in Figures 2.10b and 2.9 is notable and an indication that duration elongation due to site response is the driving effect for the differences in RVT and TS analyses.

The changes in duration shown in Figure 2.10 can be used to empirically modify the D_{rms} used in the RVT calculation for the surface S_a. The original D_{rms} used in equation 2.1 is multiplied by the ratios in Figure 2.10b for each magnitude/site combination, which modifies the a_{rms} for the S_a at the surface and the corresponding AF. The ratios of RVT/TS at the natural site frequency when using the corrected durations are shown in Figure 2.11. Using this duration correction brings the RVT results within +/- 5% of the TS results, except for two points that represent the deepest site excited by the

smallest earthquakes of *M* 5.0 and *M* 5.5. For these last two cases, the duration correction reduced that ratio of RVT/TS but the ratio remains noticeably larger than 1.0.

It is important to note that for the empirical duration modification used in Figure 2.11 to be applied broadly to RVT site response analyses, the change in duration due to site response must be known a priori. Currently this change in duration cannot be predicted without performing a suite of site response analyses in the time domain, but empirical models can be developed and this work is currently underway by the authors. Nonetheless, an empirical prediction of the duration at the ground surface likely will not provide as good agreement as shown in Figure 2.11.

2.4.4 Influence of Input Motion Frequency Content on RVT-TS Comparisons

To investigate further the difference between RVT and TS results for the deepest site and the two smallest earthquake magnitudes (i.e., $f_{site}/f_c < 0.5$) after the duration correction is applied (Figure 2.11), additional RVT and TS analyses were conducted for the 316 m site excited by earthquakes of *M* 5.0, *M* 6.5, and *M* 8.0. A duration of 23.1 s is used (i.e., the duration of M 8.0 event) for each event in an effort to isolate the effect of frequency content from the effect of duration elongation. This D_{gm} is large enough that the influence of duration elongation caused by the site will be small and will not significantly affect the RVT results. Figure 2.12 shows the site amplification results for the three magnitudes separately for the TS and the RVT analyses. The TS results across the three earthquake magnitudes are in general agreement with each other (Figure 2.12a), except at the first mode where the amplification for the *M 5.0* event is about 25% smaller than for *M* 6.5 and *M* 8.0 events. Conversely, the RVT site amplification is insensitive to earthquake magnitude (Figure 2.12b).

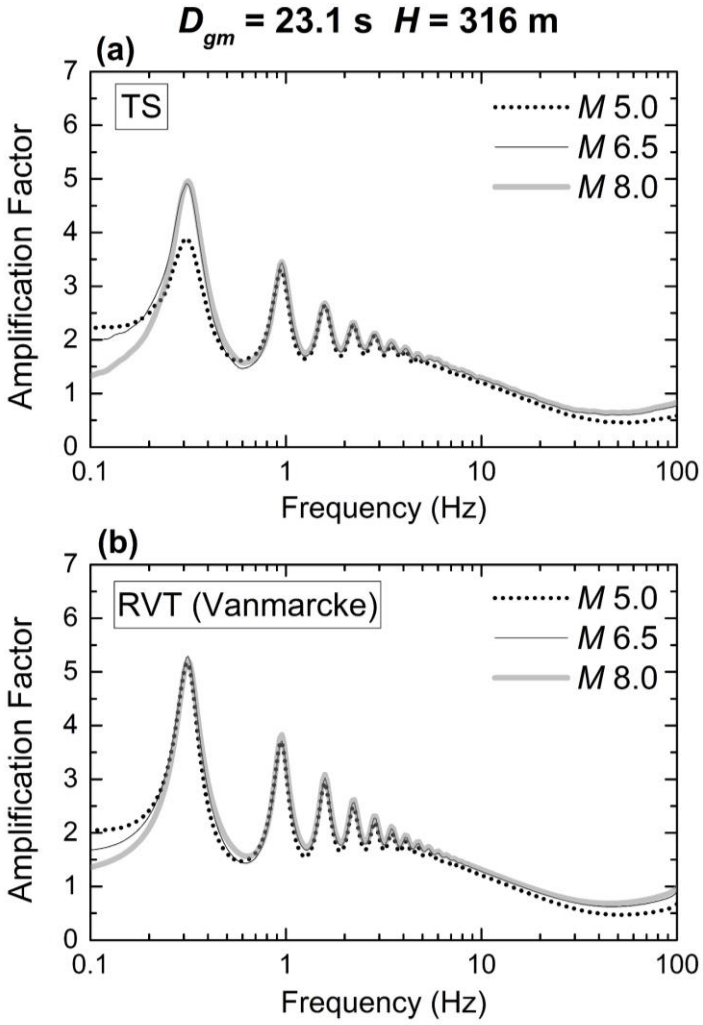

Figure 2.12: Effect of frequency content of input motion, as indicated by earthquake magnitude, on (a) TS and (b) RVT site amplification for H = 316 m site.

These results indicate that the largest values of RVT/TS shown in Figure 2.11 are caused because the RVT analyses cannot accurately capture the effect of the frequency content of the input motion on site amplification for small magnitude earthquakes. When the earthquake magnitude is small, f_{site} for a deep site is located far down the decaying potion of the rock FAS such that the second mode contributes considerably to

the oscillator response (Figure 2.8b). The second mode peak in the FAS results in a larger bandwidth factor ($\delta \sim 0.5$) that represents a more broad-band process. Thus, the bandwidth measurement used in the current peak factor cannot capture the multi-peak spectral shape of the oscillator response when the higher modes contribute significantly to the response.

2.4.5 Influence of $V_{s,rock}$ and Seismological Parameters on the RVT- TS Comparisons

Two additional suites of analyses were performed to investigate: (1) the effect of the shear wave velocity of the rock half space ($V_{s,rock}$) on the RVT-TS comparisons and (2) the effect of the seismological parameters used to develop the input rock motions on the RVT-TS comparisons. Each set of analyses considered the same three sites and seven earthquake magnitudes used in previous analyses and the Vanmracke peak factor.

Analyses were performed with $V_{s,rock}$ = 1,000 m/s and the CENA seismological parameters (Table 2.1), and the RVT/TS values at the first mode are plotted versus f_{site}/f_c in Figure 2.13. The RVT/TS values are shown with and without the empirical duration correction that accounts for the change in duration due to the site response. The shape of the data in Figure 2.13 for $V_{s,rock}$ = 1,000 m/s is similar to that in Figure 2.9 for $V_{s,rock}$ = 3,000 m/s except that the RVT/TS values for $V_{s,rock}$ = 1,000 m/s are much smaller. For the 100 m and 32 m sites, the RVT *AF* is within +/-5% of the TS *AF* (i.e., RVT/TS < 1.05) for all the scenarios considered, even when the duration correction is not included. Even under the most unfavorable cases (i.e., the 316 m site with f_{site}/f_c less than 1.0), the ratio of RVT/TS is less than 1.15 after the duration correction is applied. The more favorable comparison between RVT and TS for $V_{s,rock}$ = 1,000 m/s is due to a smaller amount of duration elongation under these conditions. The smaller $V_{s,rock}$

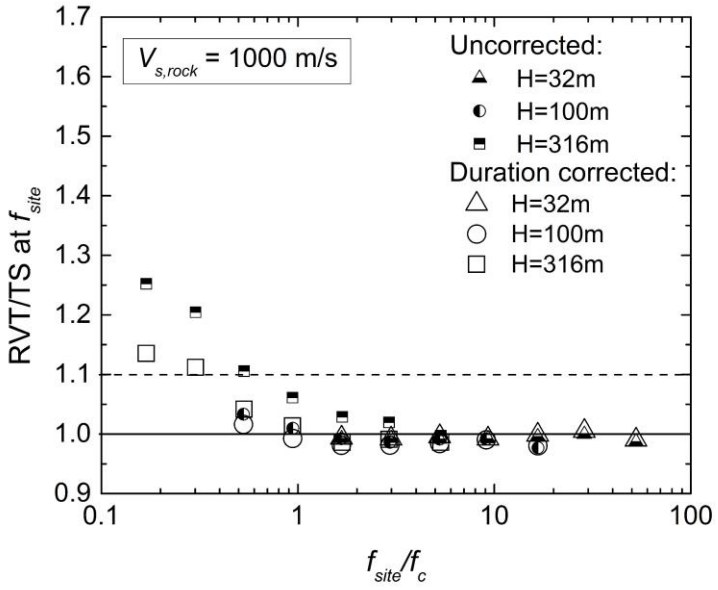

Figure 2.13: Ratio of RVT/TS site amplification at first-mode site frequency as a function of f_{site}/f_c for sites with $V_{s,rock}$ = 1000 m/s and CENA input motions.

produces smaller amplitudes in the site transfer function and allows more motion to escape the soil deposit into the underlying half-space during shaking. As a result, the amplitude of the surface motion decays more quickly after the main portion of the input motion ends, leading to less duration elongation.

The final set of analyses were performed with $V_{s,rock}$ = 1,000 m/s and seismological parameters for Western Northern America (WNA). The parameters for the WNA seismological model and ground motion duration are the same as those used in Kottke and Rathje (2013). The ratio of RVT/TS at the first mode frequency from the analyses using the WNA seismological model are plotted against f_{site}/f_c in Figure 2.14. Again, the RVT/TS values are shown with and without the empirical duration correction that accounts for the change in duration due to the site response. For the 100 m and 32

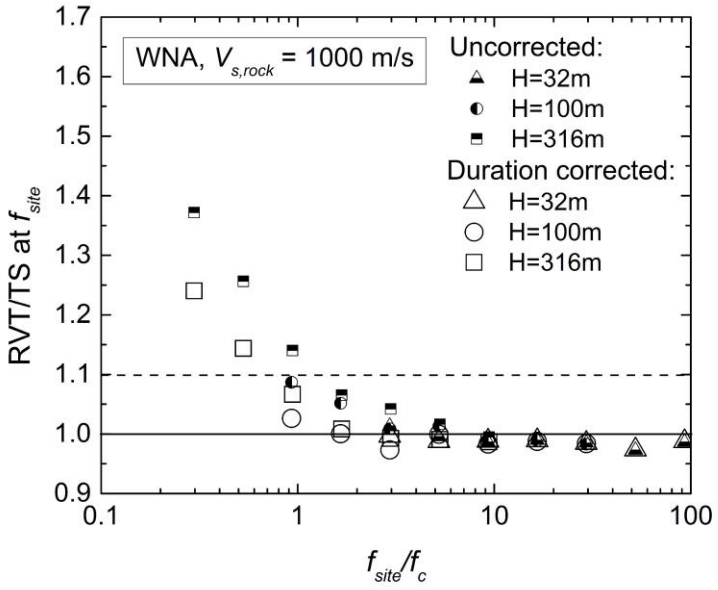

Figure 2.14: Ratio of RVT/TS site amplification at first-mode site frequency as a function of f_{site}/f_c for sites with $V_{s,rock}$ = 1000 m/s and western North America (WNA) input motions.

m sites, the RVT *AF* is within +/-10% of the TS *AF* for all the scenarios considered, even when the duration correction is not included. These values are brought to within +/-5% when the duration correction is included. For the 316 m site, most of the RVT/TS values are less than 1.1 after the duration correction is applied, except for the two points with f_{site}/f_c less than 1.0, which represent earthquake magnitudes of 5.0 and 5.5. The values in Figure 2.14 for WNA are somewhat larger than those in Figure 2.13 for CENA.

The results from this study illustrate that the impedance contrast at the soil/rock interface influences the differences between TS and RVT analyses, with a sharper impedance contrast causing stronger resonances and larger differences between TS and RVT. The site profiles in this study were purposely made simple to better understand the factors influencing the differences between TS and RVT analyses, but the profiles

also have large impedance contrasts which may be unrealistic for some regions, such as parts of western North America. The presence of a shear-wave velocity gradient in the soil as it approaches the rock half-space will likely reduce the differences between TS and RVT analyses.

2.5 DISCUSSION AND CONCLUSIONS

This article describes two different RVT peak factor models and their influence on linear-elastic RVT site response results relative to TS site response analysis. The two peak factor models are the Cartwright and Longuet-Higgins (1956) model (i.e., CL peak factor) and the Vanmarcke (1975) model (i.e, Vanmarcke peak factor). The CL peak factor model has traditionally been used in stochastic ground motion simulations (e.g., Boore 2003) and RVT site response analyses (e.g., Kottke and Rathje 2013), but the Vanmarcke peak factor accounts for the statistical dependence of peaks in a signal, which is important for narrow-band processes such as oscillator responses in seismic analyses.

It is important to note that RVT response spectra for rock conditions generated using either the CL peak factor or the Vanmarcke peak factor do not agree favorably with response spectra from stochastically simulated rock TS when using the ground-motion duration (D_{gm}) in the RVT analysis (Boore and Thompson, 2015). Although the rock FAS have no site resonances, a modified duration (i.e., D_{rms}) is still needed to account for issues related to the change in duration due to the oscillator response. The modified duration is empirically derived and thus depends on the peak factor model used. Thus, it is important to use the D_{rms} model that was developed for the peak factor model being used in the analysis. It is for this reason that, in this study, the Boore and Thompson

(2012) D_{rms} model was used with the CL peak factor, and the Boore and Thompson (2015) D_{rms} model was used with the Vanmarcke peak factor.

The site amplification results presented here show that the *AF* at the modal frequencies of a site predicted by RVT analysis is larger than predicted by TS analysis. The RVT site amplification predicted using the Vanmarcke peak factor is more similar to the TS site amplification than the RVT site amplification predicted using the CL peak factor because the Vanmarcke peak factor model more accurately models the narrow band oscillator response. Specifically, the Vanmarcke peak factor decreases with narrowing bandwidth (i.e., smaller δ), which reduces the surface S_a predicted by RVT and makes the *AF* more similar to the results from TS analysis. Therefore, the Vanmarcke peak factor model is recommended for use in both RVT-based stochastic ground motion simulations (e.g., Boore and Thompson 2015) and RVT site response analyses.

Although the Vanmarcke peak factor predicts RVT site amplification similar to TS analysis, differences remain for some situations. The results presented in this paper show that the overprediction of *AF* by RVT at the first mode frequency of a site is influenced predominantly by the site frequency (f_{site}) and the earthquake magnitude. For a given earthquake magnitude the ratio of RVT/TS increases as f_{site} decreases and for a given f_{site} the ratio of RVT/TS increases with decreasing earthquake magnitude. The larger *AF* predicted by RVT for both of these cases is caused by an increase in ground motion duration that is due to the dynamic response of the site. This longer duration at the ground surface is not taken into account in current implementations of RVT site response analysis and thus the smaller duration that is used in the RVT analysis generates an overestimation of a_{rms} (Equation 2.1) and thus an overprediction of the spectral acceleration and *AF* at the ground surface. This increase in duration is most

significant for low frequency sites and for the short duration input motions associated with small magnitude earthquakes. The combined effects of site frequency and earthquake magnitude on the RVT/TS ratio can be quantified by f_{site}/f_c, where f_c is the corner frequency of the input motion and is magnitude-dependent. When the RVT/TS values are plotted vs. f_{site}/f_c, RVT/TS increases as f_{site}/f_c decreases.

In addition to site frequency and earthquake magnitude, the ratio of RVT/TS is also affected by the shear wave velocity of the rock ($V_{s,rock}$) and the seismological parameters used to model the input ground motions. The ratio of RVT/TS increases as $V_{s,rock}$ increases due to the larger increases in duration that occur as waves are trapped in the sediment layers when the underlying rock half-space is stiffer. For the seismological parameters investigated in this study, the ratio of RVT/TS was larger for WNA parameters than CENA parameters due predominantly to the shorter durations of the WNA input motions.

For all the cases considered, the RVT amplification predicted when using the Vanmarcke *pf* is within +/-10% of the TS values for $f_{site}/f_c \geq 3.0$. When the increased duration of the surface motions are taken into account, the RVT amplification is within +/-10% of the TS values for $f_{site}/f_c \geq 0.5$. The cases with $f_{site}/f_c < 0.5$ represent deeper sites excited by small magnitude earthquakes, which are not commonly design situations that are of engineering interest. If these cases are of interest, the overprediction of *AF* at the first mode site frequency may be between 15% and 25% when the increase in duration is taken into account.

2.6 DATA AND RESOURCES

The stochastic time series used in the analysis were created using the latest version of the Stochastic-Method SIMulation (SMSIM) programs obtained from http://daveboore.com/software_online.html (last accessed November 2015). The time series site response simulations performed in this study were conducted using the program Strata (http://nees.org/resources/strata, last accessed November 2015) and the random vibration theory site response analyses were performed using scripts written in MATLAB (http://www.mathworks.com, last accessed November 2015).

2.7 ACKNOWLEDGEMENTS

This research was supported by funding from Pacific Gas & Electric, Co. through Dr. Norman Abrahamson and the Nuclear Regulatory Commission under grant NRC-HQ-60-15-C-0005. This support is gratefully acknowledged. The research also benefitted from useful discussions with Prof. Armen Der Kiureghian from the University of California at Berkeley, and Prof. Lance Manuel from the University of Texas. We also acknowledge the review comments provided by Dr. Eric Thompson and Dr. David Boore from the U.S. Geological Survey, as well as by an anonymous reviewer.

2.8 REFERENCES

Atkinson, G. M., & Boore, D. M. (2014). The attenuation of Fourier amplitudes for rock sites in eastern North America. *Bull. Seism. Soc. Am.* **104(1)** 513-528.

Boore, D. M. (1983). Stochastic simulation of high-frequency ground motions based on seismological models of the radiated spectra. *Bull. Seism. Soc. Am.* **73(6A)** 1865-1894.

Boore, D. M. (2003). Simulation of ground motion using the stochastic method. *Pure Appl. Geophys.* **160(3-4)** 635-676.

Boore, D. M. (2005). *SMSIM: Fortran programs for simulating ground motions from earthquakes: Version 2.3: A Revision of OFR 96-80-A*. *U.S. Geol. Surv. Dept. Interior*, http://www.daveboore.com/pubs_online/2005_smsim_manual_v2.3.pdf (last accessed May 2005).

Boore, D.M. (2015). *Point-Source Stochastic-Method Simulations of Ground Motions for the PEER NGA-East Project*, Chapter 2 in NGA-East: Median Ground-Motion Models for the Central and Eastern North America Region, PEER Report 2015/04, Pacific Earthquake Engineering Research Center, 11-49.

Boore, D. M., and W. B. Joyner (1984). A note on the use of random vibration theory to predict peak amplitudes of transient signals. *Bull. Seism. Soc. Am.* **74(5)** 2035-2039.

Boore, D. M., and E. M. Thompson (2012). Empirical Improvements for Estimating Earthquake Response Spectra with Random-Vibration Theory. *Bull. Seism. Soc. Am.* **102(2)** 761-772.

Boore, D.M., and E. M. Thompson (2015). Revisions to some parameters used in stochastic-method simulations of ground motion, *Bull. Seism. Soc. Am.* **105(2A)** 1029-1041.

Brune, J. N. (1970). Tectonic stress and the spectra of seismic shear waves from earthquakes. *J. Geophys. Res.* **75(26)** 4997-5009.

Brune, J. N. (1971). Correction. *J. Geophys. Res.* **76(20)** 5002.

Cartwright, D. E., and M. S. Longuet-Higgins (1956). The statistical distribution of the maxima of a random function. *Proc. Roy. Soc. Lond. Math. Phys. Sci.* **237(1209)** 212-232.

Cramér, H. (1966). On the intersections between the trajectories of a normal stationary stochastic process and a high level, *Arkiv för Matematik* **6(4)** 337-349.

Crandall, S. H., and W. D. Mark (1963). *Random Vibration in Mechanical Systems*, Academic Press, New York, 107.

Crandall, S. H., K. L. Chandiramani, and R. G. Cook (1966). Some first-passage problems in random vibration. *J. Appl. Mech.* **33(3)** 532-538.

Davenport, A. G. (1964). Note on the distribution of the largest value of a random function with application to gust loading. *ICE Proceedings* **28(2)** 187-196.

Der Kiureghian, A. (1980). Structural response to stationary excitation. *J. Eng. Mech. Div.* **106(6)** 1195-1213.

Ditlevsen, O. (1971). Extremes and First Passage Times with Applications in Civil Engineering. Thesis, Technical University of Denmark, Copenhagen.

Graizer, V. (2011). Treasure Island geotechnical array: Case study for site response analysis, *Proc. of the 4th IASPEI/IAEE International Symposium: Effect of Surface Geology on Seismic Motion*, University of California Santa Barbara, 23–26 August 2011.

Graizer, V. (2014). Comment on "Comparison of time series and random-vibration theory site-response methods" by Albert R. Kottke and Ellen M. Rathje. *Bull. Seism. Soc. Am.* **104(1)** 540-546.

Igusa, T., and A. D. Kiureghian (1985). Generation of floor response spectra including oscillator-structure interaction. *Earthquake Eng. Struct. Dynam.* **13(5)** 661-676.

Kottke, A. R., and E. M. Rathje (2008). *Technical manual for Strata*. University of California, Berkeley.

Kottke, A. R., and E. M. Rathje (2013). Comparison of Time Series and Random-Vibration Theory Site-Response Methods. *Bull. Seism. Soc. Am.* **103(3)** 2111-2127.

Liu, L., and S. Pezeshk (1999). An improvement on the estimation of pseudoresponse spectral velocity using RVT method. *Bull. Seism. Soc. Am.* **89(5)** 1384-1389.

Rathje, E. M., and M. C. Ozbey (2006). Site-specific validation of random vibration theory-based seismic site response analysis. *J. Geotech. Geoenviron. Eng.* **132(7)** 911-922.

Seifried, A., and G. Toro (2015). Improved estimation of site response using random vibration theory, SSA Annual Meeting, *Seismol. Res. Lett.* **86(2B)** 716-717.

Silva, W. J., N. Abrahamson, G. Toro, and C. Costantino (1997). *Description and validation of the stochastic ground motion model*. Submitted to Brookhaven National Laboratory, Associated Universities, Inc. Upton, New York.

Vanmarcke, E. H. (1970). Parameters of the spectral density function: Their significance in the time and frequency domains*, Department of Civil Engineering, M.I.T. Research Report No. R70-58.*

Vanmarcke, E. H. (1972). Properties of spectral moments with applications to random vibration. *J. Eng. Mech. Div.* **98(2)** 425-446.

Vanmarcke, E. H. (1975). On the distribution of the first-passage time for normal stationary random processes. *J. Appl. Mech.* **42(1)** 215-220.

Chapter 3: Development of Ground Motion Duration Models for Use in Random Vibration Theory Site Response Analysis

Xiaoyue Wang[3], Ellen M. Rathje[3]*

Abstract

Random vibration theory (RVT) site response analysis is an attractive alternative to time series (TS) analysis because it does not require input acceleration-time histories. A critical part of the RVT approach is computing the root-mean-square (*rms*) of the oscillator response from the Fourier Amplitude Spectrum and the key to this computation is the duration of the oscillator response. Various studies have developed models that predict the appropriate *rms* duration (D_{rms}) for RVT analysis. However, these models fail to consider the influence of the dynamic site response on the duration of the oscillator response. Using the D_{rms} from these models to compute the RVT surface response spectra results in larger site amplification predictions from RVT relative to TS analysis. This paper investigates the influence of site response on the duration of oscillator responses for use in RVT site response analysis. Using the results from TS analysis, an empirical model is developed that predicts the modification of D_{rms} due to site response as a function of various properties of the site. The modified D_{rms} generally results in RVT site response predictions at the site modal frequencies within +/-10% of the TS values.

[3]Department of Civil, Architectural and Environmental Engineering, The University of Texas, 301 E Dean Keeton Stop C1792, Austin, TX, USA 78712
*Corresponding author. Phone: +1-512-232-3683. E-mail: e.rathje@mail.utexas.edu.

3.1 INTRODUCTION

Random Vibration Theory (RVT) site response analysis is widely used as an alternative to time series (TS) site response analysis. Unlike TS analysis, which requires the specification of input acceleration-time histories to drive the dynamic response, RVT site response analysis uses only the Fourier Amplitude Spectrum (FAS) and the duration of motion as input. Thus, the RVT approach eliminates the effort to select the input time series, which is an attractive feature when performing probabilistic site response analyses where multiple hazard levels and earthquake scenarios are considered, or in tectonic regions where insufficient earthquake recordings are available. As a result, the use of RVT site response analysis has become standard in seismic hazard studies for nuclear facilities (Regulatory Guide 1.208; Nuclear Regulatory Commission [NRC] 2007).

A critical part of the RVT approach is computing the root-mean-square (*rms*) of the oscillator response from the Fourier Amplitude Spectrum and the key to this computation is the duration of the oscillator response. Various studies have developed models that predict the appropriate *rms* duration (D_{rms}) for RVT analysis (e.g., Boore and Thompson 2015). However, these models fail to consider the influence of the dynamic site response on the duration the oscillator response. Using the D_{rms} from these models to compute the RVT surface response spectra results in larger site amplification predictions from RVT relative to TS analysis (Wang and Rathje 2016). This paper investigates the influence of site response on the duration of oscillator responses for use in RVT site response analysis.

3.2 RVT Site Response Analysis

The details of RVT as applied to earthquake ground motion simulation and site response analysis can be found elsewhere (e.g., Boore 2003, Kottke and Rathje 2013, Wang and Rathje 2016), but the general framework is provided here.

The RVT approach is based on the theory that the peak of a signal can be estimated as the product of its root-mean-square (*rms*) value and an estimated peak factor (*pf*). Parseval's theorem is used to compute the *rms* acceleration (a_{rms}) of an acceleration-time history with a duration D_{rms} from its FAS (Boore and Joyner 1984):

$$a_{rms} = \sqrt{\frac{1}{D_{rms}} \int_0^{D_{rms}} |a(t)|^2 dt} = \sqrt{\frac{2}{D_{rms}} \int_0^{\infty} |FAS(f)|^2 df} \tag{3.1}$$

When using RVT to predict peak ground acceleration (PGA), D_{rms} is equal to the ground motion duration (D_{gm}). When RVT analysis is used to predict the spectral acceleration (S_a), D_{rms} is larger than D_{gm} because the signal is lengthened due to the response of the oscillator (Boore and Joyner 1984).

Many researchers have proposed peak factor models based on extreme value statistics to describe the probability distribution of the peak factor. In engineering seismology and site response applications, the Cartwright and Longuet-Higgins (1956) peak factor model has been the most commonly used, yet it was developed following an over-simplified assumption that the peaks of a signal are independent and follow a Poisson process. Wang and Rathje (2016) showed that by accounting for the statistical dependence between peaks of a signal, the Vanmarcke (1975) peak factor model is superior to the Cartwright and Longuet-Higgins (1956) model when applied to site response analysis. More recently, some researchers in engineering seismology have

moved towards using the Vanmarcke (1975) peak factor model in ground motion simulations (e.g., Boore and Thompson 2015).

The application of the RVT approach to site response analysis has been evaluated by various researchers through comparisons with TS site response analyses. Kottke and Rathje (2013) revealed that RVT analysis using the Cartwright and Longuet-Higgins (1956) peak factor may predict site amplification at the natural frequencies of a site 20 ~ 50 % larger than the amplification given by TS analysis, and noted that the larger amplification is related to the fact that RVT site response analysis does not account for the increase in ground motion duration due to site response. More recently, Wang and Rathje (2016) showed that the difference between the site amplification predicted using RVT and TS analyses can be improved if the Vanmarcke (1975) peak factor model is used instead of the Cartwright and Longuet-Higgins (1956) model. The Vanmarcke peak factor provides better estimates of site response because it considers the statistical dependence between peaks, which is important for narrow-band processes such as associated with site response and oscillator responses.

Wang and Rathje (2016) also demonstrated that if the increase in ground motion duration due to the dynamic response of the site is taken into account in the prediction of surface response, the difference between RVT and TS amplification is further reduced. Figure 3.1 shows results from Wang and Rathje (2016), where the ratio of RVT to TS amplification at the natural frequency of the site (i.e. the frequency of the first mode) is plotted against the ratio of the first mode site frequency to the corner frequency of the input motion (f_{site}/f_c). Results are shown for three sites with different soil thicknesses, each subjected to earthquake magnitudes ranging from 5.0 to 8.0. Figure 3.1 shows separately the RVT/TS results using the D_{rms} of the input ground motion and the RVT/TS results computed using a modified duration that accounts for the increase in

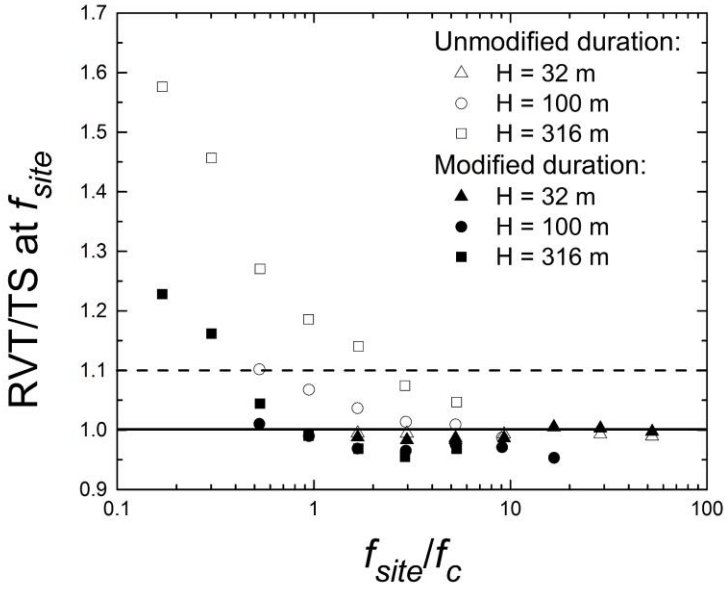

Figure 3.1: Ratio of RVT/TS site amplification at first mode site frequency as a function of f_{site}/f_c for a range of earthquake magnitudes (data from Wang and Rathje 2016).

ground motion duration at the surface. Figure 3.1 clearly shows that the RVT analysis with the duration modified for site response effects provides RVT/TS ratios that are generally close to 1.0. This result demonstrates that incorporating the effects of site response on duration can improve the prediction of RVT amplification and reduce the discrepancy between RVT and TS site amplification.

The modification of duration used by Wang and Rathje (2016) was directly computed from the surface acceleration-time histories computed by the TS site response analyses. However, an important advantage of RVT site response analysis is that it does not require the use of time series. Thus, to apply a duration modification to RVT, the development of a duration model is necessary such that the effect of site response on duration can be predicted without performing any TS analysis. This paper investigates

the change of ground motion duration due to one-dimensional site response. Stochastically simulated time series motions are used as input and sites with different characteristics (e.g., different natural frequencies, different half-space velocities) are considered. Each site is subjected to input motions representing a wide range of earthquake magnitudes and multiple distances. These cases are investigated in an effort to understand the effects of natural site frequency, site transfer function, and earthquake magnitude/distance on the change in ground motion due to site response. Based on the simulation results, a model is developed that empirically predicts the change of duration at the ground surface due to site response.

3.3 DURATIONS USED IN RVT ANALYSIS

3.3.1 *RMS* Duration

In RVT analysis, the prediction of S_a needs an accurate estimation of a_{rms} (equation 3.1) which requires an accurate estimate of the duration D_{rms}. When the a_{rms} of the ground motion is of concern in the analysis, D_{rms} is taken as the duration of the ground motion (D_{gm}). As a result, D_{gm} is used for RVT analysis when predicting PGA. However, when using RVT analysis to predict S_a, the a_{rms} of the oscillator response is of concern. In this case, D_{rms} should be taken so that it represents the duration of the oscillator response. The concept that D_{rms} may not be equal to D_{gm} was first proposed by Boore and Joyner (1984), who noted that D_{rms} is greater than D_{gm} for oscillator responses because the oscillation continues to exist after the earthquake excitation ends. Boore and Joyner (1984) developed a model that estimates D_{rms} as a function of D_{gm}, the oscillator decay time, and the oscillator natural period. This model was empirically developed not based on direct measurement of oscillator response

durations, but rather based on D_{rms} values that would produce RVT predictions of response spectra consistent with those from time domain stochastic simulations.

Boore and Thompson (2012) proposed a new model for D_{rms} that was developed in a similar manner as Boore and Joyner (1984) but consisted of a more complex functional form that better models the D_{rms} values over a broad range of oscillator frequencies. The Boore and Thompson (2012) model coefficients vary with earthquake magnitude, distance, and for different seismological conditions (i.e., western vs. central and eastern North America). Compared with the Boore and Joyner (1984) D_{rms} model (BJ84), the Boore and Thompson (2012) D_{rms} model (BT12) produces RVT predictions of response spectra more consistent with those from time series stochastic simulations over a wider range of magnitudes, distances, and seismological conditions.

Because D_{rms} models are developed from empirical comparisons between RVT response spectra and the average response spectra from time domain stochastic simulations, they are directly linked to the peak factor model used in the RVT analysis. The BJ84 and BT12 D_{rms} models were both developed using the Cartwright and Longuet-Higgins (1956) peak factor model and thus are only valid for analyses that use the Cartwright and Longuet-Higgins (1956) peak factor model. Recently, Boore and Thomson (2015) developed a D_{rms} model (BT15) based on RVT analyses using the Vanmarcke (1975) peak factor model. The functional form of the BT15 D_{rms} model is the same as in the BT12 model, but the coefficients are different.

3.3.2 Effect of Site Response on Ground Motion Durations

The previous studies on duration have focused only on broad-band rock motions and the influence of the oscillator response on the ground motion or oscillator response

duration. Site response will also change the ground motion and oscillator response duration, but in specific ways related to the site-specific characteristics of the soil deposit. Figure 3.2 provides an example of the effect of site response on ground motion and oscillator response durations using a stochastically simulated input rock motion. The site for this analysis is 316 m thick with a shear wave velocity of 400 m/s (f_{site} ~ 0.32 Hz) and the underlying rock half-space has a shear wave velocity of 3,000 m/s. The rock motion was generated using SMSIM (Boore 2005) for a *M* 6.5 earthquake and a distance of 5 km with the D_{gm} specified as 9.3 s. Shown in Figure 3.2 are the rock and surface motion times series, as well as the oscillator responses (with 5% damping) for the surface and rock motions for select natural frequencies. For each acceleration-time history the computed significant duration (D_{5-95}, computed from the time between 5% and 95% of the Arias Intensity of the motion) is provided.

The rock motion is shown in Figure 3.2a and the D_{5-95} of the motion is the same as the specified D_{gm} of 9.3 s. The oscillator responses for the rock motion for oscillator frequencies (f_{osc}) of 0.95 Hz, 0.32 Hz, and 0.1 Hz are shown in Figures 3.2b to 3.2d. The D_{5-95} durations of the oscillator responses are 10.7 s, 18.6 s, and 44.2 s, respectively, for these oscillator frequencies. These durations are longer than the duration of the original rock motion because of the oscillator response and its free vibration decay after the rock motion excitation stops. The increase in the duration becomes more significant as the oscillator frequency decreases. Comparing the surface motion with the rock motion in Figure 3.2, it is observed that the frequency content of the motion is changed due to site response and the duration of the motion increases slightly

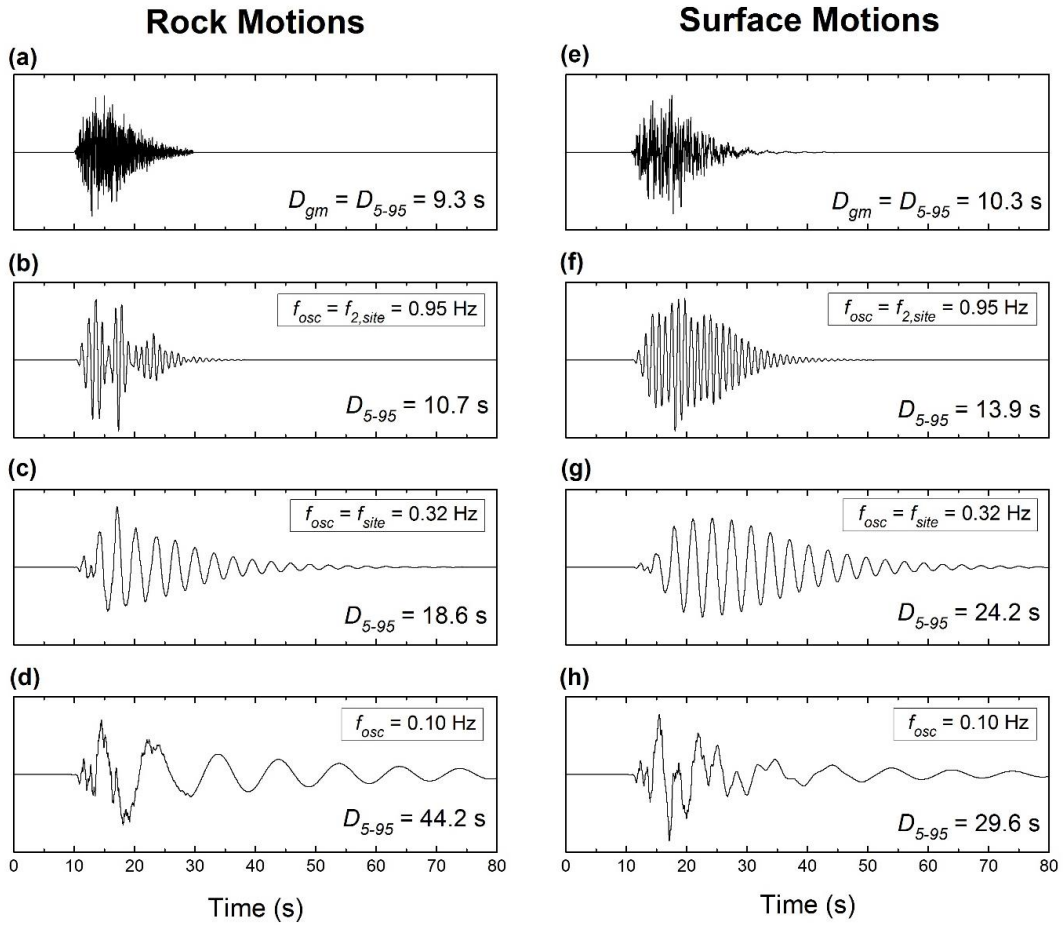

Figure 3.2: Acceleration-time histories of rock and surface motions, as well as the oscillator responses for these motions for different oscillator frequencies.

from 9.3 s to 10.3 s. However, the difference between the D_{5-95} of the oscillator responses for the rock and surface motions are more significant. At f_{osc} = 0.95 Hz the duration of the oscillator response is 3.2 s longer for the surface motion than for the rock motion and at f_{osc} = 0.32 Hz the increase in duration is 5.6 s. These larger increases are due to the site response being concentrated at these frequencies, as these frequencies represent the second and first mode frequencies, respectively, of the site. The enhanced response at these frequencies results in a stronger vibration beyond the duration of

excitation, which contributes to a longer duration. Interestingly, at f_{osc} = 0.10 Hz, an oscillator frequency less than f_{site}, the duration of the oscillator response decreases from 44.2 s to 29.6 s for the surface motion. This shortening of the oscillator response duration at the surface for a low frequency oscillator may be explained by the destructive interference between the vibration at the oscillator frequency and the vibration at the modal frequency of the site, which reduces the free vibration decay portion of the response (Figures 3.2h).

As shown in Figure 3.2, despite the similarity in the durations of the rock and surface motions, the duration of oscillator responses to the rock and surface motions can be quite different. The change in the duration of the oscillator response is due to the (generally) constructive interference between the dynamic response of the site at the modal frequencies and the dynamic response of the oscillator at the same frequency. These results suggest that the duration used for the RVT calculation of the rock response spectrum should not be used for the RVT calculation of the surface response spectrum. Instead, a different value of duration is needed for the estimation of surface response in RVT site response analysis.

It is important to note that the existing empirical D_{rms} models (e.g., BT15) were all developed to match RVT response spectra with the average response spectra obtained from a set of stochastically simulated acceleration-time series for rock site conditions. These D_{rms} values can provide RVT response spectra that better match time domain response spectra, yet they do not represent any physical characteristic of an actual oscillator response. To assess the difference between predicted D_{rms} values and those based on oscillator responses, the average D_{5-95} obtained from a group of stochastically generated time series are compared with the predicted D_{rms} values for three different D_{rms} models. Figure 3.3 plots the D_{rms} and D_{5-95} values as a function of oscillator

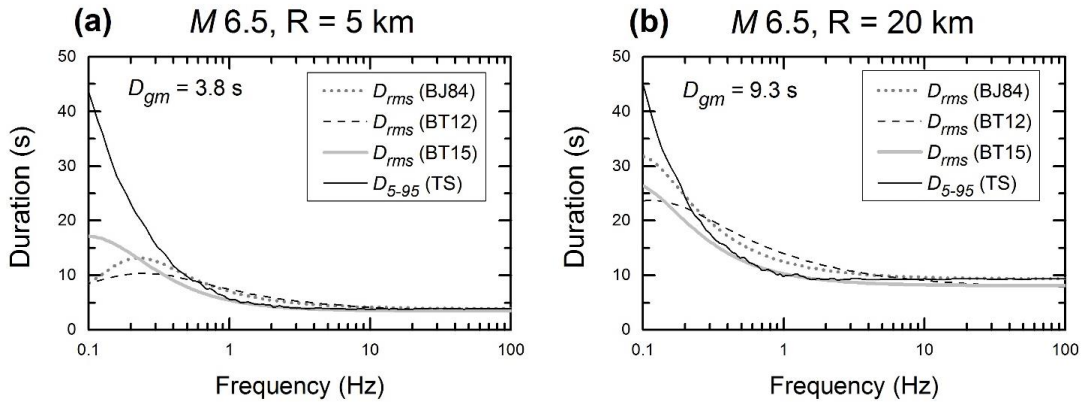

Figure 3.3: Average significant duration (D_{5-95}) of oscillator responses for time-domain, stochastically-simulated rock motions and *rms* durations (D_{rms}) from different empirical models.

frequency for two magnitude/distance scenarios. The D_{5-95} from the time series increases as the oscillator frequency decreases, with most of the increase occurring at frequencies less than 1.0 Hz. This trend is consistent with what the results show in Figure 3.2. At frequencies greater than about 1.0 Hz, the values of D_{5-95} stabilize to the D_{gm} values because the high frequency oscillator response is damped too quickly to affect the duration of the motion. The D_{rms} models predict significantly different values of duration, particularly for frequencies less than about 0.5 to 1.0 Hz. For instance, when the oscillator frequency is 0.2 Hz the D_{rms} models predict durations 5 to 15 s smaller than the observed D_{5-95} for the two earthquake scenarios shown. The difference is more significant for the scenario with the smaller D_{gm} (Figure 3.3a) and the BT15 D_{rms} predicts values closest to the observed D_{5-95}.

It is clear from Figure 3.2 that site response changes the duration of the oscillator response. However, the differences between the measured D_{5-95} and the empirical D_{rms} models (Figure 3.3) indicate that simply using the measured D_{5-95} in an RVT

analysis will not generate response spectra that are consistent with time series response spectra (recall that the D_{rms} models were developed to ensure RVT response spectra are consistent with TS response spectra). Thus, the approach taken here is to investigate how site response changes the D_{5-95} of the oscillator responses, develop a model to predict this change in D_{5-95}, and use this change in D_{5-95} to modify the D_{rms} values predicted for the rock motion to account for the site response.

3.4 ANALYSES PERFORMED

To investigate the influence of site response on the duration of oscillator responses, a large suite of site response analyses are performed using time domain input motions. The time domain input motions are stochastically generated for a range of magnitudes and distances, and are used as input into linear-elastic, time-domain site response analyses for a range of sites with different site characteristics. The D_{5-95} of the oscillator responses for the input rock motions and the computed surface motions are used to investigate the change in oscillator response duration due to site response.

3.4.1 Input Ground Motions

The input ground motion acceleration-time histories were generated by the program SMSIM (Boore 2005) using stochastic simulation (Boore 1983). For the stochastic simulation, the FAS was generated using a single corner frequency source spectrum (Boore 2003) and the ground motion duration (D_{gm}) was specified from Boore and Thompson (2015). A summary of the seismological parameters used in the stochastic simulations, including the stress drop ($\Delta\sigma$) and site diminution (κ), is provided in Table 3.1. Twenty-one earthquake scenarios for central and eastern North America

Table 3.1: Stochastic input parameters used in development of time series input motions using SMSIM

Parameter	Value
Source spectrum	Brune ω-squared point source
Stress drop $\Delta\sigma$ (bar)	400
Site diminution κ (s)	0.006
Density of crust ρ (g/cm^3)	2.8
Shear wave velocity of crust β (km/sec)	3.7
Geometrical spreading	Atkinson and Boore (2014)
Path attenuation	Atkinson and Boore (2014)
Crustal amplification	Boore (2014)

(CENA) conditions, representing three distances (5 km, 20 km, and 100 km) and seven magnitudes linearly spaced between *M* 5.0 to *M* 8.0, are considered. CENA conditions were used because seismological parameters and durations were recently updated for this region by Boore (2015). For each earthquake magnitude and distance, a suite of 100 time series was generated to account for motion-to-motion variability and to provide a stable estimate of the duration. The D_{gm} value associated with the different earthquake scenarios varies from 1.4 s to 41.8 s, as summarized in Figure 3.4.

3.4.2 Site Profiles

Nine hypothetical soil sites are used for the linear-elastic site response analyses. Each hypothetical site consists of a single layer soil deposit and an underlying rock half-space. The shear wave velocity of the soil layer is 400 m/s, three different soil depths (H = 100 m, 178 m, and 316 m) are considered along with three different shear wave velocities of the rock layer ($V_{s,rock}$ = 1,000 m/s, 1,730 m/s, and 3,000 m/s). The unit weight of the soil layer and of the rock layer are 18 kN/m^3 and 22 kN/m^3, respectively,

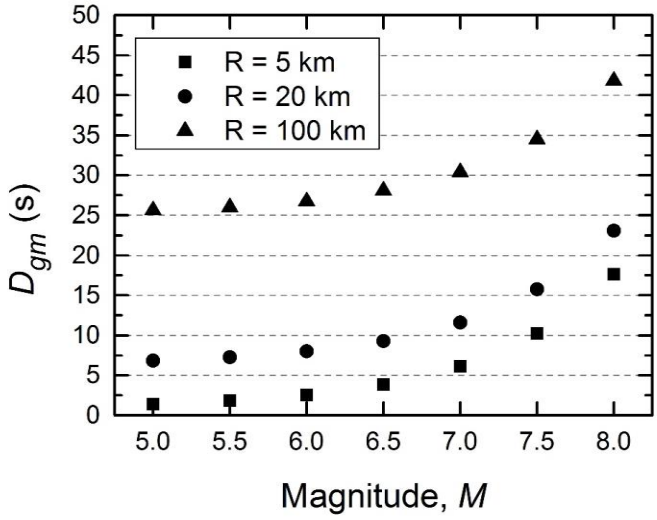

Figure 3.4: Ground motion durations (D_{gm}) for all earthquake scenarios used in this study.

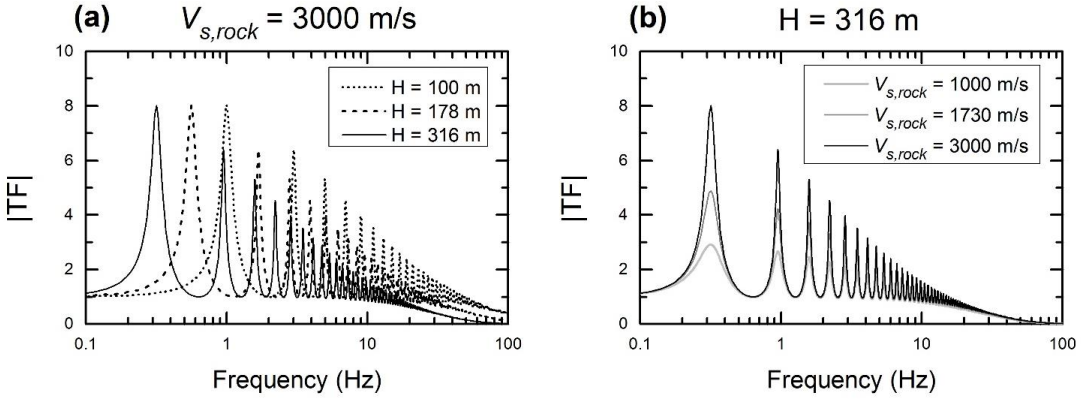

Figure 3.5: Theoretical site transfer functions for selected hypothetical site profiles used in this study.

and the damping ratio for both layers is 1%. The influence of the different soil depths and $V_{s.rock}$ on the site transfer functions are shown in Figure 3.5. The natural frequencies for the different depths are 1.0 Hz, 0.56 Hz, and 0.32 Hz, and the variation in $V_{s,rock}$ changes the peak in the transfer function by about a factor of 3. The different

sites allow for the investigation of how site frequency and the peak amplitudes in the transfer function influences changes in duration.

3.5 OSCILLATOR DURATIONS FOR ROCK MOTIONS

The duration of the oscillator response obtained from the time series was computed as the time between the accumulation of 5% and 95% of the Arias Intensity of the oscillator acceleration response (D_{5-95}). This definition of duration was used because the D_{5-95} of the rock motions that are stochastically generated is consistent with the D_{gm} values specified for these motions. The average of the D_{5-95} from the suite of 100 time series is taken as a stable estimate of the duration. To differentiate between the oscillator durations for rock motions and for surface motions, D_{5-95} is noted as $D_{5-95,rock}$ for rock and as $D_{5-95,surf}$ for the surface.

The values of $D_{5-95,rock}$ are computed for all seven magnitudes and three distances and for a range of oscillator frequencies between 0.1 Hz and 100 Hz. Figure 3.6a shows the variation of $D_{5-95,rock}$ with oscillator frequency for four earthquake scenarios with diverse D_{gm} ranging from 3.8 s to 25.6 s. In all four cases $D_{5-95,rock}$ is approximately equal to D_{gm} at frequencies greater than about 1 ~ 5 Hz, and it significantly increases as the oscillator frequency decreases. However, for each earthquake scenario the rate of increase in $D_{5-95,rock}$ and the threshold frequency below which this increase occurs are different. It is interesting that at an oscillator frequency of 0.1 Hz the $D_{5-95,rock}$ is relatively similar for all of the values of D_{gm}. $D_{5-95,rock}$ is normalized by D_{gm} in Figure 3.6b. The normalized duration at high frequencies approaches 1.0 regardless of the D_{gm}, but the threshold frequency below which $D_{5-95,rock}/D_{gm}$ increases changes with D_{gm}. At shorter D_{gm}, the threshold frequency

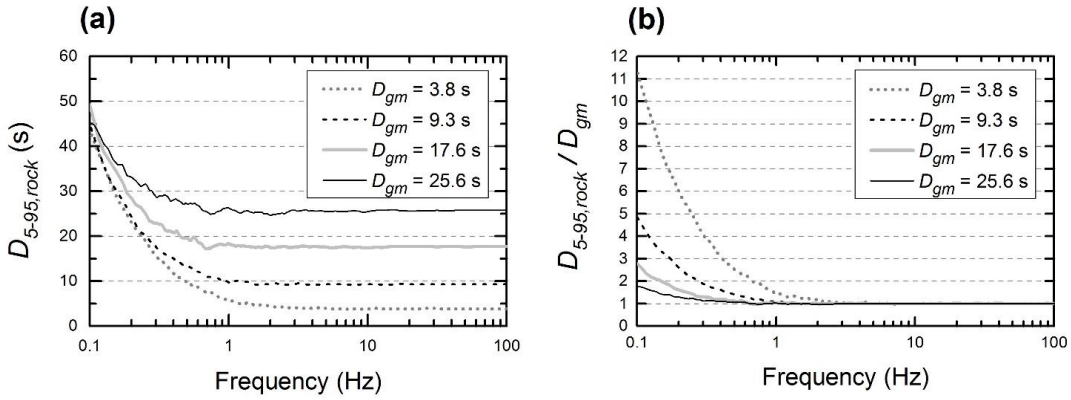

Figure 3.6: Variation of $D_{5-95,rock}$ and $D_{5-95,rock}/D_{gm}$ with oscillator frequency for a range of D_{gm}.

increases and the rate of increase of $D_{5-95,rock}/D_{gm}$ at frequencies less than the threshold frequency is larger. Figure 3.6b suggests that the variation of $D_{5-95,rock}/D_{gm}$ with frequency can be modelled directly as a function of D_{gm} rather than as a function of magnitude and distance.

An inverted hyperbolic functional form is used to describe the variation of $D_{5-95,rock}/D_{gm}$ with frequency. The general form of an inverted hyperbola in a two-dimensional plane with an origin of (0, 0) is:

$$y = y_o - \frac{x}{a+bx} \tag{3.2}$$

in which y_o is the intercept at x = 0.0, a is a parameter that controls the initial slope of the hyperbola ($1/a$ represents the initial slope), and b is a parameter that controls the height of the hyperbola ($1/b$ represents the height). Equation 3.2 is applied to a space where the x-axis represents frequency (f) and starts from 0.1 Hz, and the y-axis represents $D_{5-95,rock}/D_{gm}$ and starts from 0. As a result, equation 3.2 is rewritten as:

$$D_{5-95,rock}/D_{gm} = \begin{cases} Dur_o - \frac{(f-0.1)}{a+b(f-0.1)} & (0.1\,Hz \le f < f_{lim}) \\ 1.0 & (f \ge f_{lim}) \end{cases} \quad (3.3)$$

where Dur_o is the $D_{5-95,rock}/D_{gm}$ intercept when $f = 0.1\,Hz$, and a and b are the hyperbolic parameters that control the initial slope and height of the parabola, respectively. The inverted hyperbola is not allowed to extend below 1.0 at high frequencies and f_{lim} is the threshold frequency above which $D_{5-95,rock}/D_{gm}$ is set to 1.0. Figure 3.7 is an illustration of the functional form described in Equation 3.3, as well as the truncation at $D_{5-95,rock}/D_{gm}$ equal to 1.0. Note that $1/b$ represents the height of the un-truncated hyperbola, and corresponds to the difference between Dur_o and the minimum $D_{5-95,rock}/D_{gm}$ of the hyperbola (Dur_{min} in Figure 3.7).

To use equation 3.3 in a predictive manner, the model parameters a, b, f_{lim}, Dur_o, and Dur_{min} must be specified, and these parameters vary with D_{gm}. Taking

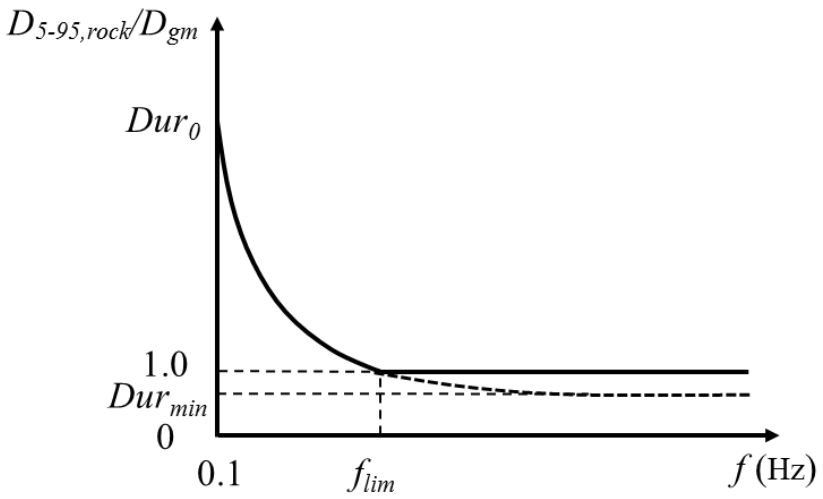

Figure 3.7: Functional form of model to predict $D_{5-95,rock}/D_{gm}$ as a function of frequency.

$Dur_o - Dur_{min} = 1/b$ and enforcing a relationship between a, b, Dur_o, and f_{lim} that ensures continuity of equation 3.3 at $f = f_{lim}$, both a and b can be computed from the three parameters, Dur_0, Dur_{min}, and f_{lim}:

$$a = \left[\frac{1}{Dur_0 - 1} - \frac{1}{Dur_0 - Dur_{min}}\right] \cdot (f_{lim} - 0.1) \quad (3.4)$$

and

$$b = \frac{1}{Dur_0 - Dur_{min}} \quad (3.5)$$

Thus, only the parameters f_{lim}, Dur_o, and Dur_{min} are needed to define the inverted hyperbola.

Equation 3.3 is used along with equations 3.4 and 3.5 to fit $D_{5-95,rock}/D_{gm}$ versus f curves for each earth scenario and associated D_{gm}. The derived values of f_{lim}, Dur_o, and Dur_{min} are used to develop predictive models of these parameters as a function of D_{gm}. The derived values and the predictive models are shown in Figure 3.8. The results indicate that f_{lim}, Dur_o, and Dur_{min} can all be predicted accurately ($R^2 \geq 0.95$) as a function of D_{gm} alone, regardless of the magnitude and distance of the earthquake scenario. Figure 3.8d shows predicted $D_{5-95,rock}/D_{gm}$ values from equations 3.3 to 3.5 using parameters estimated from the regression results in Figure 3.8. The predictions are shown for the same four earthquake scenarios shown in Figure 3.6, and comparison between these figures show good agreement between the model predictions and data. The largest difference occurs for the shortest D_{gm} (i.e., 3.8 s) at an oscillator frequency of 0.1 Hz, where the predicted value of $D_{5-95,rock}/D_{gm}$ is about 1.0 s (9%) smaller than the value shown in Figure 3.6.

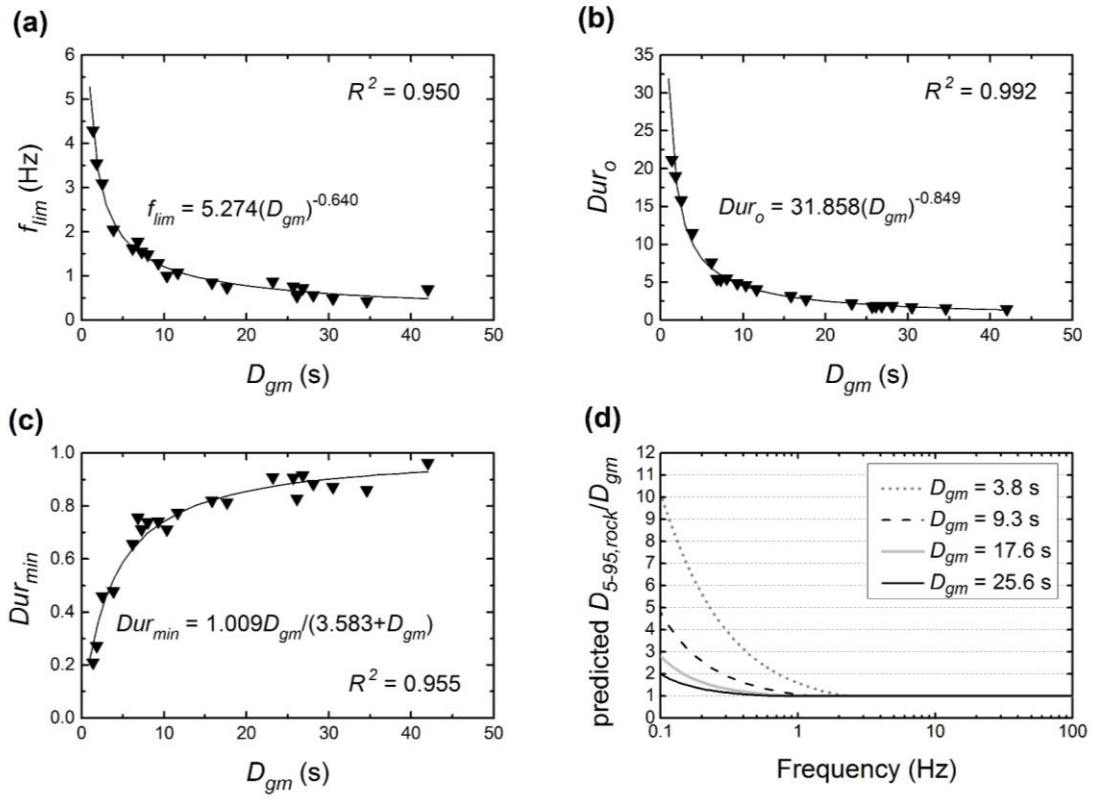

Figure 3.8: Parameters in $D_{5-95,rock}/D_{gm}$ model and predicted values of $D_{5-95,rock}/D_{gm}$ for a range of D_{gm}.

It is important to note that $D_{5-95,rock}$, if used directly in RVT analysis for rock response prediction, does not result in agreement between RVT and TS results when the excitation is shorter than the oscillator period. However, the study of the duration of rock response represented by $D_{5-95,rock}$ is essential in the understanding of the duration of surface response.

3.6 OSCILLATOR DURATIONS FOR SURFACE MOTIONS

The values of $D_{5-95,surf}$ are computed for the oscillator response of the computed surface motions for the nine sites subjected to the rock motions developed for a

range of magnitudes and distances, as discussed earlier. Figure 3.9 shows the variation of $D_{5-95,surf}$ with frequency for the 316 m site with $V_{s,rock}$ = 3,000 m/s for two selected earthquake scenarios. For each earthquake, $D_{5-95,rock}$ is plotted along with $D_{5-95,surf}$ for comparison. Several features can be observed in Figure 3.9. At higher frequencies $D_{5-95,surf}$ is very similar to $D_{5-95,rock}$, although the duration at the surface may be slightly larger due to the dynamic response of the site. Importantly, local peaks occur at specific frequencies for $D_{5-95,surf}$ and these peaks are not present for $D_{5-95,rock}$. These peaks occur at the modal frequencies of the site due to the enhanced motion present at these frequencies, which amplifies the duration of shaking of an oscillator at the same frequency. The increase in duration is most pronounced at the first mode of the site, but is also observable at the first couple of higher modes. Finally, at frequencies less than the first mode frequency of the site, $D_{5-95,surf}$ is shorter than $D_{5-95,rock}$ for smaller values of D_{gm} (Figure 3.9a) due to destructive interference. Destructive interference occurs for oscillator responses at the surface when the natural site frequency is smaller than the corner frequency of the input FAS, thus it occurs when a deep site is subjected to a moderate to small earthquake. This explains why $D_{5-95,surf}$ is shorter than $D_{5-95,rock}$ by as large as 10 s in the *M* 6.5, R = 20 km case (Figure 3.9a) at 0.1 Hz, whereas in the *M* 8.0, R = 5 km case (Figure 3.9b) $D_{5-95,surf} \sim D_{5-95,rock}$ at low frequencies.

The goal of this study is to predict the duration elongation due to site response, such that a more accurate estimate of the surface duration can be used in RVT site response analysis to improve the prediction of site amplification. Therefore, among the features observed in Figure 3.9, the difference between $D_{5-95,surf}$ and $D_{5-95,rock}$ at or near the modal frequencies is of the most interest and is the focus of the modeling efforts.

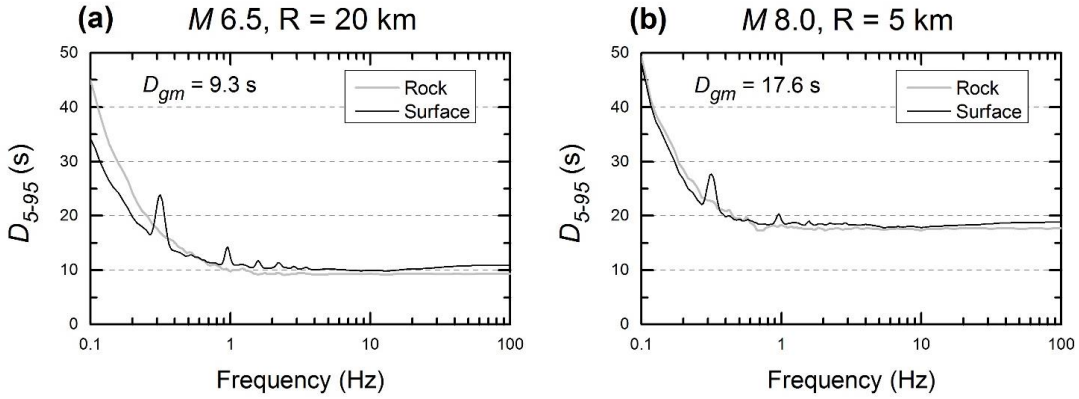

Figure 3.9: Variation of $D_{5-95,surf}$ and $D_{5-95,rock}$ with oscillator frequency for a site with H = 316 m and $V_{s,rock}$ = 3,000 m/s for two earthquake scenarios.

To investigate the factors that influence the difference between $D_{5-95,surf}$ and $D_{5-95,rock}$ at the modal frequencies, the duration difference ($\Delta D = D_{5-95,surf} - D_{5-95,rock}$) is computed for different earthquake magnitudes and distances (i.e., D_{gm}), site thicknesses, and sites with different shear wave velocities of rock. Figure 3.10 shows the influence of these factors by plotting ΔD versus oscillator frequency for different values of the various parameters. Figure 3.10a shows ΔD for earthquake scenarios with different D_{gm} for the 316 m site with $V_{s,rock}$ = 3,000 m/s. It is observed that the amplitude of ΔD at the modal frequencies is mode-dependent, with the largest value at the first mode and the smaller values higher modes. The amplitude of ΔD at each mode is influenced by the value of D_{gm}, with the smallest D_{gm} experiencing the largest ΔD. The values of ΔD for different site thicknesses, which correspond to different natural site frequencies (f_{site}), are shown in Figure 3.10b. As the thickness increases, and the corresponding f_{site} decreases, the peaks of ΔD shift to smaller frequencies accordingly. Importantly, the peak ΔD becomes smaller as the site

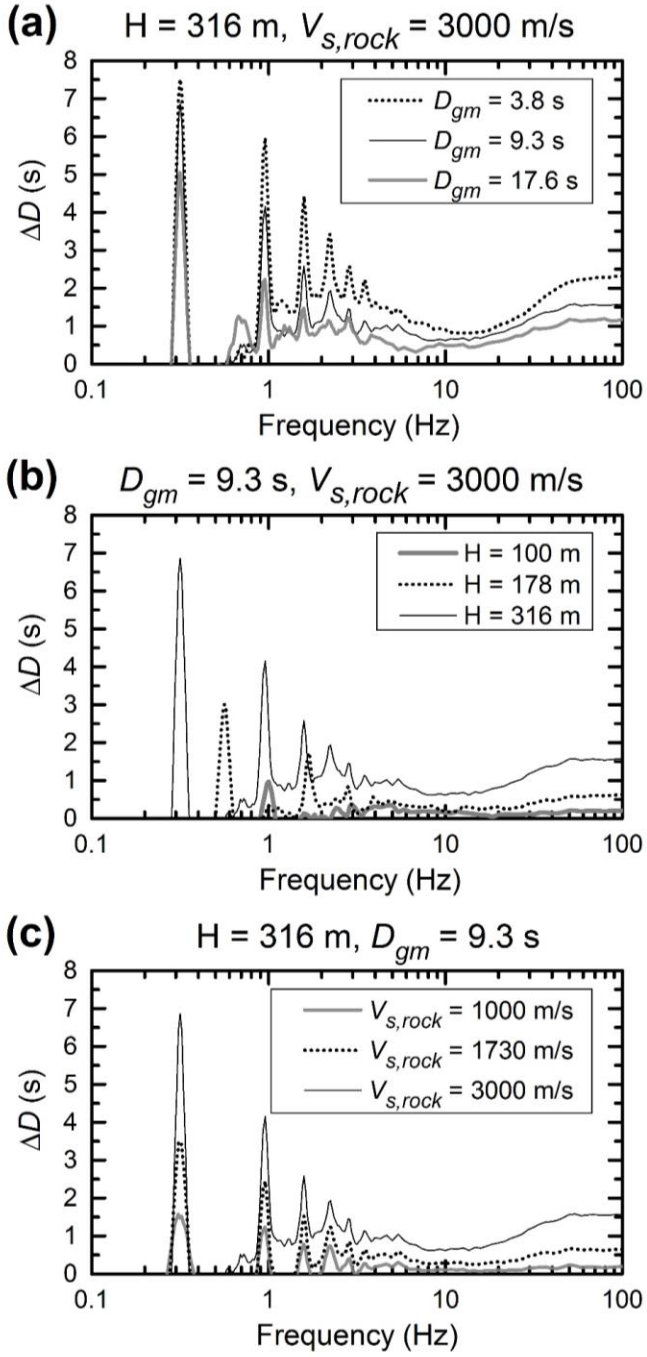

Figure 3.10: The change in the duration of the oscillator response ($\Delta D = D_{5-95,surf} - D_{5-95,rock}$) as a function of frequency due to site response for (a) different D_{gm}, (b) different site thicknesses, and (c) different $V_{s,rock}$.

thickness decreases (i.e., f_{site} increases), indicating that the amplitude of ΔD is also related to the specific value of f_{site}. Finally, Figure 3.10c illustrates ΔD for different values of $V_{s,rock}$. At the first mode, the peak ΔD is ~ 7.0 s for the case with the largest $V_{s,rock}$ (i.e., the largest impedance contrast) yet is only 1.5 s for the case with the smallest $V_{s,rock}$ (i.e., the smallest impedance contrast). A similar trend is observed at the second and third modes as well. This result indicates that the increase in $D_{5-95,surf}$ is larger when there is a strong impedance within the site profile. A stronger impedance contrast leads to a transfer function with larger peaks, which generates stronger amplification and the larger ΔD. Figure 3.10 provides insight regarding not only the amplitude of the peak ΔD, but also the width of the ΔD peak. For each mode, the width of the ΔD peak does not vary considerably with any of the factors investigated, and in general, the first mode peak has the largest width and the high modes have smaller widths.

In the modelling of ΔD, the description of each ΔD peak at a modal frequency

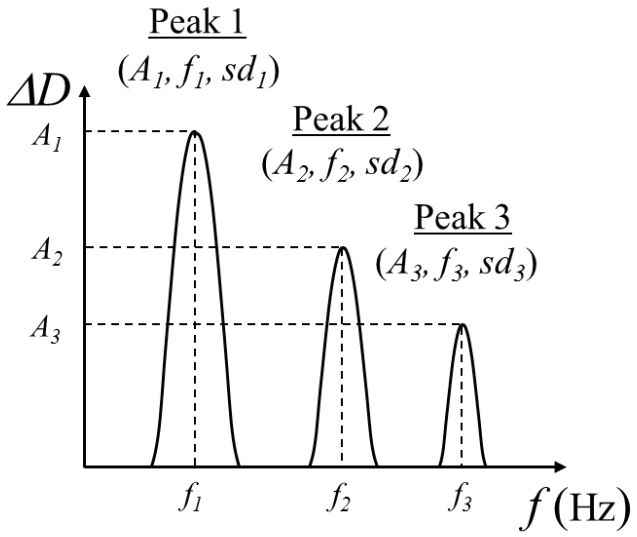

Figure 3.11: Functional form of model to predict $\Delta D = D_{5-95,surf} - D_{5-95,rock}$.

needs three parameters – amplitude, frequency where the maximum occurs, and width. A Gaussian function in log-space is selected as the functional form to describe the ΔD peak as a function of frequency. This equation is used due to its simplicity and the fact that it fits the shape of the peaks shown in Figure 3.10 generally well. The equation of ΔD can be written as the superposition of three Gaussian functions, each associated with a separate modal frequency:

$$\Delta D(f) = \sum_{i=1}^{3} A_i \cdot e^{-\frac{(\ln(f)-\ln(f_i))^2}{2*sd_i^2}} \tag{3.6}$$

in which i = 1, 2, 3 represents the mode, A_i represents the amplitude of the peak at mode i, f_i represents the frequency at the center of the peak for mode i, and sd_i represents the standard deviation (in log-space) that controls the width of the peak at mode i. The functional form of the ΔD model is shown in Figure 3.11. The value of f_i is known to be equal to the modal frequency of the site and is obtained from the site transfer function. Therefore, only A_i and sd_i need to be estimated, among which A_i is the most critical parameter because it is used to estimate the $D_{5-95,surf}$ at the modal frequencies.

As shown in Figure 3.10, the value of A_i is related to D_{gm}. Figure 3.12 shows the values of A_i derived from the ΔD data as a function of D_{gm} for different site profiles as well as modes. The value of A_i for the first mode (A_1) is first examined for different site thicknesses and $V_{s,rock}$ (Figures 3.12a, b). As shown in these figures, for a specific site A_1 decreases with increasing D_{gm}, and for a specific D_{gm} A_1 increases with site thickness and with $V_{s,rock}$. Figure 3.12c investigates the mode-dependence of A_i, revealing that for a specific D_{gm}, A_1 is always the largest and A_3 is always the

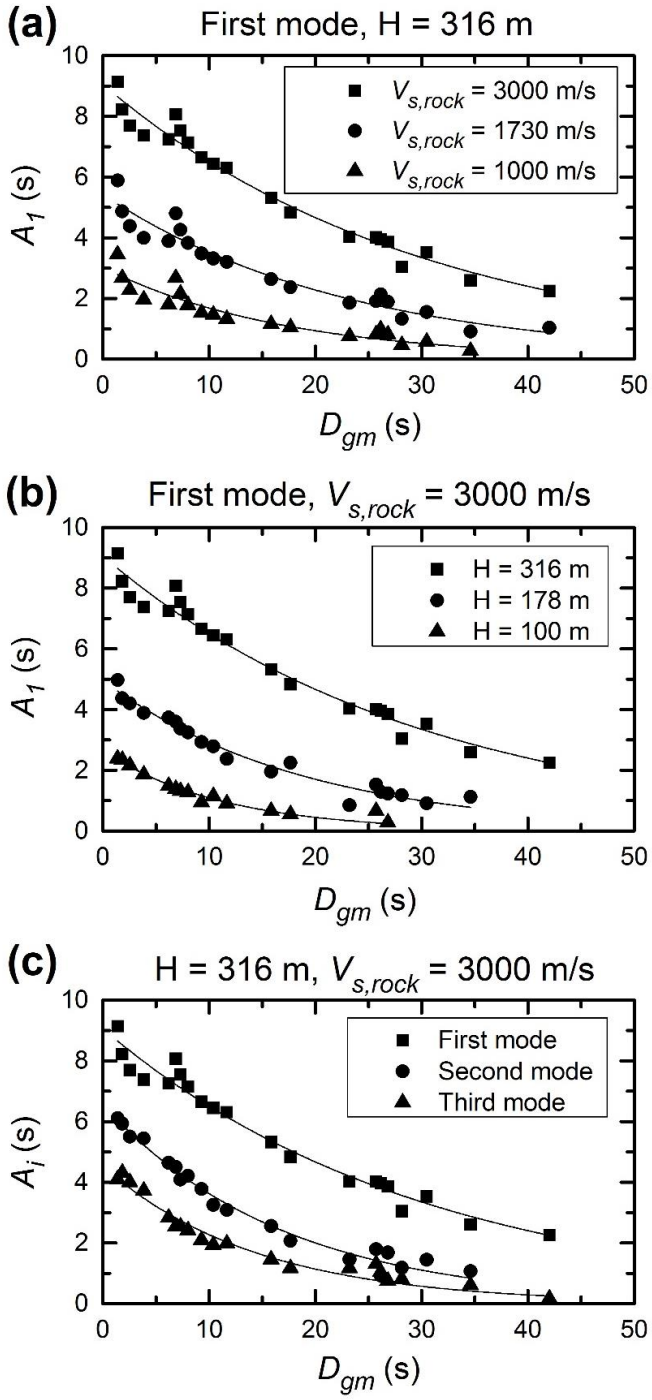

Figure 3.12: Variation of amplitude A_i with D_{gm} for (a) different $V_{s,rock}$, (b) different site thicknesses, and (c) different modes.

smallest. The relationship between A_i and D_{gm} is fit with a functional form that is written as:

$$A_i = C_i \cdot e^{-D_{gm}/m_i} \ (i = 1,2,3) \tag{3.7}$$

where C_i is the intercept and $1/m_i$ is the decay rate for mode i. A_i decreases more rapidly with larger $1/m_i$ (i.e., smaller m_i).

Equation 3.7 is fit to the A_i data for each site and the values of C_i and m_i are investigated as a function of site thickness, $V_{s,rock}$, and the mode (i.e., i = 1, 2, 3). The intercept C_1 of the amplitude at the first mode, A_1, is first studied. According to Figure 3.12, C_1 increases with both site thickness and $V_{s,rock}$. When natural site frequency (f_{site}) is used to represent the site thickness, the data show that the relationship between C_1 and ($1/f_{site}$) is approximately linear. The influence of $V_{s,rock}$ on C_1 can be represented by the amplitude of the site transfer function at the first mode site frequency ($Amp_{|TF|,1}$), and the data show that the relationship between C_1 and $Amp_{|TF|,1}$ is also linear. The combined effect of f_{site} and $Amp_{|TF|,1}$ on the variation of C_1 is shown in Figure 3.13a by plotting C_1 versus the ratio $Amp_{TF,1}/f_{site}$ for all sites considered. The data show that C_1 increases linearly with $Amp_{TF,1}/f_{site}$ and equation $C_1 = 0.35 \cdot Amp_{|TF|,1}/f_{site}$ fits the data very well and can be used to estimate C_1.

Figure 3.13b shows the variation of C_i/C_1 with f_{site}/f_i (i = 1, 2, 3) for all sites considered, where f_i is the frequency corresponding to the frequency at mode i, and $f_{site} = f_1$. Because the data are from linear-elastic site response analyses of sites with a constant shear wave velocity, f_{site}/f_i is a constant for each mode with values of 0.33 and 0.2 for the second and third modes, respectively. The values of C_i/C_1 range from

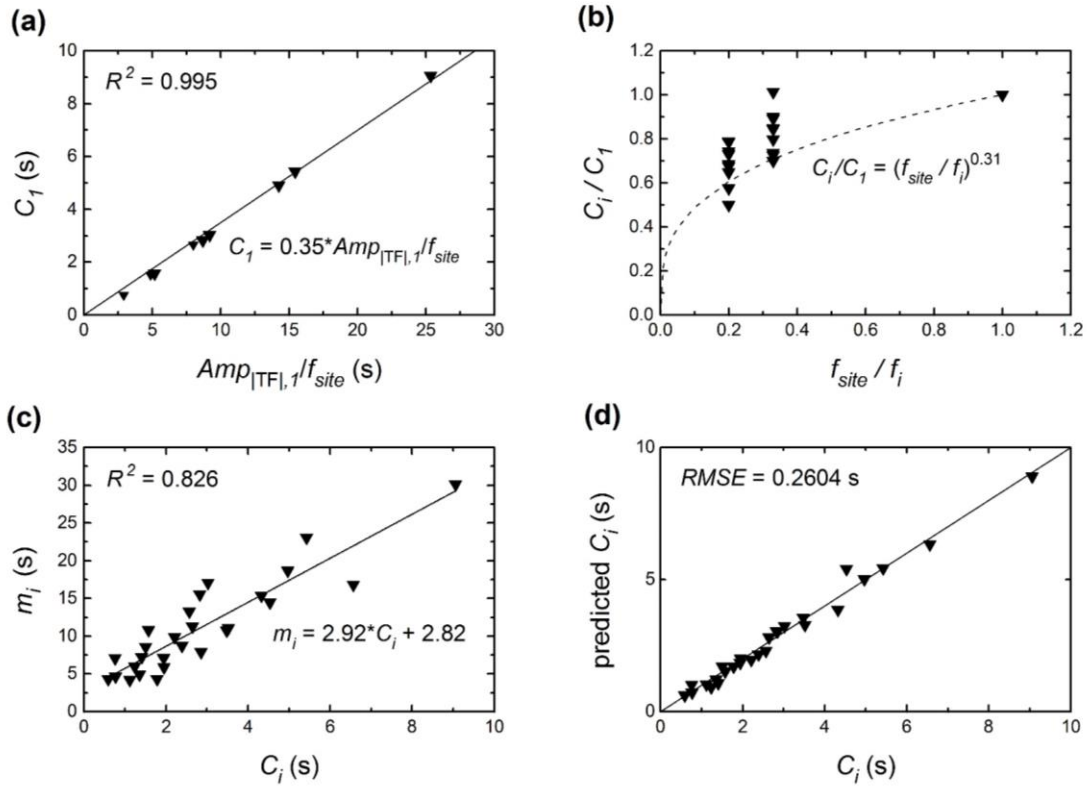

Figure 3.13: Parameters in predictive model for $\Delta D = D_{5-95,surf} - D_{5-95,rock}$.

0.7 to 1.0 for mode 2 (f_{site}/f_i = 0.33) and from 0.5 to 0.8 for mode 3 (f_{site}/f_i = 0.2). Although there is scatter in the data at each value of f_{site}/f_i, no systematic trend could be identified with other factors and thus the data in Figure 3.13b were fit with a power law with the exponent equal to 0.31.

The values of m_i derived from fitting equation 3.7 to the data indicate that, in general, m_i increases with $(1/f_{site})$ and $Amp_{|TF|,1}$ and is smaller for higher models. These trends are the same as the trends observed in the C_i values. Therefore, the values of m_i and C_i are related to each other, as shown in Figure 3.13c. The data indicate that m_i generally increases with C_i and the relationship is linear, although with some scatter. The fit to the data results in the expression $m_i = 2.92 \cdot C_i + 2.82$.

Figure 3.13d plots the predicted values of C_i against the C_i values derived directly from the data. All the data points fall on or close to the 1:1 line, indicating that the equations in Figures 3.13a and b provide an accurate estimate of C_i. The root-mean-square error (RMSE) of the C_i prediction is 0.26 s. Using the equations in Figure 3.13, C_i and m_i can be predicted as a function of f_{site} and $Amp_{|TF|,1}$ and these values can be used in equation 3.7 with the specified D_{gm} to predict the amplitude of the ΔD for a specific site.

The final parameter required for equation 3.6 is sd_i, which represents the standard deviation (in log-space) that controls the width of the ΔD peak. As shown in Figure 3.10, the width of peak is the largest for the first mode, smallest for the third mode, and its value generally does not vary much with other parameters. Therefore, three values are empirically selected for sd_i for the first three modes: 0.091, 0.081, and 0.056, respectively, for modes 1, 2, and 3.

3.7 INCORPORATING A DURATION MODIFICATION IN RVT SITE RESPONSE ANALYSIS

To modify the duration used in RVT site response analysis that has been explained for the surface motion, $D_{5-95,rock}$ and ΔD model are used to predict the ratio of $D_{5-95,surf}/D_{5-95,rock}$, and this ratio is used to modify the D_{rms} values from Boore and Thompson (2015). This approach was taken because the BT15 D_{rms} values provide accurate RVT estimates of response spectral values for rock motions, and thus should be the starting basis for the duration of motions at the ground surface. This is the same approach taken by Kottke and Rathje (2013) and Wang and Rathje (2016) to modify duration to improve RVT site amplification predictions, except in these previous studies the duration modification was taken directly from the corresponding suite of TS analyses.

Here, the modification is derived directly from the empirical duration models without any need to perform a suite of corresponding time series analyses.

To modify the duration used for the surface motion in the RVT analysis, the following procedure is followed. The D_{gm} of the rock motion is estimated using either empirical models or seismological theory. Equations 3.3 through 3.5, along with the regression equations in Figure 3.8 and the D_{gm}, are used to predict $D_{5-95,rock}$ as a function of oscillator frequency. $D_{5-95,surf}$ at each oscillator frequency is computed as the sum of $D_{5-95,rock}$ and ΔD. ΔD takes on non-zero values only at frequencies near the first three modal frequencies (f_i, with i = 1, 2, and 3), and these frequencies are obtained from the site transfer function. To predict ΔD as a function of frequency, equation 3.6 is used along with model parameters predicted from Figure 3.13 using the values of f_i and $Amp_{|TF|,1}$ (i.e., the amplitude of the site transfer function at the first mode). The $D_{5-95,rock}$ and $D_{5-95,surf}$ values are used to compute $D_{5-95,surf}/D_{5-95,rock}$ at each frequency. Finally, $D_{5-95,surf}/D_{5-95,rock}$ is multiplied by the BT15 D_{rms} values at each frequency to compute $D_{rms,surf}$, and this value is used in the *rms* calculation for the surface motion.

The influence of using $D_{rms,surf}$ instead of D_{rms} for the surface motion in RVT site response analysis is illustrated through the ratio of the site amplification from RVT and TS analyses, noted as RVT/TS. RVT/TS values for the first three modes of two selected sites (316 m and 100 m, $V_{s,rock}$ = 3,000 m/s) subjected to a range of earthquake scenarios are shown in Figure 3.14. The results are plotted versus the D_{gm} for each earthquake scenario. For the 316 m site (Figure 3.14a), the ratio of RVT/TS when the duration modification is not applied generally is above 1.0 for all D_{gm} and the ratio is larger for shorter D_{gm}. The RVT AF for the shortest D_{gm} is 1.5 to 2.2 times larger than the TS AF depending on the mode. After modifying the duration to represent

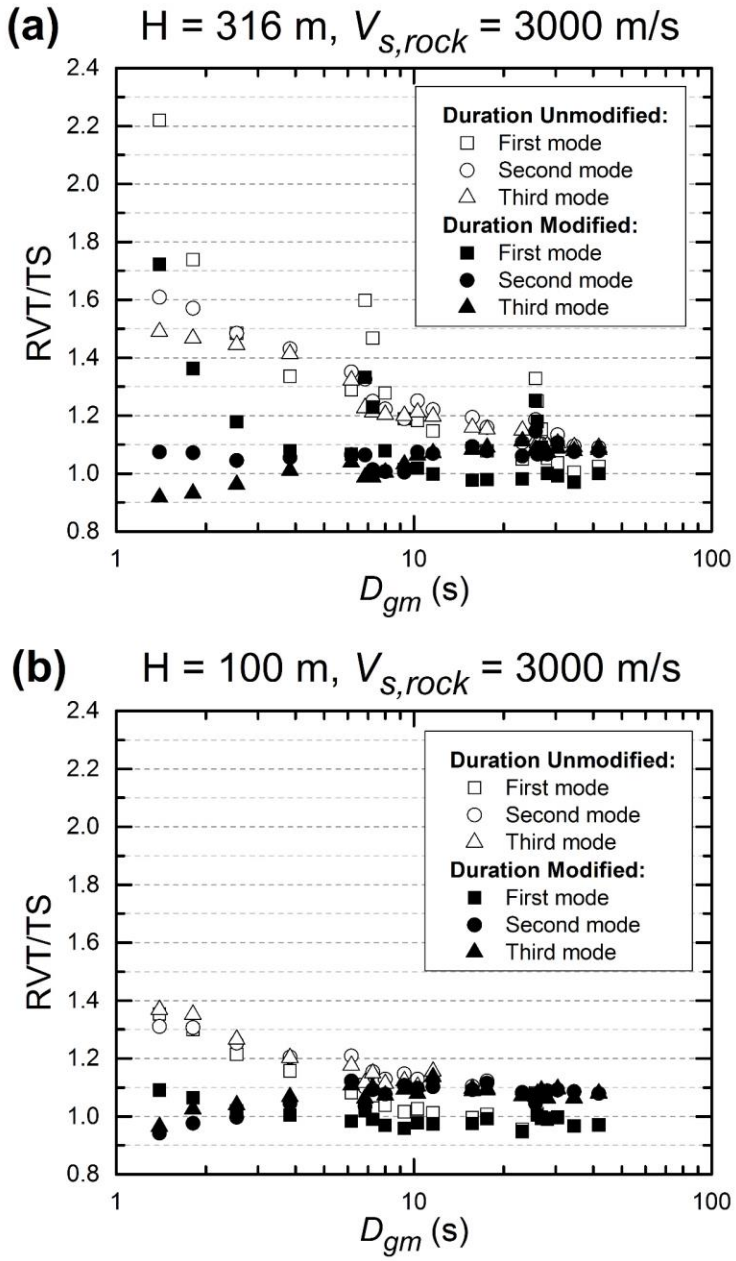

Figure 3.14: Ratio of RVT/TS site amplification at first-mode site frequency as a function of D_{gm} for RVT analyses using the D_{rms} model and using the modified $D_{rms,surf}$ model. (a) Site with H = 316 m and $V_{s,rock}$ = 3,000 m/s and (b) site with H = 100 m and $V_{s,rock}$ = 3,000 m/s.

$D_{rms,surf}$, the ratio of RVT/TS for the first three modes are all reduced and become much closer to 1.0. For the second and third modes, the differences between RVT and TS are all within +/- 10% for all earthquake scenarios after the duration modification, which is significantly smaller than the values of 20 – 60% before the duration modification. For the first mode, the duration modification results in the RVT AF within +/- 10% of the TS AF, except for a few scenarios.

Generally, the RVT/TS data vary smoothly with D_{gm} but there are three clusters of data in Figure 3.14a where RVT/TS at the first mode is much larger than the others. These clusters of points are located at D_{gm} equal to about 26 s, 7 s, and less than 2 s. These D_{gm} values are the ground motion durations associated with *M* 5.0 and *M* 5.5 earthquakes, where the input FAS have a large corner frequency. As shown in Figure 3.1, RVT/TS increases as the ratio of f_{site} to the corner frequency of the input motion (f_c) decreases, and that the duration modification provides the least improvement to RVT for sites with f_{site}/f_c less than 0.5 (Wang and Rathje 2016). The points in Figure 3.14a that increase quickly are associated with cases with f_{site}/f_c < 0.5 due to the large f_c of the small magnitude input motions. After using the duration modification for these data, RVT/TS is reduced by 10 – 25 % but the absolute value of RVT/TS still tends to be large (RVT/TS = 1.2 to 1.7).

For the 100 m site (Figure 3.14b), the values of RVT/TS are not as large as the 316 m site due to the larger f_{site} and larger f_{site}/f_c. Before the duration modification is applied, RVT/TS is larger than 1.1 only for D_{gm} less than about 10 s. After using the duration modification, the RVT AF for all D_{gm} are reduced to within about +/- 10% of the TS AF. No clusters of larger RVT/TS values are observed in Figure 3.14 because for this higher frequency site, all of the scenarios have f_{site}/f_c > 0.5.

3.8 DISCUSSION AND CONCLUSIONS

This paper investigated the duration of the oscillator response for earthquake motions and the influence of site response on this duration. The motivation for this investigation was the need to predict the duration of the oscillator response for surface ground motions computed from site response analysis. The duration of the oscillator response for the surface ground motion is needed to improve the prediction of surface response spectra from RVT site response analysis. Current implementations of RVT site response analysis use the same duration (D_{rms}) for the rock and surface motions, despite the fact that the dynamic ground response generally increases the duration of motion. Modifying D_{rms} in an RVT analysis to account for the dynamic response of the site can result in RVT predictions of site amplification that are more similar to TS predictions.

The modification to D_{rms} developed in this paper is based solely on observations of D_{5-95} of the oscillator response for input rock motions ($D_{5-95,rock}$) and computed surface motions ($D_{5-95,surf}$) from TS analysis. An empirical model for $D_{5-95,rock}$ was developed as a function of the ground motion duration (D_{gm}) and oscillator frequency. An empirical model for $D_{5-95,surf}$ was developed as a function of D_{gm}, $D_{5-95,rock}$, the frequencies of the first three modes of the site, and the transfer function amplitude at the first mode frequency of the site ($Amp_{|TF|,1}$). At each oscillator frequency, $D_{5-95,surf}/D_{5-95,rock}$ is computed from the empirical models and multiplied by the corresponding D_{rms} at each frequency to obtain $D_{rms,surf}$. This $D_{rms,surf}$ value is used in the RVT *rms* calculation for the surface motion. Using this approach, the effect of site response on the oscillator duration can be predicted for a large range of site conditions and earthquake motions without requiring any time domain site response analyses.

Using $D_{rms,surf}$ in the calculation of surface response spectra in RVT site response analysis reduces the site amplification predicted by RVT analysis, making it more consistent with the site amplification predicted by TS analysis. Before using the modified duration, the RVT site amplification at the modal frequencies for the sites analyzed was 1.1 to 2.2 times larger than the amplification from TS analysis. When the $D_{rms,surf}$ predicted by the empirical model was used in the RVT site response analysis, the vast majority of the RVT estimates of amplification were within +/- 10% of the TS amplification. The scenarios for which RVT analysis with $D_{rms,surf}$ predicted amplification substantially larger than TS analysis are associated with f_{site}/f_c < 0.5. Wang and Rathje (2016) demonstrated that for these conditions the duration modification does not adequately improve RVT analysis relative to TS analysis.

The duration models developed in this study are limited by the fact that they were based on simple shear wave velocity profiles and linear-elastic analyses. However, the duration models potentially can account for different soil profiles and equivalent-linear response because the input parameters for the duration models are based on the site transfer function. Using site transfer functions for more realistic shear wave velocity profiles and for the strain-compatible properties associated with an equivalent-linear analysis, the duration models can be applied to these conditions. Additionally, the ability of the duration modification to improve RVT site amplification estimates was assessed only at the modal site frequencies, not the entire frequency range of site amplification. These issues are addressed in the companion paper by Wang and Rathje (submitted).

3.9 Data and Resources

The stochastic time series used in the analysis were created using the latest version of the Stochastic-Method SIMulation (SMSIM) programs obtained from http://daveboore.com/software_online.html (last accessed April 2017). The durations of time series were computed using scripts written in Python (https://www.python.org, last accessed April 2017). The time-series site response analysis in this study were performed using the program Strata (http://nees.org/resorces/strata, last accessed April 2017) and the random vibration theory site response analyses were performed using scripts written in MATLAB (http://www.mathworks.com, last accessed April 2017).

3.10 Acknowledgements

This research was supported by funding from Pacific Gas & Electric, Co. through Dr. Norman Abrahamson and the Nuclear Regulatory Commission under grant NRC-HQ-60-15-C-0005. This support is gratefully acknowledged. The research also benefitted from useful discussions with Dr. David Boore from the U.S. Geological Survey, Prof. Armen Der Kiureghian from the University of California at Berkeley, and Prof. Lance Manuel from the University of Texas.

3.11 References

Boore, D. M. (1983). Stochastic simulation of high-frequency ground motions based on seismological models of the radiated spectra. *Bull. Seism. Soc. Am.* **73(6A)** 1865-1894.

Boore, D. M. (2003). Simulation of ground motion using the stochastic method. *Pure Appl. Geophys.* **160(3-4)** 635-676.

Boore, D. M. (2005). *SMSIM---Fortran programs for simulating ground motions from earthquakes: Version 2.3---A Revision of OFR 96-80-A*. US Geological Survey open-file report.

Boore, D.M. (2015). *Point-Source Stochastic-Method Simulations of Ground Motions for the PEER NGA-East Project*, Chapter 2 in NGA-East: Median Ground-Motion Models for the Central and Eastern North America Region, PEER Report 2015/04, Pacific Earthquake Engineering Research Center, 11-49.

Boore, D. M., and W. B. Joyner (1984). A note on the use of random vibration theory to predict peak amplitudes of transient signals. *Bull. Seism. Soc. Am.* **74(5)** 2035-2039.

Boore, D. M., and E. M. Thompson (2012). Empirical Improvements for Estimating Earthquake Response Spectra with Random-Vibration Theory. *Bull. Seism. Soc. Am.* **102(2)** 761-772.

Boore, D.M., and E. M. Thompson (2015). Revisions to some parameters used in stochastic-method simulations of ground motion, *Bull. Seism. Soc. Am.* **105(2A)** 1029-1041.

Cartwright, D. E., and M. S. Longuet-Higgins (1956). The statistical distribution of the maxima of a random function. *Proc. Roy. Soc. Lond. Math. Phys. Sci.* **237(1209)** 212-232.

Kottke, A. R., and E. M. Rathje (2013). Comparison of Time Series and Random-Vibration Theory Site-Response Methods. *Bull. Seism. Soc. Am.* **103(3)** 2111-2127.

Nuclear Regulatory Commission (NRC) (2007). *Regulatory Guide 1.208: A Performance-based Approach to Define the Site-specific Earthquake Ground Motion*, United States Nuclear Regulatory Commission, Washington, DC.

Vanmarcke, E. H. (1975). On the distribution of the first-passage time for normal stationary random processes. *J. Appl. Mech.* **42(1)** 215-220.

Wang, X., and Rathje, E. M. (2016). Influence of Peak Factors on Site Amplification from Random Vibration Theory Based Site-Response Analysis. *Bull. Seism. Soc. Am.* **106(4)** 1733-1746.

Chapter 4: Accounting for Changes in Duration in Random Vibration Theory Based Site Response Analysis

Xiaoyue Wang[4], Ellen M. Rathje[4]*

Abstract

Random Vibration Theory (RVT) site response analysis is commonly used in seismic hazard studies for nuclear facilities. A fundamental parameter in RVT analysis is the duration used when calculating the root-mean-square (*rms*) oscillator response (i.e., spectral acceleration) from the Fourier Amplitude Spectrum. Recent research has suggested that RVT site response analysis should incorporate the effects of site response on the duration used in predicting the *rms* oscillator response for the surface motion. Wang and Rathje (2017) developed an empirical model to predict the change in the duration of the oscillator response due to the dynamic site response. This paper evaluates the performance of RVT site response analysis using the Wang and Rathje (2017) duration modification. It is shown that for a wide range of shear wave velocity profiles and earthquake scenarios, the duration modification generally produces RVT amplification factors within +/- 10% of TS amplification factors. The same improvement is obtained for linear-elastic and equivalent-linear site response analyses. The cases where the duration modification does not fully improve the RVT site amplification predictions are associated with low frequency sites subjected to small magnitude earthquake, where the site frequency is less than one-half the corner frequency of the input motion.

[4]Department of Civil, Architectural and Environmental Engineering, The University of Texas, 301 E Dean Keeton Stop C1792, Austin, TX, USA 78712
*Corresponding author. Phone: +1-512-232-3683. E-mail: e.rathje@mail.utexas.edu.

4.1 INTRODUCTION

Random Vibration Theory (RVT) site response analysis is commonly used in seismic hazard analysis for nuclear facilities to compute the dynamic response of soil deposits (Regulatory Guide 1.208; Nuclear Regulatory Commission [NRC], 2007) because of its efficiency in computing large numbers of analyses without the need to select input motions. However, studies have shown that RVT site response analysis predicts site amplification at the natural site frequencies that are considerably larger than time series (TS) analysis, despite the fact that the two analyses use the same frequency domain transfer functions to compute the site response (Kottke and Rathje 2013, Graizer 2014). Recent research by Wang and Rathje (2016) showed that the difference between site amplification predicted using RVT and TS analyses can be partially reduced if the Vanmarcke (1975) peak factor model is used instead of the Cartwright and Longuet-Higgins (1956) model. It was also suggested that further reduction in the discrepancy between RVT and TS amplifications can be obtained if the influence of the dynamic response of the site is taken into account in the duration used in RVT site response analysis.

To apply the effect of site response on duration to the RVT analysis, Wang and Rathje (2017) developed a duration model such that this effect can be predicted a priori without using any time series. This duration model was developed empirically based on the measured durations of oscillator responses from acceleration-time histories from site response analysis. Although the duration model developed by Wang and Rathje (2017) is based on simple shear wave velocity profiles and linear-elastic analyses, the model potentially can be used for more complex shear wave velocity profiles and equivalent-linear analyses. This paper incorporates the Wang and Rathje (2017) duration modification into RVT site response analysis for a broad range of realistic shear wave

velocity profiles and for both linear-elastic (LE) and equivalent-linear (EQL) site response analyses. The performance of the RVT approach using a modified duration at the ground surface is evaluated through comparisons with the results from TS site response analyses.

4.2 MODIFIED RVT APPROACH FOR SITE RESPONSE ANALYSIS

4.2.1 RVT Framework

RVT site response analysis specifies the input motion based on a Fourier Amplitude Spectrum (FAS) and a duration. To compute peak time domain characteristics of motion (e.g., peak ground acceleration, spectral acceleration), the RVT approach takes advantage of the concept that the peak of a signal can be estimated as the product of its root-mean-square (*rms*) value and a peak factor (*pf*). The *pf*, defined as the peak to *rms* ratio for a signal, is computed from extreme value statistics. Different *pf* models have been developed, but the Vanmarcke (1975) peak factor model is recommended for use in RVT analysis for earthquake ground motions and site response (Wang and Rathje 2016). The *rms* value is computed by applying Parseval's theorem to an earthquake motion with a duration D_{rms} (Boore and Joyner 1984):

$$a_{rms} = \sqrt{\frac{1}{D_{rms}} \int_0^{D_{rms}} |a(t)|^2 dt} = \sqrt{\frac{2}{D_{rms}} \int_0^{\infty} |FAS(f)|^2 df} \quad (4.1)$$

To predict peak ground acceleration (PGA), D_{rms} is set equal to the ground motion duration (D_{gm}). To predict spectral acceleration (S_a), the dynamic response of the oscillator increases the duration such that D_{rms} is larger than D_{gm}.

Several models have been developed that predict D_{rms} as a function of D_{gm} and the oscillator properties. These models were developed empirically to provide RVT response spectra that are similar to the average response spectra from stochastic simulations in the time domain (e.g., Boore and Joyner 1984, Boore and Thompson 2012, Boore and Thomspon 2015). As a result, each D_{rms} model is linked to the peak factor model used in the RVT analysis. Among the D_{rms} models, the model developed by Boore and Thompson (2015) is the most recent model, and more importantly, it is the only model that is based on the Vanmarcke (1975) peak factor. The BT15 D_{rms} model, similar to the other D_{rms} models, was developed to model the oscillator response for ground motions for generic rock conditions; thus it should only be used in the prediction of rock response spectra in RVT analysis.

4.2.2 Outline of RVT Approach Using Modified Duration

Kottke and Rathje (2013) and Wang and Rathje (2016) suggested that the effects of site response on duration should be considered in RVT site response analysis. Thus, a duration different than the D_{rms} predicted using BT15 is needed for the estimation of surface response in RVT site response analysis. The duration model developed by Wang and Rathje (2017) quantifies the influence of site response on the duration of the oscillator response, and the Wang and Rathje (2017) model is incorporated into RVT site response analysis in this study to modify the duration used for the calculation of the surface response spectrum.

The outline of the RVT approach using modified durations is illustrated in Figure 4.1. Unchanged from the standard RVT analysis, the prediction of a rock response spectrum uses the rock FAS and the D_{rms} at each oscillator frequency with Equation 4.1

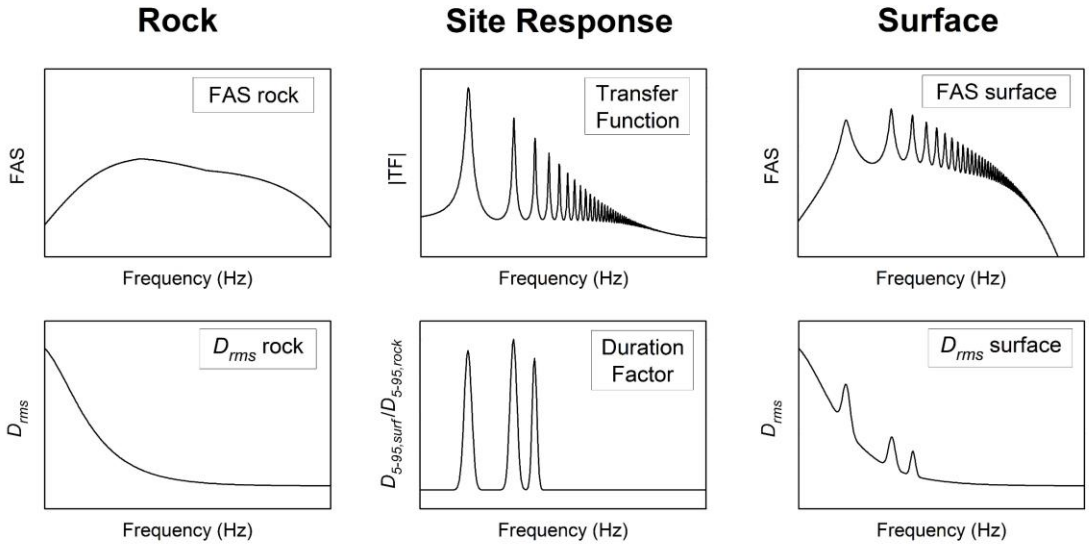

Figure 4.1: Framework of the RVT approach using a modified duration at the ground surface.

to calculate the *rms* spectral acceleration. The values of D_{rms} are obtained from a D_{rms} model, such as the BT15 model, and a specified D_{gm}. The dynamic response of the site transforms not only the FAS, but also the duration of the oscillator response used in the calculation of the *rms* acceleration. To compute the surface response spectrum, the RVT approach adopts a new method to account for this change in the duration of the oscillator response.

The dynamic response of a site is concentrated at the modal frequencies of the site and is quantified by the amplitude of the site transfer function (|TF|). The |TF| transfers the rock FAS into a surface FAS and RVT analysis uses this surface FAS in the estimation of the surface response spectrum in both the *rms* acceleration calculation and the peak factor calculation. The increase in wave amplitudes at the modal frequencies also works to elongate the duration of the oscillator responses at these frequencies. The ratio of $D_{5-95,surf}/D_{5-95,rock}$ is used to represent the influence of site properties on

duration (Figure 4.1). The ratio of $D_{5-95,surf}/D_{5-95,rock}$ is multiplied by the BT15 D_{rms} at each frequency to compute $D_{rms,surf}$, and $D_{rms,surf}$ is used in the RVT analysis along with the surface FAS in the calculation of *rms* acceleration for the prediction of surface response spectrum.

The ratio of $D_{5-95,surf}/D_{5-95,rock}$ is obtained using the model developed in Wang and Rathje (2017). This approach is summarized here. The value of $D_{5-95,rock}$ is computed as a function of frequency and D_{gm} using the inverted parabola model of Wang and Rathje (2017). The increase in duration at the ground surface (ΔD) is predicted from the site modal frequencies and the amplitude of the site transfer function at the first mode. $D_{5-95,surf}$ is computed as the sum of $D_{5-95,rock}$ and ΔD at each frequency. The ratio of $D_{5-95,surf}/D_{5-95,rock}$ is computed using the values of $D_{5-95,rock}$ and $D_{5-95,surf}$ at each frequency.

The Wang and Rathje (2017) duration model that predict $D_{5-95,surf}$ was developed based on site response analyses using simple shear wave velocity profiles and assuming linear-elastic soil properties. However, the effects of site response on the duration are predicted as a function of characteristics of the site transfer function (i.e., the site modal frequencies and the amplitude of the site transfer function at the first mode), and thus the predictive model for the modified duration can potentially be extended to sites with more complex velocity profiles and nonlinear soil properties associated with EQL analyses. In these cases, the parameters for the duration model are derived from the site transfer function of the realistic shear wave velocity profiles and for the strain-compatible properties associated with an EQL analysis.

4.3 ANALYSES PERFORMED

A number of shear wave velocity profiles, both hypothetical and realistic profiles measured in the field, are used to test the performance of the RVT site response approach using the modified duration model. For each site, input motions from earthquakes with a wide range of magnitudes and several distances are considered. Both RVT and TS analyses are performed, and the site amplification from the two approaches are compared. In addition to LE site response analyses, EQL site response analyses are performed to evaluate whether the duration modification performs adequately when using the strain-compatible soil properties.

4.3.1 Input Ground Motions

The ground motion acceleration-time histories used for the TS site response analysis were stochastically simulated using the program SMSIM (Boore 2005) and single corner frequency source spectrum (Boore 2003). The important seismological parameters describing the shape of the FAS, including the stress drop ($\Delta\sigma$) and site diminution (κ), are summarized in Table 4.1. The ground motion duration (D_{gm}) used for the stochastic simulations were derived from Boore and Thompson (2015). Earthquake scenarios for central and eastern North America (CENA) conditions were considered, because the seismological parameters and durations were recently updated for this region (Boore 2015). Multiple earthquake magnitudes and distances were used to investigate the effects of the input motion intensity, duration, and frequency content. Seven earthquake magnitudes spaced linearly from 5.0 to 8.0 and placed at distances of 5 km, 20 km, and 100 km were used. For each earthquake magnitude and distance, a suite of 100 time series was generated to provide a stable estimate of the average site amplification. The D_{gm} values used to generate the average FAS of the suite of time

Table 4.1: Stochastic input parameters used in development of time series input motions using SMSIM

Parameter	Value
Source spectrum	Brune ω-squared point source
Stress drop $\Delta\sigma$ (bar)	400
Site diminution κ (s)	0.006
Density of crust ρ (g/cm^3)	2.8
Shear wave velocity of crust β (km/sec)	3.7
Geometrical spreading	Atkinson and Boore (2014)
Path attenuation	Atkinson and Boore (2014)
Crustal amplification	Boore (2014)

series ranged from 1.4 s to 41.8 s. These are the same values used in Wang and Rathje (2017). The input motions for the RVT site response analysis used the same FAS and D_{gm} as used by the stochastic simulation. In this way the input ground motions for use in TS and RVT analyses are consistent with each other.

4.3.2 Site Profiles

A total of 16 soil profiles were used in this study, the nine hypothetical sites from Wang and Rathje (2017) and an additional seven realistic sites. Each hypothetical site consists of a single soil layer underlain by a rock half-space. Three different soil depths (H = 100 m, 178 m, and 316 m) and three different half-space shear wave velocities ($V_{s,rock}$ = 1,000 m/s, 1,730 m/s, and 3,000 m/s) were used to represent a range of natural site frequencies and impedance contrasts. The seven realistic sites have more complicated shear wave velocity profiles than the hypothetical sites (Figure 4.2). These shear wave velocity profiles represent the Calvert Cliffs (CC) site in Maryland (UniStar Nuclear 2007) and six Kik-Net downhole array sites in Japan (open to the public at

http://www.kik.bosai.go.jp/kik/index_en.shtml). Note that the depths of the shear wave velocity profiles from realistic sites in Figure 4.2 vary significantly, with the shallowest site representing about 200 m and the deepest site representing over 1200 m. The near-surface shear wave velocities range from about 100 m/s to 400 m/s for the sites, and shear wave velocity of the half-space at the bottom of the profiles range from 1,000 m/s to 3,260 m/s.

Figure 4.3 shows the theoretical transfer functions for the hypothetical and realistic sites for LE conditions assuming 1% damping for each layer. For the

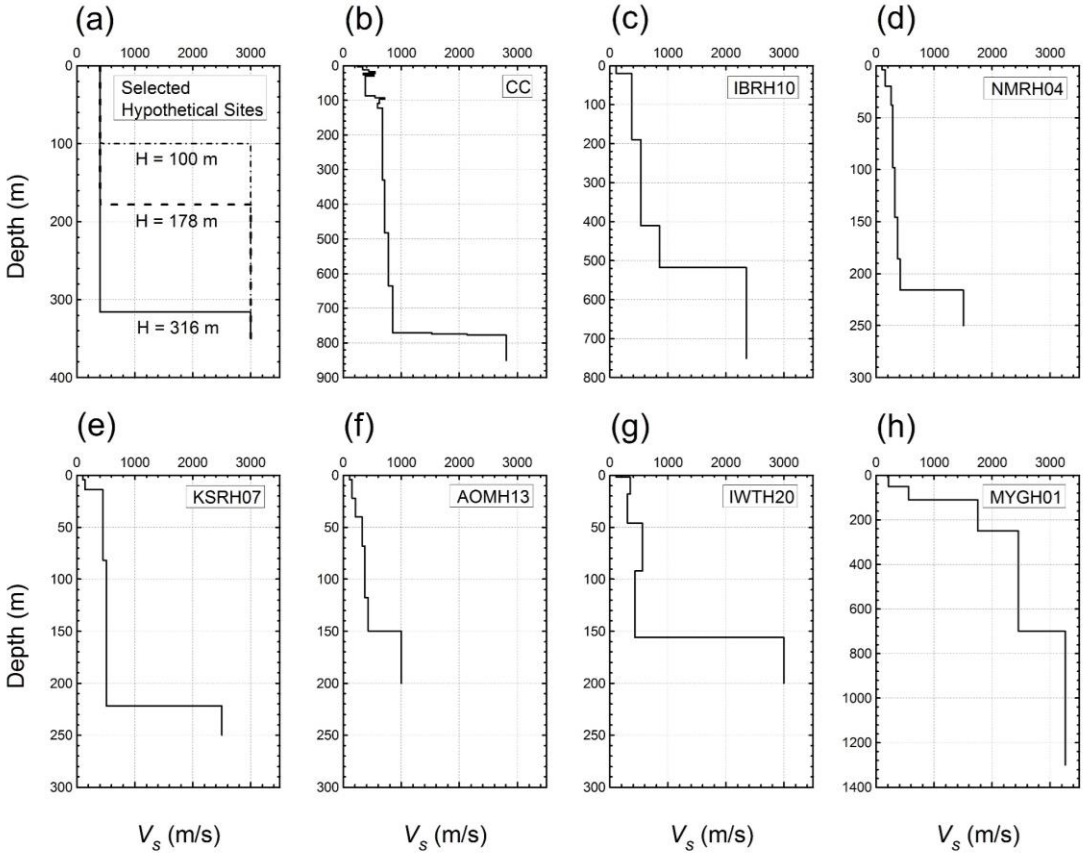

Figure 4.2: Shear wave velocity profiles of hypothetical and realistic sites used in this study.

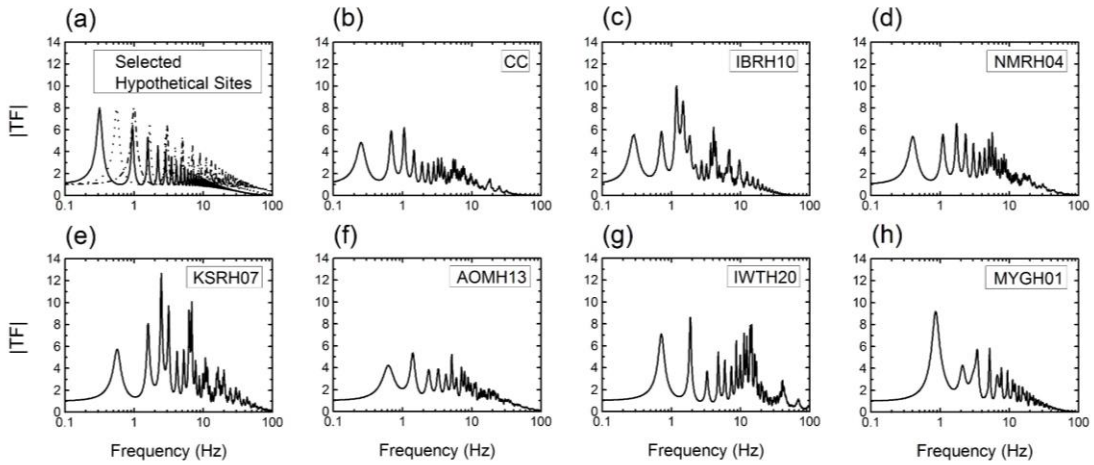

Figure 4.3: Linear-elastic transfer functions for hypothetical and realistic site profiles.

hypothetical sites (Figure 4.3a, for $V_{s,rock}$ = 3,000 m/s) the peaks at the first mode all have about the same amplitude of 8.0, but the peak occurs at the different natural site frequencies (f_{site}). Each of the higher modes has a smaller amplitude than the previous mode. For the same hypothetical sites with $V_{s,rock}$ of 1,000 m/s and 1,730 m/s (not shown), the amplitudes of the first mode peaks are 2.9 and 4.9, respectively. For the realistic sites, Figure 4.3 shows the transfer functions in order from the site with the lowest natural frequency (CC site, f_{site} = 0.25 Hz) to the site with the highest natural frequency (MYGH01 site, f_{site} = 0.86 Hz). Because the realistic sites have non-uniform velocity profiles and different $V_{s,rock}$ (Figure 4.2), each of the transfer functions has a unique shape and the amplitudes at f_{site} ranges widely from 4.2 to 9.2. For many of the realistic sites, the peaks in the transfer function at the higher modes are similar, or larger, than the first mode peak.

In the LE analysis, the material damping for both the soil and rock layers were assumed constant and equal to 1%. In the EQL analysis, which considers strain-

compatible soil properties, nonlinear modulus reduction and damping curves were assigned to the soil layers. The empirical model of Darendeli and Stokoe (2001) was used to generate these nonlinear curves, using the confining pressure derived from the site profile as well as assumed values of plasticity index (PI = 15) and over-consolidation ratio (OCR = 1.0).

4.4 RVT-TS SITE RESPONSE COMPARISONS: LINEAR-ELASTIC CONDITIONS

Time series (TS) and RVT site response analyses are performed for the range of site conditions and input motions discussed previously. The RVT analyses are performed with and without the duration modification from Wang and Rathje (2017). The site response results are shown in terms of the ratio of the surface spectral acceleration to rock spectral acceleration, called the amplification factor (*AF*). For the TS analysis, the *AF* is shown in terms of the mathematical mean of the *AF* values from a suite of 100 time series motions. Full *AF* spectra are first examined for specific cases, and then the *AF* values at the modal site frequencies are compiled for all the cases to show the general performance of the RVT site response analysis when using the modified duration.

4.4.1 Results for Hypothetical Sites

The results from linear-elastic site response analyses for the hypothetical sites are discussed first. These hypothetical sites were used to develop the Wang and Rathje (2017) duration model, and thus the performance should be the best for these cases. Figure 4.4 shows the *AF* results for the 100 m and 316 m hypothetical sites with $V_{s,rock}$ = 3,000 m/s for two earthquake scenarios. For the 316 m site subjected to a *M* 6.5, R =

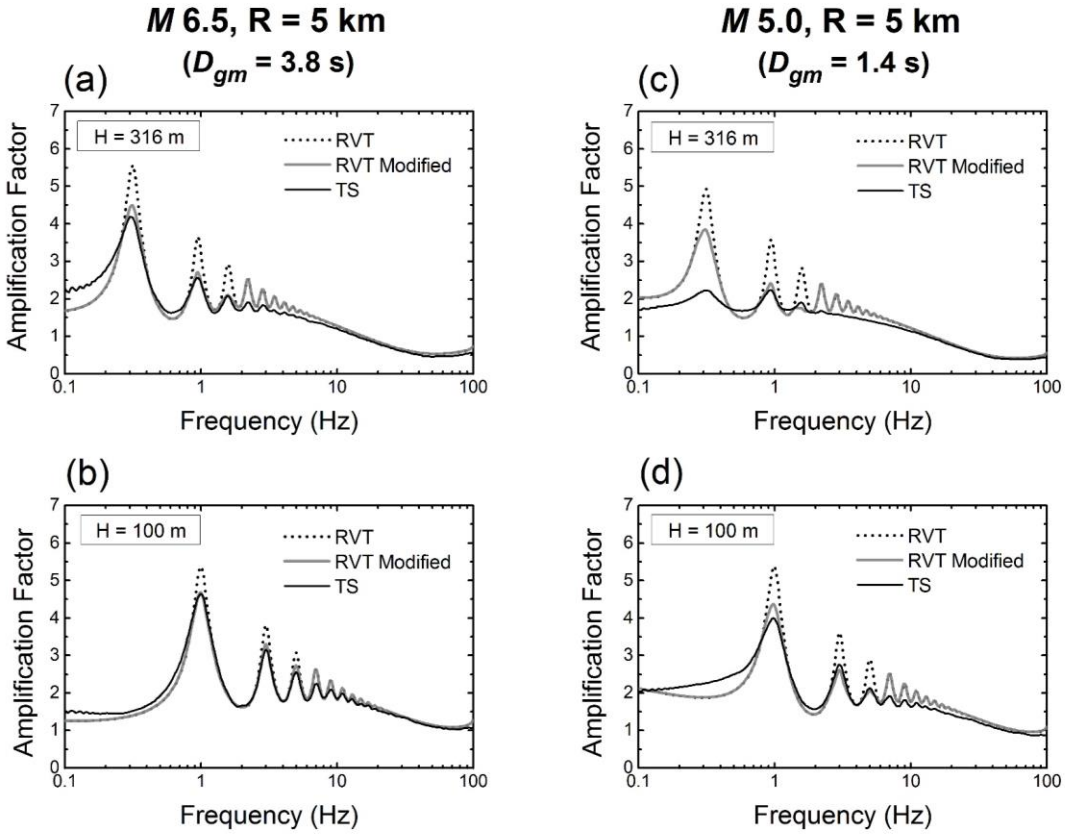

Figure 4.4: *AF* results from linear-elastic RVT and TS analyses for H = 316 m and 100 m hypothetical sites with $V_{s,rock}$ = 3,000 m/s and selected earthquake scenarios.

5 km earthquake motion (Figure 4.4a, D_{gm} = 3.8 s), the RVT *AF* values obtained using the original duration are 30 to 40% larger than the *TS* values at the modal frequencies. When using the modified duration, the RVT *AF* at the site frequencies match the TS *AF* very well. Similar results are observed for the 100 m site subjected to the same earthquake scenario (Figure 4.4b). For the 316 m site subjected to a *M* 5.0, R = 5 km earthquake motion (Figure 4.4c, D_{gm} = 1.4 s), the RVT *AF* values using the original duration are significantly larger than the TS *AF* values (almost 2.5 times larger at the first mode). Using the modified duration improves the RVT-TS match at the second and

third modes, but the RVT *AF* at the first mode remains about 1.6 times larger than the TS *AF*. The significant difference remains in this case because, as described in Wang and Rathje (2016), RVT cannot capture the detailed characteristics of the oscillator response when the natural site frequency is smaller than about half of the corner frequency (f_c) of the input motion (i.e., $f_{site}/f_c \leq 0.5$) due to the significant contribution from the second mode of the site. For the 316 m site (f_{site} = 0.32 Hz) and a *M* 5.0 earthquake (f_c = 1.89 Hz), the ratio of f_{site}/f_c is 0.17 and the effect is significant. For the 100 m site (f_{site} = 1.0 Hz) subjected to the same earthquake scenario, the ratio of f_{site}/f_c is 0.53 and the duration modification successfully improves the RVT *AF* values at modal frequencies (Figure 4.4d). In addition to showing the improvement achieved by the RVT duration modification at the peak values of the *AF* spectra, Figure 4.4 demonstrates that RVT duration modification maintains a realistic shape of the RVT *AF* relative to TS analysis.

To compile the *AF* results for a range of earthquake scenarios, the ratio of RVT *AF* to TS *AF*, noted as RVT/TS, can be plotted as a function of D_{gm} (Figure 4.5). Figure 4.5a shows the RVT/TS results versus D_{gm} for the same two hypothetical sites shown in Figure 4.4, but subjected to all 21 earthquake magnitude/distance scenarios. Figure 4.5a shows the data for the first mode of each site, and the RVT results are computed using the original duration approach. Generally, RVT/TS increases with decreasing D_{gm} for each site, but the data for the 316 m site take on larger values than for the 100 m site. Additionally, the RVT/TS values for the 316 m site approach 1.0 at D_{gm} ~ 30-40 s, while for the 100 m site the RVT/TS values approach 1.0 at D_{gm} ~ 10 s. Based on these observations, the ratio of RVT/TS is more pronounced at smaller D_{gm} and for smaller f_{site}. These effects can be taken into account by considering $D_{gm} \cdot f_{site}$, which represents the ratio between the ground motion duration and the first mode

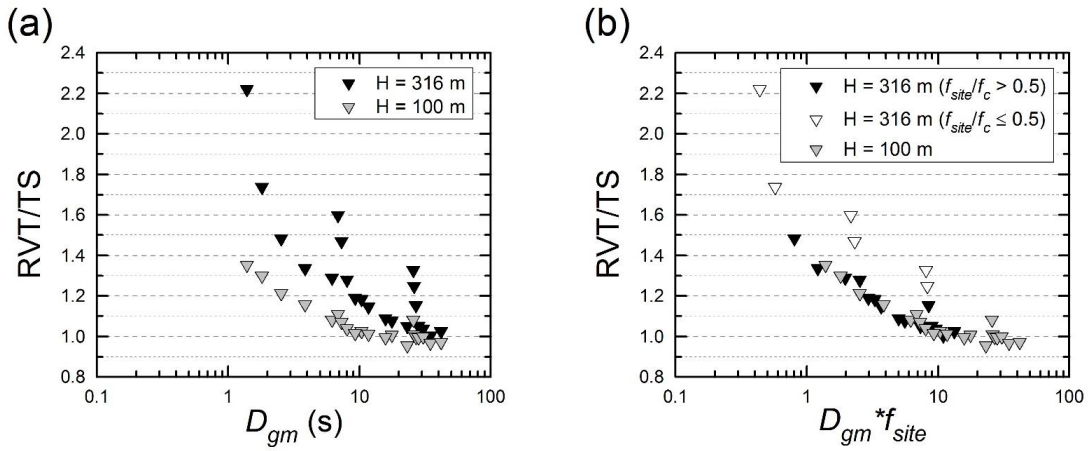

Figure 4.5: Ratio of RVT/TS at the first mode frequency from linear-elastic analysis for the H = 316 m and 100 m hypothetical sites ($V_{s,rock}$ = 3,000 m/s) and all earthquake scenarios. RVT analyses use the original, unmodified duration.

site period. As $D_{gm} \cdot f_{site}$ increases, D_{gm} becomes larger relative to the site period, the duration elongation effects due to site response become smaller, and RVT/TS approaches 1.0. The data in Figure 4.5a are re-plotted in Figure 4.5b using $D_{gm} \cdot f_{site}$, and in this figure the data for the 316 m and 100 m sites follow the same trend. As noted in Wang and Rathje (2017), three clusters of data associated with the 316 m site (at D_{gm} ~ 26 s, 7 s, and 1-2 s) appear to deviate from the general trend in Figure 4.5. These data represent small magnitude earthquakes with $f_{site}/f_c \leq$ 0.5, where RVT analysis does not accurately capture the oscillator response and thus the points do not follow the trend for the data with $f_{site}/f_c >$ 0.5.

Figure 4.6 shows RVT/TS vs. $D_{gm} \cdot f_{site}$ for all nine hypothetical sites, each subjected to the 21 earthquake magnitude/distance scenarios. $D_{gm} \cdot f_{site}$ takes on values between about 0.4 and 40 for these cases. RVT/TS values using the modified duration are shown separately for cases with $f_{site}/f_c > 0.5$ and with $f_{site}/f_c \leq 0.5$. For the first mode (Figure 4.6a), the modified duration results in RVT/TS close to 1.0 for all

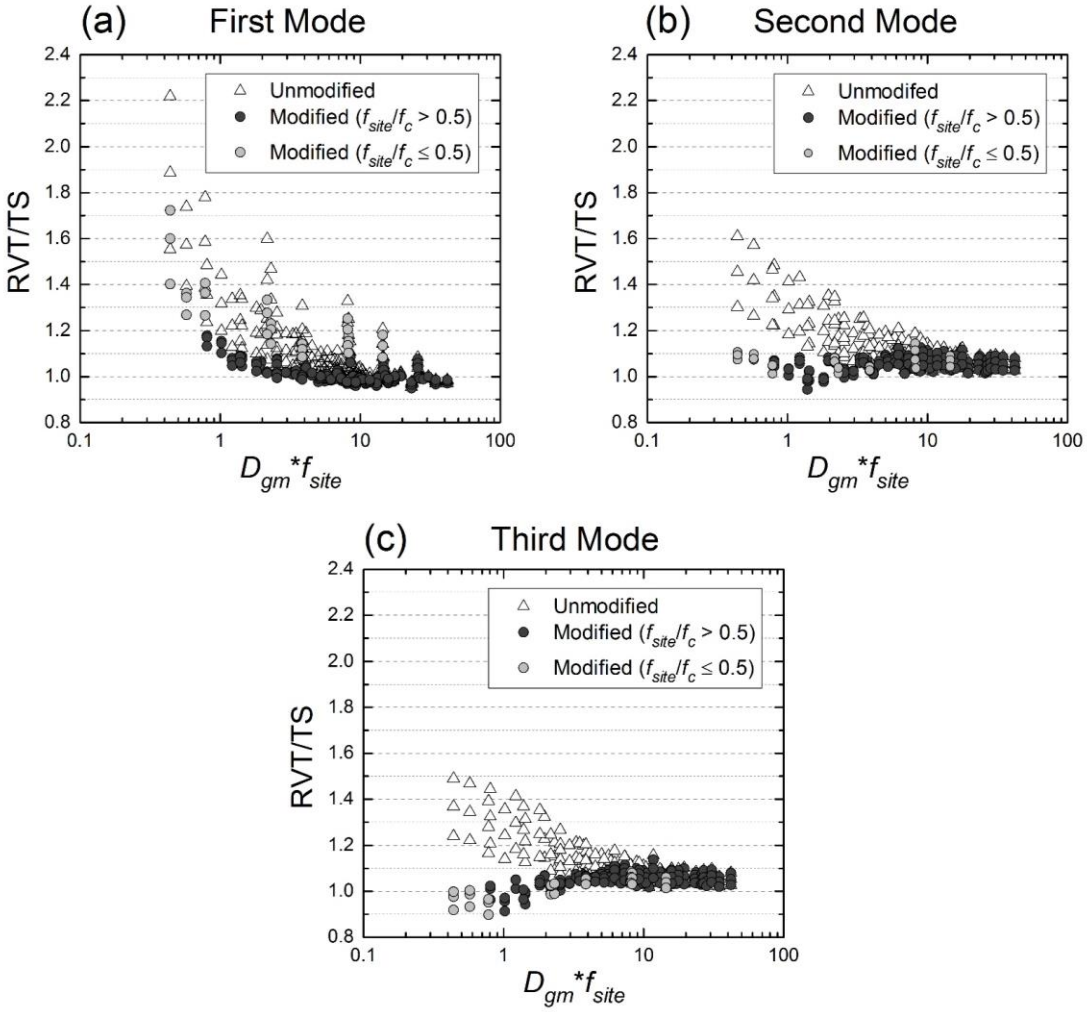

Figure 4.6: Ratio of RVT/TS at modal frequencies as a function of $D_{gm} \cdot f_{site}$ from linear-elastic analysis for all hypothetical sites and all earthquake scenarios.

values of $D_{gm} \cdot f_{site}$ for all cases with $f_{site}/f_c > 0.5$. Without the duration modification, RVT/TS for these cases was between 1.1 and 1.5. For the cases with $f_{site}/f_c \leq 0.5$, the duration modification does not generate values RVT/TS as close to 1.0. The vast majority of these cases have RVT/TS larger than 1.1, with the largest value about 1.7. The results shown in Figure 4.6a for 9 hypothetical sites and 21

earthquake scenarios are consistent with the results from Wang and Rathje (2016), which were based on only three sites and 7 earthquake scenarios. The data in Figure 4.6a confirm that $f_{site}/f_c = 0.5$ is an appropriate barrier that separates the cases ($f_{site}/f_c \leq 0.5$) where duration modification works very well to remove the differences between RVT and TS analyses at the first mode from the cases ($f_{site}/f_c > 0.5$) where duration modification only partially reduces the difference between RVT and TS.

Figures 6b and c show the RVT/TS results for the second and third modes of the sites. For these higher modes, RVT/TS varies smoothly with $D_{gm} \cdot f_{site}$ and no clusters of data are observed, which indicates that the RVT *AF* at the second and third modes are not affected by f_{site}/f_c. The largest values of RVT/TS for analyses using the unmodified duration are about 1.6 and 1.5 for the second and third modes, respectively. When using modified duration, the values of RVT/TS are reduced to between 0.9 and 1.1, which indicates satisfactory improvement to the RVT analysis. In general, the RVT *AF* using the duration modification is within +/- 10% of the TS *AF* regardless of the f_{site}/f_c for the second and third modes. For the third mode (Figure 4.6c), the modified RVT/TS at smaller $D_{gm} \cdot f_{site}$ are systematically smaller than 1.0 but still have values greater than 0.9. It is likely that these smaller values are due to the scatter in the regression for the duration modification for higher modes (Wang and Rathje 2017).

The results in Figure 4.6 indicate that the duration modification developed by Wang and Rathje (2017) improves linear-elastic site amplification predictions from RVT site response analyses for a wide range of earthquake scenarios for sites that have simple shear wave velocity profiles. The only exceptions are cases with $f_{site}/f_c \leq 0.5$ and these exceptions only occur at the first mode.

4.4.2 Results for Realistic Sites

The realistic sites have layered and more complex shear wave velocity profiles, and thus represent a broader cross-section of potential soil sites. Linear-elastic site response analyses using the TS and RVT approach are performed for the realistic sites. Figure 4.7 shows RVT and TS *AF* spectra for three cases – the CC site (f_{site} = 0.25 Hz) for a *M* 6.5, R = 5 km earthquake, the KSRH07 site (f_{site} = 0.57 Hz) for a *M* 6.0, R = 5 km earthquake, and the MYGH01 site (f_{site} = 0.86 Hz) for a *M* 5.5, R = 5 km earthquake. These site and earthquake scenario combinations were selected to ensure $f_{site}/f_c > 0.5$ and to focus on smaller D_{gm} where duration elongation is the most significant.

For the CC site (f_{site}/f_c = 0.74, Figure 4.7a), the RVT *AF* at the first three modes are about 30% larger than the TS *AF* when using the unmodified duration. The duration modification brings the RVT *AF* within 10% of the TS *AF* for the first mode, and at the second and third modes RVT and TS are essentially the same. For the KSRH07 site (f_{site}/f_c = 0.95, Figure 4.7b), the RVT *AF* are about 30% larger than the TS *AF* for the first three modes when using the unmodified duration. The largest *AF* for the KSRH07 site actually occurs at the third mode of the site (~ 2.3 Hz) due to the large peak in the |TF| at the third mode (Figure 4.3e) that is the result of the thin, softer layer near the surface (Figure 4.2e). Despite the fact that the shape of |TF| for the KSRH07 site differs greatly from the |TF| of the hypothetical sites (Figure 4.3a), the RVT analysis using the modified duration successfully reduces the difference between the RVT and TS *AF* at the first three modes.

For the MYGH01 site (f_{site}/f_c = 0.81, Figure 4.7c), the RVT *AF* is about 25% larger than the TS *AF* for the first mode when using the unmodified duration, but the difference is significantly less at the second and third modes. The *AF* is much larger at

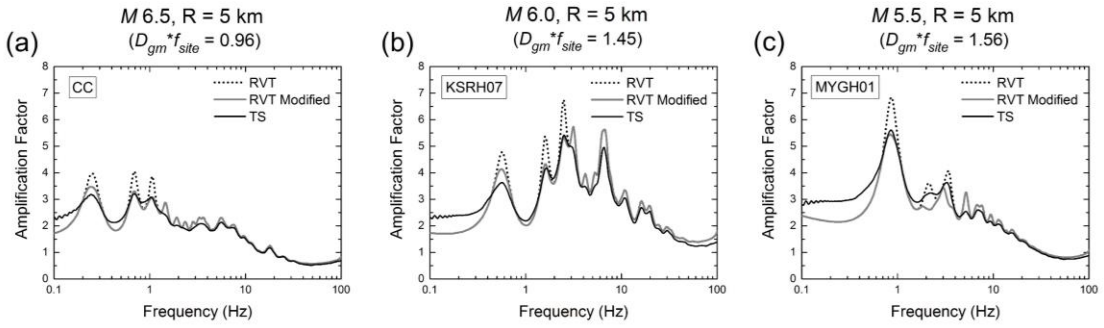

Figure 4.7: *AF* results from linear-elastic RVT and TS analyses for selected realistic sites and earthquake scenarios.

the first mode (*AF* ~ 5.5) as compared to the second and third modes (*AF* ~ 3), which is directly due to the larger peak in the |TF| at the first mode as compared to the higher modes (Figure 4.3g). The smaller amplitudes in the |TF| at the higher modes generates less duration elongation at these modes, and thus the RVT and TS *AF* are more similar. After the duration modification is applied, the RVT and TS *AF* match very well at the first mode but at the second and third modes the RVT *AF* become about 20% smaller than the TS *AF*, indicating excessive duration modification at the higher modes. The duration modification for all three modes is related to the amplitude of the transfer function at the first mode ($Amp_{|TF|,1}$); thus a large $Amp_{|TF|,1}$ results in a large duration modification and a large reduction in the RVT *AF* for all three modes. The hypothetical sites also have larger $Amp_{|TF|}$ at the first mode compared with the higher modes, but the difference is not as large as for MYGH01. Duration modification models that utilize directly the $Amp_{|TF|}$ for each mode were investigated, but these models did not perform well for sites where the $Amp_{|TF|}$ at the higher modes are larger than at the first mode.

To compile the *AF* results for all of the realistic sites and earthquake scenarios, the ratio of RVT/TS is plotted against $D_{gm} \cdot f_{site}$ in Figure 4.8. The $D_{gm} \cdot f_{site}$ for

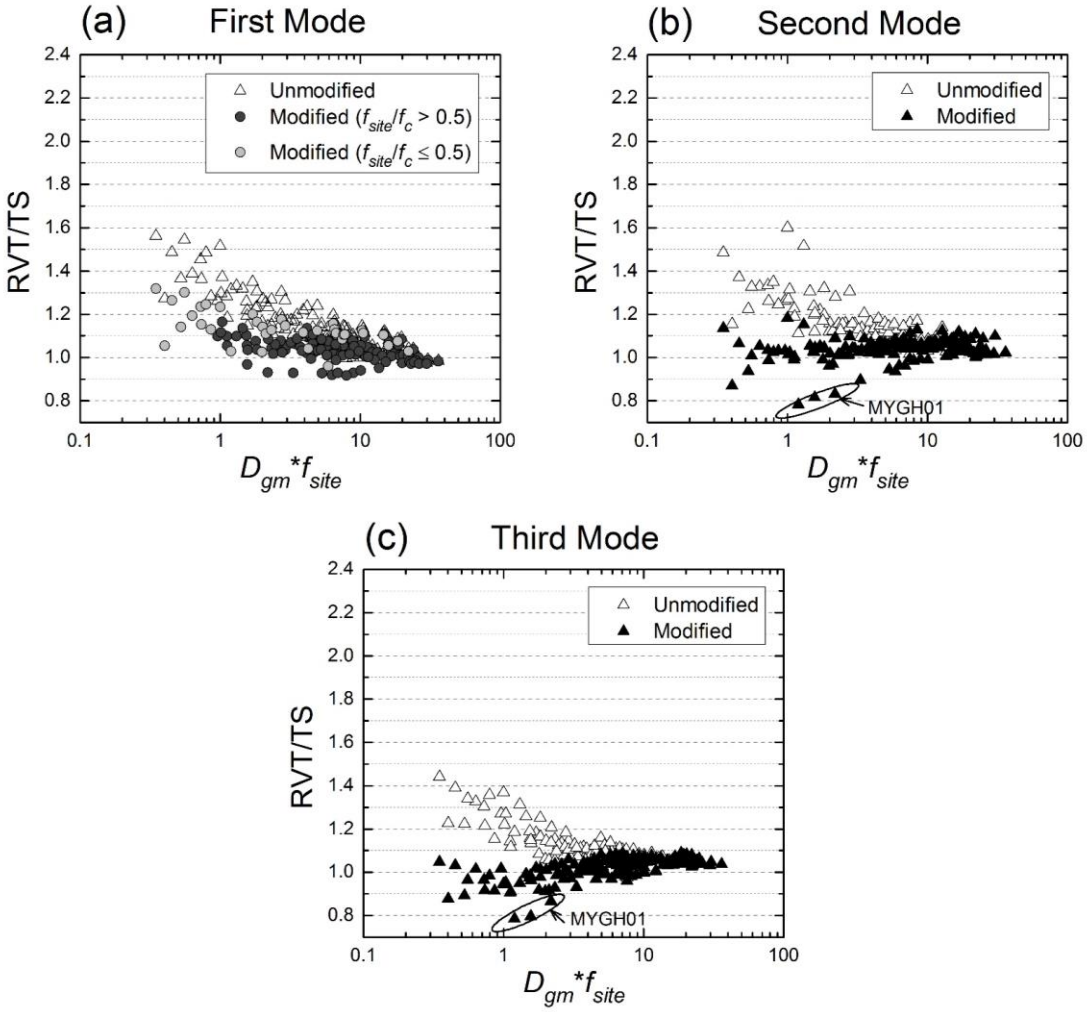

Figure 4.8: Ratio of RVT/TS at modal frequencies as a function of $D_{gm} \cdot f_{site}$ from linear-elastic analysis for all realistic sites and all earthquake scenarios.

the realistic sites range from 0.3 to 40, similar to the data for the hypothetical sites. Again, the results for scenarios with $f_{site}/f_c > 0.5$ are distinguished from the results with $f_{site}/f_c \leq 0.5$. Similar to the results for the hypothetical sites, RVT/TS increases with decreasing $D_{gm} \cdot f_{site}$when the original, unmodified duration is used in the RVT analysis. The largest value of RVT/TS is approximately 1.6 for the first mode of the

realistic sites, while this value was as large as 2.2 for the hypothetical sites (Figure 4.6). For the cases with $f_{site}/f_c > 0.5$, when the duration modification is applied almost all of the RVT/TS are within the range of 0.9 to 1.1 range for the first mode. For the cases with $f_{site}/f_c \leq 0.5$, the RVT/TS are mostly above 1.1 after the duration modification is applied, but the values are still greatly reduced compared with the RVT/TS before the duration modification. For the second and third modes (Figures 4.8b and c), the duration modification brings the RVT *AF* for all $D_{gm} \cdot f_{site}$ within +/- 10% of the TS *AF* except for some cases for the MGYH01 site where RVT/TS is as small as about 0.8. It appears from Figure 4.8 that despite the complexity of the realistic site profiles, the duration modification developed by Wang and Rathje (2017) adequately improves the RVT amplification relative to TS analysis for $f_{site}/f_c > 0.5$.

4.5 RVT-TS SITE RESPONSE COMPARISONS: EQUIVALENT-LINEAR CONDITIONS

Equivalent-linear (EQL) analyses are performed for the realistic shear wave velocity profiles to investigate the difference between RVT and TS amplification at different input motion intensities and induced shear strain levels.

The input motions for the EQL analysis are based on the same earthquake magnitudes and distances used in the LE analysis. However, the source spectrum used in SMSIM is representative of a point source, which is only appropriate for smaller magnitude earthquakes or for larger magnitude earthquakes at larger distances. For larger earthquakes at shorter distances, the large extent of the fault rupture cannot be modeled as a point source. In these cases, seismic waves arrive at a site from different parts of the fault rupture at a range of distances. If one uses the closest distance to the fault (R_{CD}) in an SMSIM simulation for a large magnitude earthquake, excessively large

levels of shaking are predicted. This issue was not critical for LE analysis, but for EQL analysis the modeling of appropriate intensities of ground shaking is essential to ensure realistic estimates of the induced strain.

To account for the effect that the motions at a site are generated from different segments of the fault rupture, an effective distance (R_{EFF}) can be used in a point-source simulation instead of R_{CD} (Boore 2009). R_{EFF} represents an equivalent point-source distance that accounts for the effects of the different distances associated with each segment of the fault rupture, and R_{EFF} is always equal to or larger than R_{CD}. In this study, the site is assumed to be located perpendicular to the mid-point of the rupture of a linear fault, and values of R_{EFF} were computed for each magnitude and three values of R_{CD} (5 km, 20 km, and 100 km). For the smaller magnitudes and for R_{CD} = 100 km, the computed $R_{EFF} \sim R_{CD}$, but for the larger magnitudes and at shorter distances $R_{EFF} > R_{CD}$. For R_{CD} = 5 km R_{EFF} varies from 5 to 15 km, for R_{CD} = 20 km R_{EFF} varies from 20 to 35 km, and for R_{CD} = 100 km R_{EFF} varies from 100 to 115 km.

The response spectra of the input motions generated using *M* and R_{EFF} are shown in Figure 4.9. In general, for each R_{CD} the rock response spectra increase with magnitude. However, for closer distances (R_{CD} = 5 km and 20 km) there is a magnitude

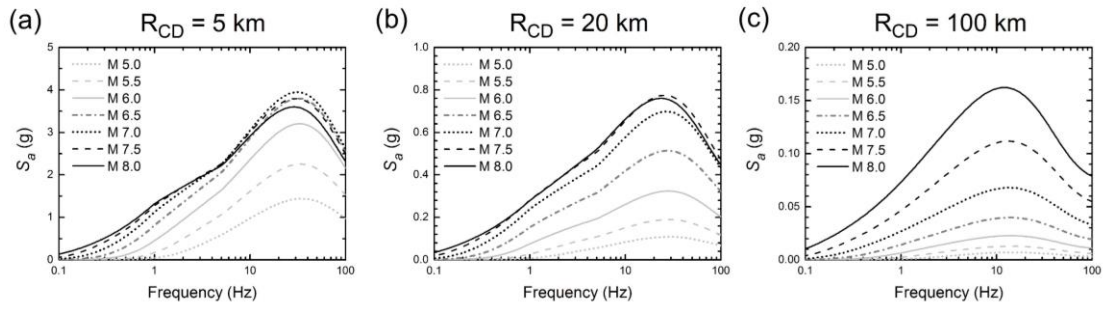

Figure 4.9: Response spectra of input motions generated using SMSIM (Boore 2005) and accounting for finite-source effects.

above which the response spectra do not change considerably with *M*. This occurs at *M* > 6.0 for R_{CD} = 5 km and at *M* > 7.0 for R_{CD} = 20 km. This magnitude saturation occurs because the increase in earthquake energy associated with larger *M* is offset by an increase in R_{EFF} due to the increased length of fault rupture. When using R_{EFF} the input response spectra have more realistic intensities with the largest S_a ~ 4.0 g and the largest PGA ~ 1.6 g.

Figure 4.10 compares the RVT and TS EQL results for selected cases for the CC site that illustrate the influence of input intensity and induced strain levels on the results. Across the three input motions shown, the first peak of the *AF* spectra shifts to the left, indicating a decrease in f_{site} as the input intensity increases with decreasing R_{CD}. This decrease in f_{site} is caused by the larger values of induced shear strain, which leads to a smaller stiffness through the nonlinear modulus reduction curve for the soil. For *M* = 6.5, R_{CD} = 100 km with $D_{gm} \cdot f_{site}$ = 7.05 (f_{site}/f_c = 0.61, Figure 4.10a), the RVT and TS *AF* are very similar due to the agreement in the induced shear strain profiles (Figure 4.10d) and the large value of $D_{gm} \cdot f_{site}$. Note that the original ground motion duration is used in the RVT calculation of the maximum shear strain. The RVT *AF* at the first three modes are larger than the TS *AF* by about 10%, but the duration modification does not reduce this difference because of the large value of $D_{gm} \cdot f_{site}$.

For *M* = 6.5, R_{CD} = 20 km with $D_{gm} \cdot f_{site}$ = 2.34 (f_{site}/f_c = 0.71, Figure 4.10b), the site amplification is reduced at each mode relative to the R_{CD} = 100 km input motion in Figure 4.10a, particularly at the higher modes, due to the larger values of induced shear strain (Figure 4.10e). The induced strains obtained from RVT and TS analysis are very similar at all depths, with relative differences less than 10%. The difference between the RVT and TS *AF* are larger here than for the R_{CD} = 100 km input motion due to the smaller value of $D_{gm} \cdot f_{site}$, but the duration modification successfully

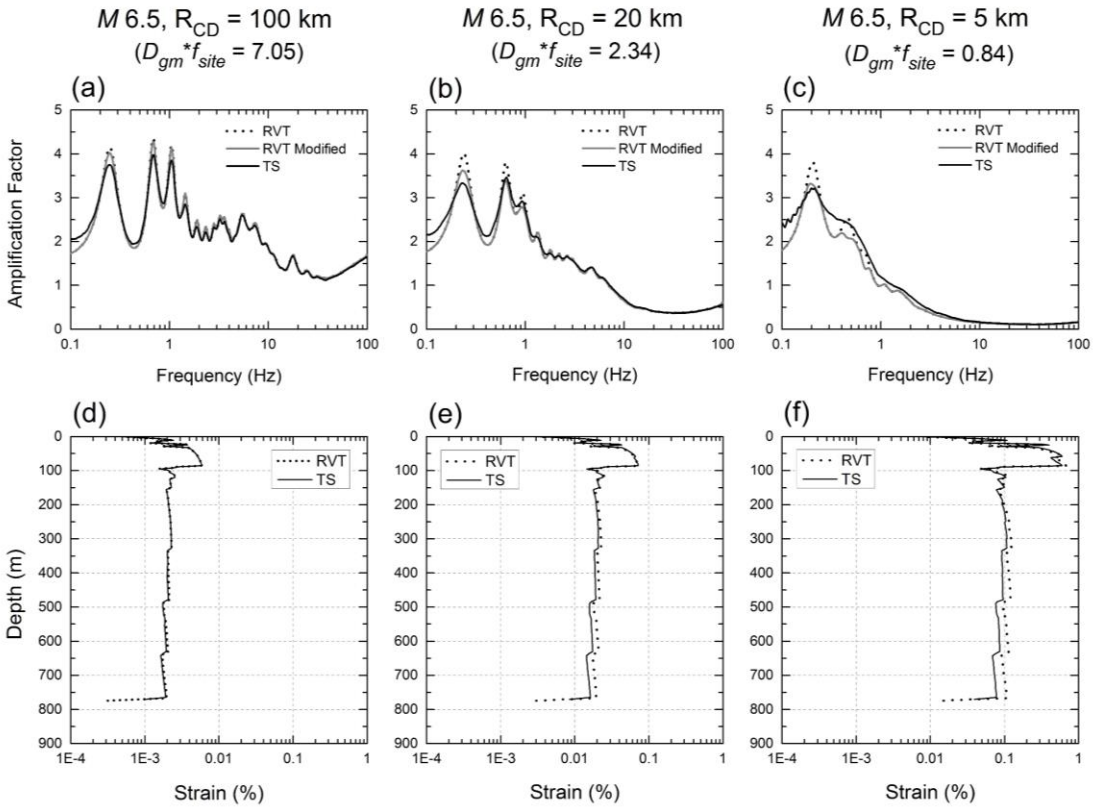

Figure 4.10: *AF* results and shear strain profiles from equivalent linear RVT and TS analyses for the CC site subjected to ground motions with different intensities.

improves the RVT *AF* at the modal frequencies. In this case, after the duration modification is applied, the RVT *AF* is within 10% if the TS *AF*.

The *M* 6.5, R_{CD} = 5 km scenario with $D_{gm} \cdot f_{site}$ = 0.84 (f_{site}/f_c = 0.74, Figure 4.10c) induces the largest shear strains with values mostly between 0.1% and 1.0% (Figure 4.10f). The large strain level further reduces the natural site frequency and more significantly damps out the higher modes. In fact, only the first mode is observed clearly in the *AF* spectra in Figure 4.10c. At the first mode, the RVT *AF* is larger than the TS *AF* by about 20%, and using the duration modification in the RVT analysis results in an excellent match with the TS analysis. However, at frequencies between 0.3 Hz to 1.0

Hz, the RVT *AF* becomes smaller than the TS *AF* by about 5% to 15% when the duration modification is applied. These frequencies represent the frequency range associated with the second and third modes of the site. A possible explanation for this is that the strains predicted by RVT are 20% to 30% larger than those predicted by TS analysis at depths larger than 300 m. The RVT predicted strains are larger likely because the duration used in the computation of maximum strain may be longer than the ground motion duration due to the fact that strains are more closely associated with ground velocity than ground acceleration (Kottke and Rathje 2013). Nonetheless, the duration modification results in the RVT *AF* having a similar shape as the TS *AF* across the frequencies shown.

The data from EQL analysis are compiled and plotted in terms of RVT/TS versus $D_{gm} \cdot f_{site}$ in Figure 4.11. Results are only shown for analyses where the maximum shear strain was less than 1.0%, because EQL analysis becomes unreliable at larger strains. Note that the f_{site} used to compute $D_{gm} \cdot f_{site}$ in Figure 4.11 is obtained from the EQL analysis, so it is generally smaller than the small-strain f_{site} used in the LE analysis. Conversely, the D_{gm} used to compute $D_{gm} \cdot f_{site}$ is equal to or greater than used in the LE analysis because R_{EFF} is used instead of R_{CD}. Similar to the results for LE conditions, the EQL RVT analyses predict larger *AF* than TS analysis and this effect is most pronounced at smaller $D_{gm} \cdot f_{site}$. When using the unmodified duration RVT predicts amplification at the first mode as much as 1.6 times larger than the TS analysis, and the duration modification reduces the values of RVT/TS and makes them closer to 1.0. For the cases with $f_{site}/f_c > 0.5$, all the RVT/TS are concentrated around 1.0. For the cases with $f_{site}/f_c \leq 0.5$, only about half of the RVT/TS values are between 0.9 and 1.1 after the duration modification is applied. For the second and third modes, more than half of the modified RVT/TS values are between 0.9 and 1.1, except for the range of

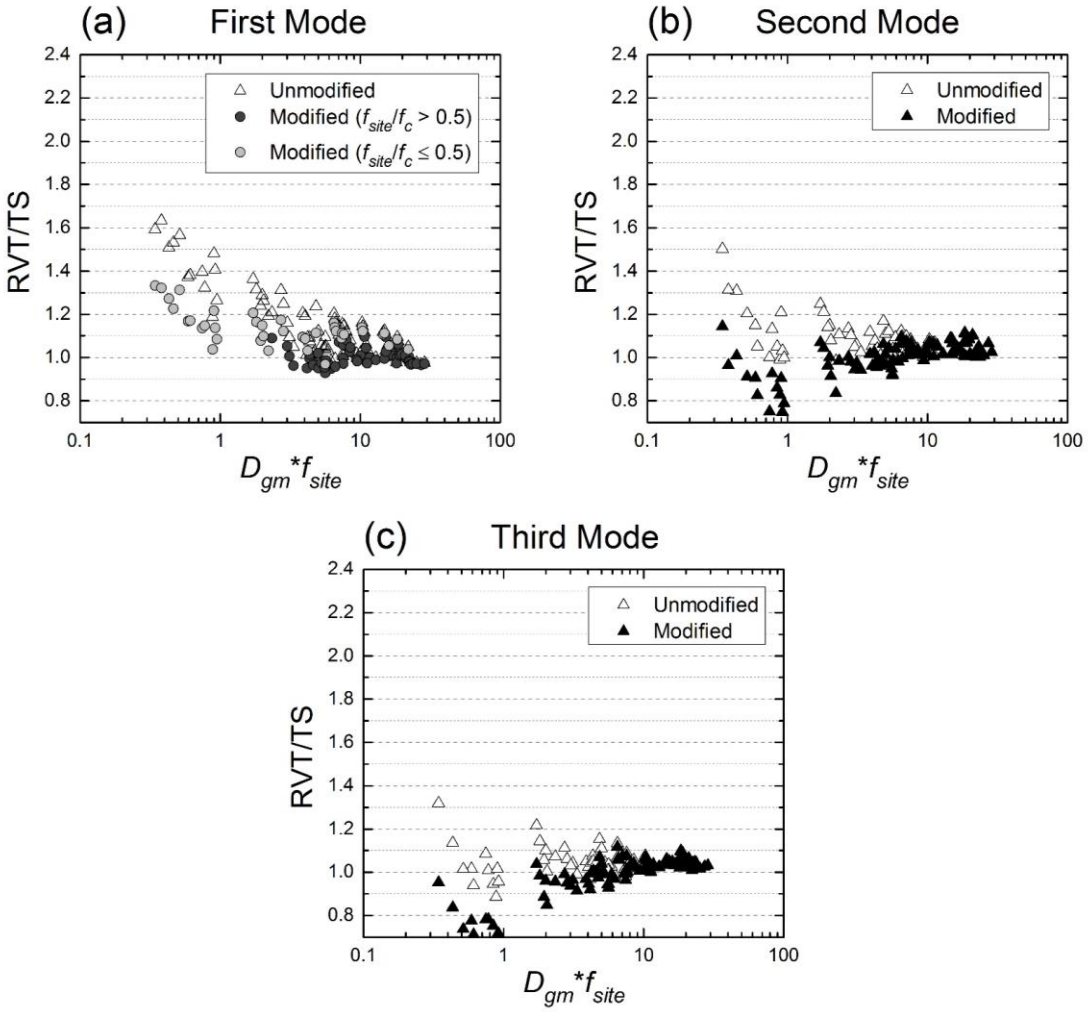

Figure 4.11: Ratio of RVT/TS at modal frequencies as a function of $D_{gm} \cdot f_{site}$ from equivalent-linear analysis for all realistic sites and all earthquake scenarios.

$D_{gm} \cdot f_{site}$ ~ 0.6 – 2.0 where the modified RVT/TS values become significantly smaller than 0.9. These $D_{gm} \cdot f_{site}$ values correspond with scenarios of small magnitude/short distance earthquakes, where the largest discrepancies are found between RVT and TS induced shear strains.

In general, the RVT/TS results obtained from the EQL analyses in Figure 4.11 are consistent with the results from the LE analyses, although there appears to be somewhat more scatter in the EQL results. This scatter is likely a result of differences in the strains predicted by TS and RVT analyses. Figure 4.12 plots the maximum shear strain predicted by RVT versus the average value of the maximum shear strain for the 100 TS motions for each earthquake scenario. It is shown that when maximum shear strain is less than 0.1%, the strains obtained from RVT and TS analyses agree well. When the maximum shear strain is between 0.1 – 1%, scatter is observed, indicating that the difference between the maximum strains induced by RVT and TS analyses become larger, with the largest relative difference ~ 50%. Another issue that affects the RVT-TS comparison for EQL analyses is the influence of motion-to-motion variability in the strains generated by each TS motion for the same scenario. Because each TS motion

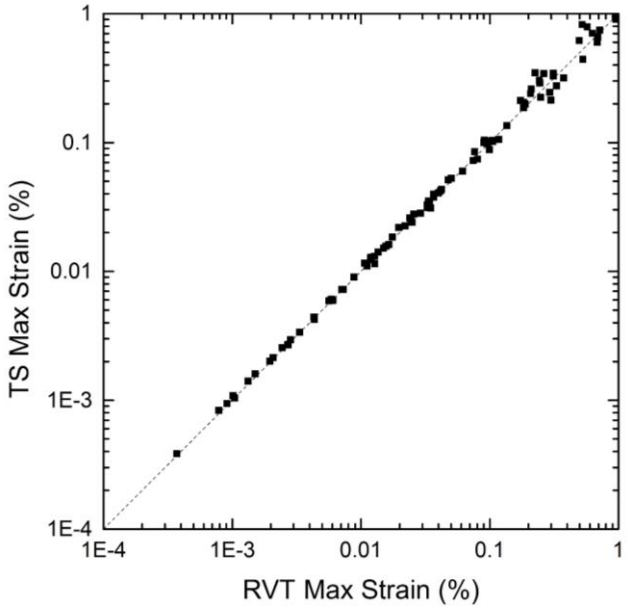

Figure 4.12: Maximum shear strain from RVT analysis vs. maximum shear strain from TS analysis.

induces a slightly different strain (i.e., across the 100 motions, the strains may vary by as much as +/- 45%, depending on the maximum strain), the associated peak in the site transfer function also varies, which reduces the *AF* at the average site frequency. Despite these issues, Figure 4.11 indicates that the duration modification appropriately reduces the RVT *AF* for EQL analysis such that it better matches the results from TS analysis, particularly when $f_{site}/f_c > 0.5$.

4.6 CONCLUSIONS

RVT site response analysis is commonly used to evaluate site effects in seismic hazard studies for nuclear facilities. However, recent research has shown that RVT can predict site amplification as much as 1.6 times larger than TS analysis at the natural frequencies of a site (Kottke and Rathje 2013, Wang and Rathje 2016), but that this effect can be reduced if the elongation of duration due to site response is taken into account. Wang and Rathje (2017) developed an empirical model to predict this duration elongation associated with the first three modes of a site, and this paper evaluated the performance of RVT site response analysis when the Wang and Rathje (2017) duration modification is incorporated.

RVT site response analysis using the modified surface duration was evaluated using both LE and EQL site response analyses. Simple, hypothetical shear wave velocity profiles, as well as more realistic and complex shear wave velocity profiles, were used in the analyses. The site amplification results from the LE analysis show that the modification of duration reduces the site amplification predicted by RVT analysis so that it is more consistent with the amplification predicted by TS analysis. Before applying the duration modification, the RVT amplification factors can be as much as 1.6 to 2.2

larger than the TS amplification factors. The largest differences are observed for cases with smaller f_{site} and input motions with smaller durations (D_{gm}). These cases, which generally correspond with $D_{gm} \cdot f_{site} < 1.0$, represent situations where the vibration of the low frequency (i.e., long period) site coupled with the short ground motion duration result in the largest duration elongation. After duration modification is applied to the RVT analysis, the vast majority of RVT amplification factors are within +/- 10% of the TS amplification factors. This improvement is observed at all of the three modes considered, and for both the hypothetical sites and realistic sites. The scenarios where the duration modification does not perform as well are associated with deep sites subjected to small magnitude earthquakes (i.e., scenarios where $f_{site}/f_c \leq 0.5$), because RVT analysis does not accurately capture the oscillator response due to the significant contribution to the response from the second mode of the site (Wang and Rathje 2016).

When strain-compatible soil properties are considered using EQL analyses, both the RVT and TS amplifications are affected similarly by the induced shear strain levels. As the induced shear strain increases, the modes shift to smaller frequencies, the peaks in amplification decrease, and the higher modes become further damped and gradually disappear. Consistent with the results from LE analysis, when the duration modification is applied to EQL RVT site response analysis, the RVT amplification factors are mostly within +/- 10% of the TS amplification factors. More scatter is observed in the difference between RVT and TS amplification for EQL analysis than for LE analysis, due predominantly to slight differences in the induced shear strains from RVT and TS analyses.

4.7 Data and Resources

The stochastic time series used in the analysis were created using the latest version of the Stochastic-Method SIMulation (SMSIM) programs obtained from http://daveboore.com/software_online.html (last accessed April 2017). The time-series site response analysis in this study were performed using the program Strata (http://nees.org/resorces/strata, last accessed April 2017) and the random vibration theory site response analyses were performed using scripts written in MATLAB (http://www.mathworks.com, last accessed April 2017).

4.8 Acknowledgements

This research was supported by funding from Pacific Gas & Electric, Co. through Dr. Norman Abrahamson and the Nuclear Regulatory Commission under grant NRC-HQ-60-15-C-0005. This support is gratefully acknowledged.

4.9 References

Boore, D. M. (2003). Simulation of ground motion using the stochastic method. *Pure Appl. Geophys.* **160(3-4)** 635-676.

Boore, D. M. (2005). *SMSIM---Fortran programs for simulating ground motions from earthquakes: Version 2.3---A Revision of OFR 96-80-A*. US Geological Survey open-file report.

Boore, D. M. (2009). Comparing Stochastic Point-Source and Finite-Source Ground-Motion Simulations: SMSIM and EXSIM. *Bull. Seism. Soc. Am.* **99(6)** 3202-3216.

Boore, D.M. (2015). *Point-Source Stochastic-Method Simulations of Ground Motions for the PEER NGA-East Project*, Chapter 2 in NGA-East: Median Ground-Motion Models

for the Central and Eastern North America Region, PEER Report 2015/04, Pacific Earthquake Engineering Research Center, 11-49.

Boore, D. M., and W. B. Joyner (1984). A note on the use of random vibration theory to predict peak amplitudes of transient signals. *Bull. Seism. Soc. Am.* **74(5)** 2035-2039.

Boore, D. M., and E. M. Thompson (2012). Empirical Improvements for Estimating Earthquake Response Spectra with Random-Vibration Theory. *Bull. Seism. Soc. Am.* **102(2)** 761-772.

Boore, D.M., and E. M. Thompson (2015). Revisions to some parameters used in stochastic-method simulations of ground motion, *Bull. Seism. Soc. Am.* **105(2A)** 1029-1041.

Cartwright, D. E., and M. S. Longuet-Higgins (1956). The statistical distribution of the maxima of a random function. *Proc. Roy. Soc. Lond. Math. Phys. Sci.* **237(1209)** 212-232.

Darendeli, M. B. (2001). Development of a new family of normalized modulus reduction and material damping curves, *Ph.D. Thesis*, The University of Texas, Austin.

Graizer, V. (2014). Comment on "Comparison of time series and random-vibration theory site-response methods" by Albert R. Kottke and Ellen M. Rathje. *Bull. Seism. Soc. Am.* **104(1)** 540-546.

Kottke, A. R., and E. M. Rathje (2013). Comparison of Time Series and Random-Vibration Theory Site-Response Methods. *Bull. Seism. Soc. Am.* **103(3)** 2111-2127.

Nuclear Regulatory Commission (NRC) (2007). *Regulatory Guide 1.208: A Performance-based Approach to Define the Site-specific Earthquake Ground Motion*, United States Nuclear Regulatory Commission, Washington, DC.

Vanmarcke, E. H. (1975). On the distribution of the first-passage time for normal stationary random processes. *J. Appl. Mech.* **42(1)** 215-220.

Wang, X., and Rathje, E. M. (2016). Influence of Peak Factors on Site Amplification from Random Vibration Theory Based Site-Response Analysis. *Bull. Seism. Soc. Am.* **106(4)** 1733-1746.

Wang, X., and Rathje, E. M. (2017). Development of Ground Motion Duration Models for Use in Random Vibration Theory Site Response Analysis.

Chapter 5: Conclusions And Recommendations For Future Work

5.1 CONCLUSIONS

This research investigated two critical parts of RVT site response analysis – the statistical peak factor model and the duration used in the calculation of the *rms* acceleration. In the investigation, RVT and time series (TS) site response analyses were performed for a wide range of sites as well as earthquake scenarios (i.e., magnitudes and distances) and the site amplification results compared. Based on the investigation, a model of peak factor that accounts for the statistical dependence between peaks is recommended for use in RVT site response analysis. In addition, a model of duration that accounts for not only the effect of oscillator response but also the effect of site properties on duration is developed. The RVT analysis that incorporated these findings is applied to various shear velocity profiles and for strain-compatible soil properties associated with equivalent-linear analysis. The site amplification results indicate that the improved RVT site response analysis generally works well to reduce the discrepancy between RVT and TS amplification for a wide range of situations.

A critical part of the RVT approach is the peak factor. The peak factor model proposed by Cartwright and Longuet-Higgins (CL peak factor, 1956) has traditionally been used in stochastic ground motion simulations (e.g., Boore 2003) and RVT site response analyses (e.g., Kottke and Rathje 2013). The Vanmarcke (1975) peak factor is an alternative model that accounts for the statistical dependence of peaks in a signal, which is important for narrow-band processes such as oscillator responses in seismic analyses. The site amplification results of this research show that the amplification factor (*AF*) predicted by RVT analysis at the modal frequencies of a site is larger than

predicted by TS analysis, regardless of which peak factor model is used. However, the RVT site amplification predicted using the Vanmarcke peak factor is more similar to the TS site amplification than the RVT site amplification predicted using the CL peak factor. Therefore, the Vanmarcke peak factor model is recommended for use in both RVT-based stochastic ground motion simulations (e.g., Boore and Thompson 2015) and RVT site response analyses.

Although the Vanmarcke peak factor predicts RVT site amplification more similar to TS analysis, differences remain for some situations. A main cause of this difference is associated with the duration used when calculating the root-mean-square (*rms*) oscillator response. Current implementations of RVT site response analysis use the same duration (i.e., D_{rms}) for the rock and surface motions. The D_{rms} accounts for the change in duration due to oscillator response and can be predicted by D_{rms} models. The D_{rms} model developed by Boore and Thompson (2015) is the most recent model, and importantly, it is the only model that is based on the Vanmarcke (1975) peak factor. However, the D_{rms} model does not consider the fact that the dynamic ground response generally increases the duration of motion and the duration of the oscillator response. Thus, the use of the D_{rms} of the input motion in the prediction of the surface response causes an excessive RVT surface response, particularly when a low frequency site is subjected to a ground motion of short duration.

To account for the influence of site response on duration, a modification to D_{rms} is developed in this research. The development of the modification model is based solely on time domain observations of D_{5-95} durations of the oscillator response for input rock motions ($D_{5-95,rock}$) and computed surface motions ($D_{5-95,surf}$) from TS analysis. Empirical models for $D_{5-95,rock}$ and $D_{5-95,surf}$ were developed as functions of the ground motion duration (D_{gm}), oscillator frequency, the frequencies of the first

three modes of the site, and the transfer function amplitude at the first mode frequency of the site ($Amp_{|TF|,1}$). At each oscillator frequency, $D_{5-95,surf}/D_{5-95,rock}$ is computed from the empirical models and multiplied by the corresponding D_{rms} at each frequency to obtain $D_{rms,surf}$. This $D_{rms,surf}$ value is used in the RVT *rms* calculation for the surface motion. Using this approach, the effect of site response on the oscillator duration can be predicted for a large range of site conditions and earthquake motions without requiring any time domain site response analyses.

RVT site response analysis using the modified surface duration (i.e., $D_{rms,surf}$) was evaluated using both linear-elastic (LE) and equivalent linear (EQL) site response analyses. Simple hypothetical shear wave velocity profiles, as well as more realistic and complex shear wave velocity profiles, were used in the analyses. The site amplification results from the LE analysis show that the modification of duration reduces the site amplification predicted by RVT analysis so that it is more consistent with the amplification predicted by TS analysis. After duration modification is applied to the RVT analysis, the vast majority of RVT amplification factors are within +/- 10% of the TS amplification factors. This improvement is observed at all of the three modes considered, and for both the hypothetical sites and realistic sites. The scenarios where the duration modification does not perform as well are associated with deep sites subjected to small magnitude earthquakes (i.e., scenarios where $f_{site}/f_c \leq 0.5$, with f_c the corner frequency of the input FAS), because RVT analysis does not accurately capture the oscillator response due to the significant contribution to the response from the second mode of the site (Wang and Rathje 2016).

When strain-compatible soil properties are considered using EQL analyses, both the RVT and TS amplifications are affected similarly by the induced shear strain levels. As the induced shear strain increases, the modes shift to smaller frequencies, the peaks in

amplification decrease, and the higher modes become further damped and gradually disappear. Consistent with the results from LE analysis, when the duration modification is applied to EQL RVT site response analysis, the RVT amplification factors are mostly within +/- 10% of the TS amplification factors. More scatter is observed in the difference between RVT and TS amplification for EQL analysis than for LE analysis, due predominantly to slight differences in the induced shear strains from RVT and TS analyses.

5.2 RECOMMENDATIONS FOR FUTURE WORK

The results from this research show that there are still a few situations where the site amplification obtained from the improved RVT analysis does not match the average TS site amplification perfectly. These cases suggest that further improvements may be needed in RVT site response analysis and the recommendations of future work are given below.

It is shown that when $f_{site}/f_c \leq 0.5$, more than a half of the cases have RVT amplifications that are significantly larger than the TS amplifications even if the recommended RVT approach is used. This result indicates that for these cases, the oscillator response due to the significant contribution to the response from the second mode of the site is not fully captured by the RVT approach. This problem is associated with the factor of bandwidth used in the peak factor model. The bandwidth factor may not accurately model the bandwidth of the signal when multiple peaks or modes are in the Fourier Amplitude Spectrum of the signal such as the surface motions. In future work, investigations could be conducted for the bandwidth factor used in the RVT approach such that the effect of multiple modes can be accounted for with more accuracy.

It is also shown that at the higher modes for the MYGH01 site, the RVT and TS amplifications originally have similar values and duration modification only make the RVT amplification ~ 20% smaller than the TS amplification. This indicates that duration modification in RVT analysis is not always necessary. Therefore, further investigations could be conducted to understand in what cases the duration modification is essential and a simple approach could be proposed to distinguish cases where duration modification is essential.

Current study focuses on a systematic comparison between RVT and TS site response analyses. Therefore, stochastic simulated earthquake motions generated for a wide range of earthquake magnitudes and distances are used as input. However, stochastic simulated motions may not have identical statistical properties with recorded earthquake motions. As a result, further study could use earthquake motion recordings in both RVT and TS analyses to test the performance of the improved RVT approach.

References

Atkinson, G. M., & Boore, D. M. (2014). The attenuation of Fourier amplitudes for rock sites in eastern North America. *Bull. Seism. Soc. Am.* **104(1)** 513-528.

Boore, D. M. (1983). Stochastic simulation of high-frequency ground motions based on seismological models of the radiated spectra. *Bull. Seism. Soc. Am.* **73(6A)** 1865-1894.

Boore, D. M. (2003). Simulation of ground motion using the stochastic method. *Pure Appl. Geophys.* **160(3-4)** 635-676.

Boore, D. M. (2005). *SMSIM: Fortran programs for simulating ground motions from earthquakes: Version 2.3: A Revision of OFR 96-80-A*. *U.S. Geol. Surv. Dept. Interior*, http://www.daveboore.com/pubs_online/2005_smsim_manual_v2.3.pdf (last accessed May 2005).

Boore, D. M. (2009). Comparing Stochastic Point-Source and Finite-Source Ground-Motion Simulations: SMSIM and EXSIM. *Bull. Seism. Soc. Am.* **99(6)** 3202-3216.

Boore, D.M. (2015). *Point-Source Stochastic-Method Simulations of Ground Motions for the PEER NGA-East Project*, Chapter 2 in NGA-East: Median Ground-Motion Models for the Central and Eastern North America Region, PEER Report 2015/04, Pacific Earthquake Engineering Research Center, 11-49.

Boore, D. M., and W. B. Joyner (1984). A note on the use of random vibration theory to predict peak amplitudes of transient signals. *Bull. Seism. Soc. Am.* **74(5)** 2035-2039.

Boore, D. M., and E. M. Thompson (2012). Empirical Improvements for Estimating Earthquake Response Spectra with Random-Vibration Theory. *Bull. Seism. Soc. Am.* **102(2)** 761-772.

Boore, D.M., and E. M. Thompson (2015). Revisions to some parameters used in stochastic-method simulations of ground motion, *Bull. Seism. Soc. Am.* **105(2A)** 1029-1041.

Brune, J. N. (1970). Tectonic stress and the spectra of seismic shear waves from earthquakes. *J. Geophys. Res.* **75(26)** 4997-5009.

Brune, J. N. (1971). Correction. *J. Geophys. Res.* **76(20)** 5002.

Cartwright, D. E., and M. S. Longuet-Higgins (1956). The statistical distribution of the maxima of a random function. *Proc. Roy. Soc. Lond. Math. Phys. Sci.* **237(1209)** 212-232.

Cramér, H. (1966). On the intersections between the trajectories of a normal stationary stochastic process and a high level, *Arkiv för Matematik* **6(4)** 337-349.

Crandall, S. H., and W. D. Mark (1963). *Random Vibration in Mechanical Systems*, Academic Press, New York, 107.

Crandall, S. H., K. L. Chandiramani, and R. G. Cook (1966). Some first-passage problems in random vibration. *J. Appl. Mech.* **33(3)** 532-538.

Darendeli, M. B. (2001). Development of a new family of normalized modulus reduction and material damping curves, *Ph.D. Thesis*, The University of Texas, Austin.

Davenport, A. G. (1964). Note on the distribution of the largest value of a random function with application to gust loading. *ICE Proceedings* **28(2)** 187-196.

Der Kiureghian, A. (1980). Structural response to stationary excitation. *J. Eng. Mech. Div.* **106(6)** 1195-1213.

Ditlevsen, O. (1971). Extremes and First Passage Times with Applications in Civil Engineering. Thesis, Technical University of Denmark, Copenhagen.

Graizer, V. (2011). Treasure Island geotechnical array: Case study for site response analysis, *Proc. of the 4th IASPEI/IAEE International Symposium: Effect of Surface Geology on Seismic Motion*, University of California Santa Barbara, 23–26 August 2011.

Graizer, V. (2014). Comment on "Comparison of time series and random-vibration theory site-response methods" by Albert R. Kottke and Ellen M. Rathje. *Bull. Seism. Soc. Am.* **104(1)** 540-546.

Igusa, T., and A. D. Kiureghian (1985). Generation of floor response spectra including oscillator-structure interaction. *Earthquake Eng. Struct. Dynam.* **13(5)** 661-676.

Kottke, A. R., and E. M. Rathje (2008). *Technical manual for Strata*. University of California, Berkeley.

Kottke, A. R., and E. M. Rathje (2013). Comparison of Time Series and Random-Vibration Theory Site-Response Methods. *Bull. Seism. Soc. Am.* **103(3)** 2111-2127.

Liu, L., and S. Pezeshk (1999). An improvement on the estimation of pseudoresponse spectral velocity using RVT method. *Bull. Seism. Soc. Am.* **89(5)** 1384-1389.

Nuclear Regulatory Commission (NRC) (2007). *Regulatory Guide 1.208: A Performance-based Approach to Define the Site-specific Earthquake Ground Motion*, United States Nuclear Regulatory Commission, Washington, DC.

Rathje, E. M., and M. C. Ozbey (2006). Site-specific validation of random vibration theory-based seismic site response analysis. *J. Geotech. Geoenviron. Eng.* **132(7)** 911-922.

Seifried, A., and G. Toro (2015). Improved estimation of site response using random vibration theory, SSA Annual Meeting, *Seismol. Res. Lett.* **86(2B)** 716-717.

Silva, W. J., N. Abrahamson, G. Toro, and C. Costantino (1997). *Description and validation of the stochastic ground motion model*. Submitted to Brookhaven National Laboratory, Associated Universities, Inc. Upton, New York.

Vanmarcke, E. H. (1970). Parameters of the spectral density function: Their significance in the time and frequency domains*, Department of Civil Engineering, M.I.T. Research Report No. R70-58.*

Vanmarcke, E. H. (1972). Properties of spectral moments with applications to random vibration. *J. Eng. Mech. Div.* **98(2)** 425-446.

Vanmarcke, E. H. (1975). On the distribution of the first-passage time for normal stationary random processes. *J. Appl. Mech.* **42(1)** 215-220.

Wang, X., and Rathje, E. M. (2016). Influence of Peak Factors on Site Amplification from Random Vibration Theory Based Site-Response Analysis. *Bull. Seism. Soc. Am.* **106(4)** 1733-1746.

Wang, X., and Rathje, E. M. (2017). Development of Ground Motion Duration Models for Use in Random Vibration Theory Site Response Analysis.